For Official Use **ENV/CHEM/NANO(2015)30/ADD1**

Organisation de Coopération et de Développement Économiques
Organisation for Economic Co-operation and Development

28-Oct-2015

English - Or. English

ENVIRONMENT DIRECTORATE
CHEMICALS COMMITTEE

ENV/CHEM/NANO(2015)30/ADD1
For Official Use

Working Party on Manufactured Nanomaterials

Draft "Nano-SIAR": SiO2

15th Meeting of the Working Party on Manufactured Nanomaterials

4-6 November 2015
OECD Conference Centre
Paris, France

Mar GONZALEZ
Tel. +(33-1) 45 24 76 96; Email: Mar.GONZALEZ@oecd.org

JT03385247

English - Or. English

Dossier for Synthetic Amorphous Silica for the

OECD WPMN TESTING PROGRAMME

OVERVIEW

1. Chemical Name: Synthetic Amorphous Silica

2. CAS Number: Silicon dioxide, general CAS number: 7631-86-9

Precipitated silica, CAS number: 112926-00-8
(NM-200, NM-201 and NM-204)

Pyrogenic/thermal silica, CAS number: 112945-52-5
(NM-202, NM-203)

3. Lead Sponsor(s): France and the European Commission

4. Co-Sponsors: BIAC, Korea, Canada, Belgium and Denmark

5. Overview of Lead Sponsor(s) and Co-Sponsors:

	Contact	**E-mail**
SPONSORS		
European Commission	Kirsten Rasmussen	Kirsten.Rasmussen@ec.europa.eu
France	Nathalie Thieriet	nathalie.thieriet@anses.fr
	Myriam Saihi	myriam.saihi@sante.gouv.fr
CO-SPONSORS		
Belgium	Juan D. Piñeros Garcet	Juan.pineros@health.fgov.be
	Paul Troisfontaines	Paul.Troisfontaines@iph.fgov.be
Korea	Kyunghee Choi Sang Hee Lee	nierchoi@me.go.kr envilee@korea.kr
BIAC (CEFIC ASASP sector group)	Joel Wilmot Monika Maier Philippe Coceht Mario Heinemann	JWI@cefic.be monika.maier@evonik.com philippe.cochet@eu.rhodia.com mario.heinemann @wacker.com
CONTRIBUTORS		
Denmark	Keld Alstrup Jensen	kaj@nrcwe.dk
Japan	Takuya IGARASHI	t-igarashi@aist.go.jp

6. Date of Submission: Initial submission: 01 Sep. 2013. Date of final Dossier: XX

7. Comments:

7.a End-points in the WPMN test programme:

The OECD Working Party on Manufactured Nanomaterials (WPMN) testing programme agreed on relevant end-points, see Annex III, for the phase 1 of the WPMN testing programme, and this dossier on synthetic amorphous silicon dioxide (SAS) provides an overview of the outcomes of the testing as well as background information and including a review of relevant literature. Detailed information on results and tests performed can be found in the annexes to the report.

According to definitions relating to nanomaterials, for example by ISO, Synthetic Amorphous Silica is a nanostructured material. The SAS industry, as co-sponsor, provided several samples of SAS to the lead sponsors, to enable selection of the most relevant sample for the Testing Programme.

The European Joint Action "NANOGENOTOX", which was active from 2009 to 2013 and co-financed by the European Commission's Directorate General for Health and Consumers (DG SANCO) and several EU Member States, has contributed significantly to this document by making available all its scientific results on characterisation and mammalian toxicology of SAS, see Annex IV for the list of associated and collaborating partners. The NANOGENOTOX project including final outcomes is presented at http://nanogenotox.eu/ .

7.b Previous review reports on amorphous silicon dioxide and silicates:

The properties of synthetic amorphous silica has already been reviewed and assessed in several contexts, and the three main review reports identified are:

1) "Synthetic Amorphous Silica and Silicates" by the UK under the OECD High Production Volume (HPV) program. The associated SAS HPV dossier was agreed at SIAM 19, 19-22 October 2004 and published by UNEP [OECD (2004a)].
2) Furthermore, ECETOC has assessed SAS and published the outcome in JACC report number 51 of September 2006 [ECETOC (2006)].
3) The Synthetic Amorphous Silica and Silicates Industry Association (SASSI) prepared a SAS Voluntary Submittal Package (25 July 2008) for the Nanoscale Materials Stewardship Program (NMSP) of the U.S. Environmental Protection Agency [SASSI (2008)].

Furthermore, a SIDS report on soluble silicates was identified:

4) "Soluble Silicates" by Germany under the OECD High Production Volume (HPV) program. The associated dossier was agreed at SIAM 18, 20-23 April 2004 and published by UNEP (OECD 2004b).

In addition to these reports, the Association of Synthetic Amorphous Silica Producers (ASASP) stated at a meeting 30 September 2009 that SAS has been registered under REACH. The European

Chemicals Agency (ECHA) has published the registration and information is available from ECHA at http://echa.europa.eu; the registration covers synthesized amorphous SiO_2.

The reports give a comprehensive review of synthetic amorphous silica obtained by different processes and as placed on the market, and contain much valuable information on the material. The reports reflect that SAS is not a newly developed nanostructured material, but has been placed on the market for decades. Nevertheless, analysing the information presented in the reports in relation to the base data set agreed for a principal material for dossiers in the sponsorship programme as described in the guidance manual for sponsors, the data presented in the reports has some weaknesses. For example, the data relate to different sources of SAS[1], which, depending on the manufacturing process and exact process parameters within each process, differ across several physical-chemical properties, including size of primary particles and/or specific surface area. The reports have only limited data on the physical-chemical characterisation of the different SASs that have used to obtain the test results presented and are thus not fulfilling the information requests in the Sponsorship Program. Under the WPMN Testing Programme, validated standard test methods should be used, e.g. OECD, DIN, ISO, or adapted as exemplified in the reports on test methods, nanomaterials and sample preparation [OECD 2009 and OECD 20012] and the agreed data set of 59 end-points should be submitted for one source. The three background reports therefore have a limited value for addressing the information needs of the Sponsorship Program.

In addition to the three reports, several scientific articles reporting outcomes of tests using specific sources of SAS have been identified, and this report gives an overview also of these articles grouped according to end-points. The literature survey is general and included searches aimed at SAS in general, not one specific source of SAS.

According to the definitions for example by ISO, SAS is a nanostructured material. The SAS industry, as co-sponsor, provided several samples of SAS to the lead sponsors, to enable selection of the most relevant sample for the sponsorship programme.

[1] SAS from different producers, obtained through different chemical processes, and with different particle-sizes.

TABLE OF CONTENTS

1. GENERAL INFORMATION

1.1 SUBSTANCE INFORMATION

CAS Number:	Silicon dioxide, general CAS number: 7631-86-9 Precipitated silica (NM-200, NM-201 and NM-204), CAS number: 112926-00-8 Pyrogenic silica (NM-202 and NM-203), CAS number: 112945-52-5
EINECS Number	231-545-4
OECD Name	Silicon dioxide
IUPAC Name:	Silicon dioxide
Molecular Formula:	SiO_2
Molecular Weight:	60.08 g/mol
Synonyms:	Synthetic amorphous silica, SAS, silica

The principal material in the OECD WPMN test programme is NM-200 which is a precipitated synthetic amorphous silicon dioxide (SAS). The two alternate materials NM-201 and NM-204 are also precipitated materials, whereas the alternate materials NM-202 and NM-203 are both pyrogenic SAS. The materials in the NM series are provided by the JRC Nanomaterials Repository, see http://ihcp.jrc.ec.europa.eu/our_activities/nanotechnology/nanomaterials-repository, that has subsampled representative nanomaterials (Roebben at al. 2013) initially for the OECD WPMN testing programme. The background for material selection is given in Annex I. In addition, Korea submitted information for a laboratory synthesized material and manufactured in Sykgyung AT, and Japan contributed in *vitro test* results of nanotek SiO_2. BIAC provided data on the test information pertaining to the High Production Volume (HPV) program resulting in the report "Synthetic Amorphous Silica and Silicates" by the UK under the OECD, which was agreed at SIAM 19, 19-22 October 2004 and published by UNEP (OECD 2004a).

1.2 DETAILS ON CHEMICAL CATEGORY

The spatial arrangement of SiO_2 is formed by strong, directional covalent bonds, and has a well-defined local structure: four oxygen (red) atoms are arrayed at the corners of a tetrahedron around a central silicon atom (yellow), see Figure 1.

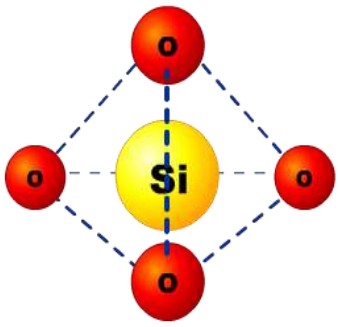

Figure 1. Structure of silicon dioxide.

The bond angles around O-Si-O are essentially the tetrahedral angle, 109 degrees; the Si-O distance is 1.61 A (0.16 nm) with very little variation. The bond angle Si-O-Si, θ_{SiOSi}, is nominally about 147 degrees, but can vary from about 120 to 180 degrees with very little change in bond energy. Furthermore, rotation of the bond about the axis is almost completely free, see Figure 2.

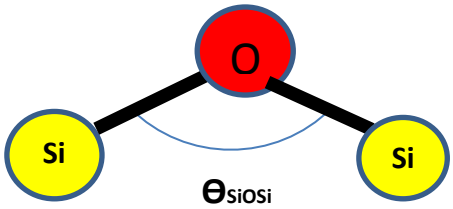

Figure 2. Silicon-Oxygen-Silicon variation of bond angle.

These observations can be summarised as follows: the "tetrahedra" formed by the SiO_4 groups must touch each other at their corners, but can do so at widely varying angles, which is also known as the Zachariesen-Warren model for the structure of SiO_2. The result of this flexibility in the bridge bonds is that SiO_2, while it has many different possible crystalline structures, can very easily form amorphous materials (i.e. materials with no long-range order). Amorphous silicon dioxide will not crystallize upon annealing at normal temperatures.

Surface chemistry

At the surface of the SAS NMs two types of groups appear: (1) hydrophobic siloxane, which is oxygen and silicon covalently bound, and (2) hydrophilic silanol (Si-OH), where the oxygen is bound to silicon and hydrogen. The number of silanol groups per unit surface area (per nm^2) varies from 5.0 to 5.7 for precipitated silica, and from 1.25 to 2.5 for pyrogenic silica. As the silanol group is hydrophilic, the solubility of SAS depends on the number of silanol groups per unit surface area, i.e. the solubility of silicon dioxide depends on route of production. Three possible spatial arrangements have been identified for silanol, see Figure 3.

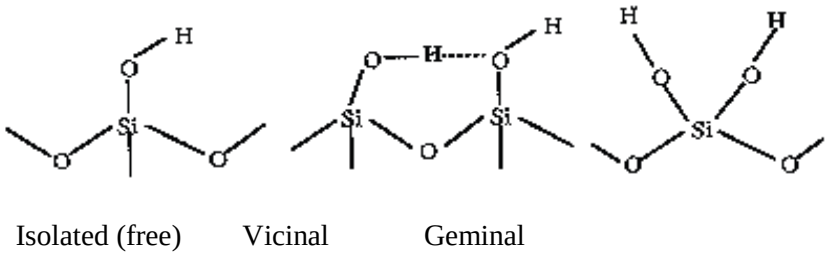

Figure 3. Spatial arrangements for silanol.

Characterisation

The principal (NM-200) and alternate materials (NM-201, NM-202, NM-203 and NM-204) were characterised in the NANOGENOTOX project as well as by the European Commission's Joint Research Centre, the JRC. Rasmussen et al. (2013) presents the collected data and information on the physical-chemical characterisation of the NM-series, giving details for both the principal and alternate materials of the NM-series, and also including a description of the test methods and procedures. Table 1 gives an overview of the physical-chemical characterisation performed and the methods used and Table 3 and Table 4 summarise the results. In addition, Korea submitted

information for a laboratory synthesized material and manufactured in Sykgyung AT, and Japan contributed in *vitro test* results of nanotek SiO_2.

Almost all of the OECD endpoints on physical-chemical testing have been completed for the principal OECD WPMN material, NM-200. Also the alternate materials, NM-201, NM-202, NM-203 and NM-204 have been extensively characterised. The determination of the octanol water coefficient is not feasible for nanomaterials, as discussed at an OECD expert meeting in Mexico, March 2013, see OECD 2014, and was considered to be not relevant for insoluble and sparingly soluble nanomaterials. The photocatalytic activity was considered to be not relevant for SAS. Analysis of intrinsic hydroxyl radical formation capacity, using the Benzoic acid probe for quantification, gave no detectable radical after 24 and 48-hour incubation.

In the NANOGENOTOX project a standardised sample preparation protocol was developed and used for the testing; the protocol addressed three types of materials, TiO_2, SiO_2 and MWCNT, and was optimized for the set of materials. Briefly, the final dispersion following the protocol has a concentration of 2.56mg/mL and sterile-filtered 0.05% w/v BSA-ultrapure water. The samples are sonicated (probe sonicator) for 16 minutes, placed in an ice bath. The energy input should be calibrated to be in the order of 3,136 MJ/m^3. The protocol is published at the project's webpage and is available at:
http://www.nanogenotox.eu/files/PDF/web%20nanogenotox%20dispersion%20protocol.pdf

The institutes participating to the characterisation of the silicon dioxides used a number of different apparatus and equipment when performing the measurements; these are listed in Rasmussen et al. 2013.

Table 1. SAS NMs: Physical and chemical characterisation performed on the NM-series (from Rasmussen et al., 2013).

Physical-chemical Properties and Material Characterization (from OECD list)	NM characterised					Method
	200	201	202	203	204	
Homogeneity	x			x		DLS
Agglomeration / aggregation	x	x	x	x		SAXS/USAXS
	x	x	x	x		DLS
	x	x	x	x		TEM
Water solubility *)	x	x	x	x	x	SDR
Crystalline phase	x	x	x	x	x	XRD
Dustiness	x	x	x	x	x	Small rotating drum
	x	x	x	x	x	Vortex shaker method
Crystallite size	x	x	x	x	x	SAXS/USAXS
	x	x	x	x	x	XRD
Representative TEM picture(s)	x	x	x	x	x	TEM
Particle size distribution	x	x	x	x	x	CLS
	x	x	x	x	x	TEM
	x	x	x	x		DLS
	x	x	x	x	x	AFM
Specific surface area (SSA)	x	x	x x	x x	x x	BET
	x	x	x	x	x	SAXS/USAXS
Volume SSA	x			x		TEM tomography
Zeta potential (surface charge)	x	x	x	x		Zeta-metry
Surface chemistry (where appropriate).	x			x		XPS
	x	x	x	x	x	TGA

Presence of coating	x	x	x	x	x	DTA
					x	GC-MS (TGA > 1 wt%)
Photo-catalytic activity						
Pour density	x	x	x	x	x	Weighing
Porosity	x	x	x	x	x	BET
Octanol-water partition coefficient, where relevant						
Redox potential	x	x	x	x	x	SDR
OH radical formation, acellular	x	x	x	x	x	Benzoic acid probe to form hydroxybenzoic acid analysed by HPLC-UV
Other relevant information (where available)						
Elemental analysis/impurities	x	x	x	x	x	Semiquantitaive ICP-OES
	x	x	x	x	x	Semiquantitaive EDS

*) the solubility was investigated in Gambles solution, Caco 2 medium, and the NANOGENOTOX dispersion medium

1.3 GENERAL SUBSTANCE INFORMATION

A. Type of Substance

Element [ ]
Inorganic [X]
Natural substance [ ]
Organic [ ]
Organometallic [ ]
Petroleum product [ ]

B. Physical State (at 20°C and 1.013 hPa)

Gaseous [ ] Liquid [ ] **Solid [X]**

C. Purity (Indicate the percentage by weight/weight)

Different analyses were performed for identifying elemental composition and surface chemistry. Such characterisation also gives information on the type and amount of impurities and the presence of a coating. The purity range of the materials studied in the NANOGENOTOX project was from 96 to 99 %. No information concerning purity was given for the materials studied by Korea and Japan. Information about protocols used and results will be given in the physical chemical data part of this report.

1.4 USE PATTERN

A. Uses

SAS is a High Production Volume (HPV) chemical which is widely used in many industries and in various applications such as synthetic resins, plastics, lacquers, vinyl coatings, varnishes, adhesives, paints, printing inks, silicone rubber, fillers in the rubber industry, tyre compounds, insulation material, liquid systems in coatings, as free-flow and anti-caking agents in powder materials, including food, as tooth paste additives, pharmaceuticals, cosmetics, as liquid carriers particularly in the manufacture of agrochemicals and animal feed, and foods, resulting in widespread exposure to these substances (Arts et al., 2007; Merget et al., 2002; Reuzel et al., 1991). SAS is also increasingly used in diagnostic and biomedical research such as cancer therapy, DNA delivery, and enzyme immobilization (Barik et al., 2008) because of its ease of production and relatively low cost; the total

volumes for these uses is though low in comparison with the industrial uses. According to SRI Consulting precipitated SAS is the most abundant nanomaterial on the market in terms of quantity[2].

The selected SASs in the NM-series are used, among others, in food applications and as reinforcement in car tires (rubber).

B Method of production (e.g., precipitation, gas phase):

The methods of production of synthetic amorphous silica are described in detail in e.g. "Integrated Pollution Prevention and Control. Reference Document on Best Available Techniques for the Manufacture of Large Volume Inorganic Chemicals - Solids and Others industry." (EC, 2007). An overview of the two main processes, the wet route (precipitation) and thermal route (flame hydrolysis) is given below. The chemistry basis for both processes is as follows: Silicon dioxide is formed when silicon is exposed to oxygen (air), and under ambient conditions a very thin layer (approximately 1 nm or 10 Å) of so-called 'native oxide' is formed on the surface. Higher temperatures and alternative environments are used to grow well-controlled layers of silicon dioxide on silicon, for example at temperatures between 600 and 1200 °C, using the so-called "dry" or "wet" oxidation with O_2 or H_2O, respectively. Process conditions, for example pH, temperature, concentration and amount of stirring, influence the size of the primary particles and the amount of aggregation and agglomeration of the silicon dioxide produced.

Thermal Route

Pyrogenic silica (sometimes called fumed silica), which is a very fine particulate form of silicon dioxide, is prepared by burning silicon tetrachloride ($SiCl_4$) or trichlorosilane ($SiHCl_3$) in an oxygen rich hydrocarbon flame to produce a "smoke" of SiO_2:

$$SiCl_4 + 2\ H_2 + O_2 \rightarrow SiO_2 + 4\ HCl$$

$$SIHCl_3 + H_2 + O_2 \rightarrow SiO_2 + 3\ HCl$$

By varying e.g. the flame temperature, flame composition and feed stock, the product's physical-chemical properties, e.g. the specific surface area and the particle size, can be controlled. NM-202 and NM-203 were synthsised via this type of process.

Wet Route

Different manufacturing methods are possible, and (**1**) decribes the way the materials NM-200, NM-201 and NM-204 were synthetized; (**2**) this process is used for synthesis of monodisperse particles (with a control of the shape and the size of the nanomaterial).

1. Amorphous silica, silica gel, is produced by the acidification of solutions of sodium silicate to produce a gelatinous precipitate that is then washed and afterwards dehydrated to produce colourless microporous silica.

   Briefly, the precipitation method reacts an alkali metal silicate dissolved in water, e.g. water glass ($Na_2O \cdot nSiO_2$; n = 2 – 4) with sulphuric acid, through a series of production steps that include raw material storage, synthesis, solid-liquid-filtration, drying and packaging. The synthesis can either be continuous or in batch.

   $$Na_2O\ x\ nSiO_2 + H_2SO_4 \rightarrow nSiO_2 + Na_2SO_4 + H_2O$$

[2] http://www.ihs.com/products/chemical/planning/scup/nanoscale-chemicals.aspx?pu=1&rd=chemihs

2. In order to obtain monodisperse SAS nanoparticles, e.g. sol-gel methods are employed such as the Stober method and the water-in-oil (w/o) micro-emulsion method. The sol-gel process is based on a series of hydrolysis, condensation and polymerisation reactions of an alkoxide. The most widely used precursors are alkoxysilanes, such as tetramethoxysilane (TMOS) and tetraethoxysilane (TEOS).

Hydrolysis is initiated by the addition of water to the silane solution under acidic, neutral, or basic conditions $Si\text{-}(OR)_4 + H_2O \rightleftharpoons (RO)_3\text{-}Si\text{-}OH + ROH$

During the condensation step a molecule, such as water or alcohol, is liberated. This leads to polymerisation and synthesis of a network of silane (Si-O-Si) and to production of nanomaterials.

$Si\text{-}(OR)_4 + HO\text{-}Si\text{-}(OR)_3 \rightleftharpoons (RO)_3\text{-}Si\text{-}O\text{-}Si\text{-}(OR)_3 + ROH$ (with alcohol)

or $(RO)_3\text{-}Si\text{-}OH + HO\text{-}Si\text{-}(OR)_3 \rightleftharpoons RO)_3\text{-}Si\text{-}O\text{-}Si\text{-}(OR)_3 + H_2O$ (with water)

2 PHYSICAL CHEMICAL DATA

2.1 Overview of Identification information and Physical Chemical Data for SAS

SAS is well described in the literature with regard to "classical[3]" physical-chemical properties and these are reported also in standard reference works; some of the "classical" physical-chemical properties are not part of the end-points agreed under the Sponsorship Program.

For physical-chemical properties listed in the Sponsorship Program as relevant for nanomaterials, some appear not to be relevant for SAS (crystalline phase and size, photocatalytic activity, redox potential, radical formation). For the relevant ones a wide range of values are presented in the three background reports [OECD (2004a), ECETOC (2006), SASSI (2008)] obtained through measurements using different SAS sources, see for example ECETOC (2006) p. 12. The water/octanol coefficient could also be relevant but currently no meaningful measurement method is available for nanomaterials. Thus the precise value of these parameters applicable to the principal material should be measured in the Sponsorship Program as information available from literature would not necessarily pertain to the principal material.

In the Joint Action NANOGENOTOX precipitated and pyrogenic synthetic amorphous silicon dioxide were characterised, see Rasmussen, 2013.

This section describes the characterisation results of the principal material (NM-200) and alternate materials (NM-201, NM-202, NM-203 and NM-204), and presentes the data characterising the Korean material.

The following Table 3 gives an overview of the information available for the end-point group *Nanomaterial Information / Identification*. Table 2 summarises the *physical chemical characterisation* data generated for the principal material (NM-200) in the Testing Programme. Table 4 summarises the *physical chemical characterisation* data generated for the WPMN Testing

[3] Melting point, boiling point, vapour pressure, flash point, auto flammability, flammability, explosive properties, oxidising properties, viscosity, water solubility, octanol-water partition coefficient.

Programme for the principal and alternate materials. An overview of the test methods used for obtaining experimental data is given in Table 1. The data for NM-201, NM-202, NM-203 and NM-204 presented in the same way as data for NM-200 in Table 2 are given in Annex V.

Table 2. Overview of results from the physical-chemical characterisation of the principal material, NM-200.

Method	Institution	Results
Homogeneity		
DLS	CEA, INRS, NRCWE	Repeated DLS studies were performed between the vials and within the vial. The observed variability between the vials is very low (2-3%) but intra-vial is much higher: 6-10%.
Agglomeration / aggregation		
SAXS	CEA	Structure and size parameters extracted from SAXS data. Gyration radius of primary particles and aggregates $2xRg_1$: 18 nm and $2xRg_2$: 440 nm, fractal dimension D_f: 2.45 and number $N_{part/agg}$ of particles per aggregate: 3600
DLS	CEA	• Ultra-pure water dispersion (intra vial study) Z-average (nm): 207.1 ± 12.3, PdI: 0.390 ± 0.041
	NRCWE	• Ultra-pure water dispersion (inter vial study) Z-average (nm): 181.5 ± 4.3, PdI: 0.238 ± 0.006
	INRS	• Ultra-pure water dispersion (intra vial study) Z-average (nm): 240.5 ± 2.3, PdI: 0.248 ± 0.006
	JRC	• Milli-Q water dispersion. Z-average (nm): peak 1: 136, peak 2: 376, PdI: 0.524 • culture media dispersion Z-average (nm): peak 1: 144.4, peak 2: 2611, PdI: 0.492 • PBS dispersion Z-average (nm): peak 1: 187.2, peak 2: 712.7, PdI: 0.532
TEM	CODA-CERVA, IMC-BAS	High porosity nanostructured material which may be considered aggregates of primary particles. Mean diamater (nm): 31 ± 3. Feret min: 21.9 nm (median of 8005) Feret max: 34.5 nm (median of 8005) Morphology of aggregates/agglomerates: low to medium sphericity, sub-angular to rounded.
TEM-tomography	CODA-CERVA	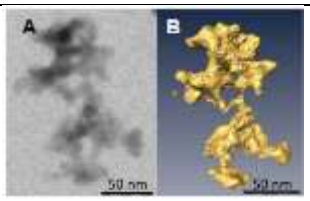 Aggregates of very complex morphology composed of a variable number of interconnected primary subunits.
AFM	CEA	Third dimension of the agglomerates/aggregates: median (of 1382): 21.9 nm
Water Solubility		
24-hour acellular *in vitro* incubation test	NRCWE	The 24-hour dissolution ratio of NM-200 was measured in three different media: 0.05% BSA in water, Gambles solution and Caco 2 media. Both NM-200 and the Al impurities are partially soluble in all media but amounts vary considerably with medium, as does the relative amounts of dissolved Al impurities compared with dissolved Si, suggesting that the solubility behaviour of the Al impurity and NM-200 depends on the medium.
Crystalline phase		
XRD	JRC	Synthetic amorphous silicon dioxide. Peaks supporting the presence of crystalline material, consistent with Na_2SO_4 were seen.

	NRCWE	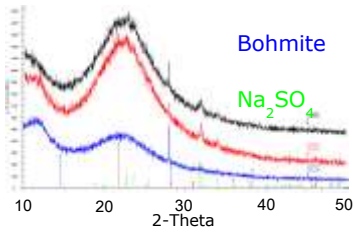	Synthetic amorphous silicon dioxide; impurities of Na_2SO_4, and Böhmite (γ-AlO(OH)) were detected.
	IMC-BAS	Synthetic amorphous silicon dioxide.	
Dustiness			
Small Rotating Drum	NRCWE	Inhalable dustiness index (n=3) 6459 ± 273 Respirable dustiness index (n=3) 293 ± 193 (mg/kg)	
Vortex Shaker Method	INRS	Respirable dustiness index (n=1) 34000 ± 0.0304 (mg/kg)	
Crystallite size			
SAXS	CEA	Amorphous material. Primary particle size: Equivalent diameter for spheres: 22nm, $2xRg_1$ is 18 nm	
XRD	JRC	Synthetic amorphous silicon dioxide. Traces of crystalline material seen around 2-Theta equal to 32° and 34°, which is consistent with the suggested presence of Na_2SO_4	
	NRCWE	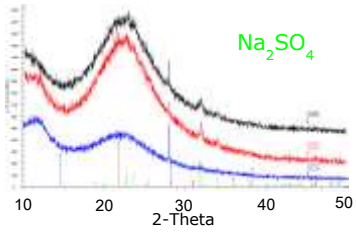	Synthetic amorphous silicon dioxide. Crystalline impurities of Na_2SO_4
	IMC-BAS	Synthetic amorphous silicon dioxide	

Representative TEM picture(s)		
TEM	CODA-CERVA, IMC-BAS	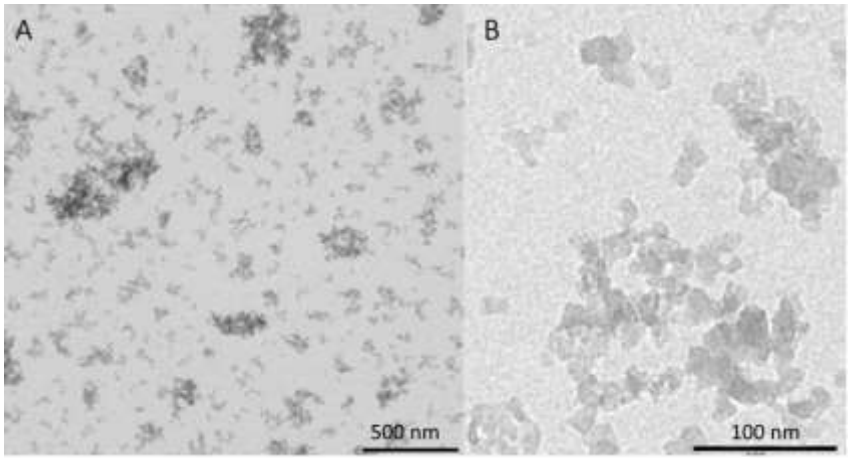 Aggregates with dense, complex structure
Particle size distribution		
SAXS	CEA	Primary particle size: Equivalent diameter for spheres: 22 nm, $2xRg_1$ is 18nm
TEM	CODA-CERVA	Primary particle size: 14 ± 7 nm
	IMC-BAS	Primary particle size: 18 nm
	INRS	Primary particle size: 23 ± 8 nm
TEM	CODA-CERVA, IMC-BAS	Number (expressed in %) of SAS NM particles smaller than 100nm, 50nm and 10nm <100 nm - 88.7%, <50 nm - 69.8% <10 nm - 1.7%
DLS	CEA	The material is polydisperse. The intensity size distribution, which consists of two main peaks is very broad and revels the presence of large aggregates of few microns.
	JRC	The material is polydisperse. The intensity size distribution, which consists of two main peaks is very broad and revels the presence of large aggregates of few microns. (see Aggregation/ Agglomeration results)
	NRCWE	The material is polydisperse. (see Aggregation/ Agglomeration results)
	INRS	The material is polydisperse. (see Aggregation/ Agglomeration results)
CLS	JRC	Peak (nm): 75 - 95, CLS Pdl: 10.18
Specific Surface Area		
BET	IMC-BAS	189.16 (m^2/g)
SAXS	CEA	123.3 ± 4.9 (m^2/g)
Volume Specific Surface Area		
TEM tomography	CODA-CERVA	342 ± 36 (m^2/cm^3) (Volume specific surface area)
Zeta Potential (surface charge)		
Zetametry	CEA	NM-200 forms a stable suspension, with negatively to neutral charged nanoparticles. The zeta potential, however, varied greatly as function of pH and reached - 45 mV around pH 7. IEP <2
	JRC	Zeta potential at pH 7, milliQ water: -47.5 (mV). Zeta potential at pH 7.1, PBS: - 18 (mV)

Surface Chemistry		
XPS	JRC	The following elements were identified in the surface of NM-200: O (70.8 at %), Si (24.1 at %), C (4.1 at %), Na (1.0 at %) and S (0.1 at %). The presence of C is considered to be due to surface contamination.
TGA	NRCWE	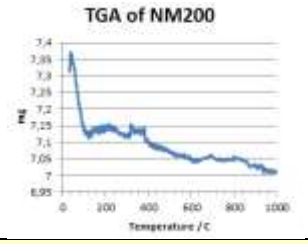 Significant mass loss was observed below 100°C (water). A 3 wt % gradual mass loss was observed above 110°C and may indicate some associated organic compounds.
Photo-catalytic activity		
End-point not relevant for SAS		
Pour-density		
Weighing	INRS	0.12 g/cm^3 (8 wt% water content)
Porosity		
BET	IMC-BAS	Micropore volume (mL/g): 0.01181
Octanol-water partition coefficient,		
End-point not relevant		
Redox potential		
OxoDish fluorescent sensor plate for O_2 detection	NRCWE	The evolution of O_2 level during 24-hour incubation was measured in three different media. Different dO_2 values were observed for these media. In the 0.05% BSA-water and Gambles solution NM-200 showed negligible reactivity. In Caco 2 media, a negative dose-response relation was observed with decreasing dO_2 level with increasing concentration of NM-200. The results suggest that NM-200 is inactive or reductive in the different incubation media.
Radical formation		
HPLC + UV	NRCWE	Using the benzoic acid probe to form 4 hydroxy benzoic acid in a phosphate buffered hydrous solution gave no detectable concentration OH radicals.
Composition		
EDS	IMC-BAS	Na - 8800 ppm, Al - 4600 ppm, S - 8700 ppm, Si - 44.77 (wt %), O (wt%) calculated - 53.02
ICP-OES		Impurities > 0.01 %: Al, Ca, Na (> 0.1 %), S (> 0.1 %) Impurities 0.005 - 0.01 % : Fe, K Impurities 0.001 – 0.005 %: Mg, Zr

Table 3. Summary of the Nanomaterial Information / Identification end-points for the silicon dioxides investigated.

NANOMATERIAL ENDPOINTS	SiO_2 Principal Material	SiO_2 [Silicon Dioxide (SAS)] Alternate Materials			
	Silicon Dioxide (SAS) NM-200 (precipitated)	NM-201 (precipitated)	NM-202 (pyrogenic)	NM-203 (pyrogenic)	NM-204 (precipitated)
Nanomaterial name	Silicon Dioxide (SAS) NM-200	Silicon Dioxide (SAS) NM-201	Silicon Dioxide (SAS) NM-202	Silicon Dioxide (SAS) NM-203	Silicon Dioxide (SAS) NM-204
CAS Number	General CAS No. for SiO_2: 7631-86-9				
CAS Number	112926-00-8 for precipitated silicon dioxide	112926-00-8 for precipitated silicon dioxide	112945-52-5 for pyrogenic silicon dioxide	112945-52-5 for pyrogenic silicon dioxide	112926-00-8 for precipitated silicon dioxide
Structural formula / molecular structure	SiO_2, strong, directional covalent bonds, and has a well-defined local structure: four oxygen atoms are arrayed at the corners of a tetrahedron around a central silicon atom				
Composition	Purity: $\geq$ 96% SiO_2, 2.7% Na_2SO_4 0.7% AlO(OH)	Purity: $\geq$ 97% SiO_2, 1.4% Na_2SO_4 1.2% AlO(OH)	Purity: $\geq$ 99% SiO_2 0.7% AlO(OH)	Purity: $\geq$ 99% SiO_2 0.7% AlO(OH)	Purity: $\geq$ 98% SiO_2 0.6% Na_2SO_4 0.8% AlO(OH)
Analytical Method(s) of detection	Overview in NIOSH manual of analytical methods http://www.cdc.gov/niosh/docs/2003-154/pdfs/7501.pdf				
Basic morphology	White, fluffy, amorphous powder				
Surface chemistry	Neither coated nor modified.	Neither coated nor modified.	Neither coated nor modified.	Neither coated nor modified.	Coated
Commercial uses	Multiple. It is a High Production Volume (HPV) chemical; for example car tyres (rubber), printing inks, paints.				
	Cosmetics, food, animal feed, etc.	Cosmetics, animal feed, food, etc.	Cosmetics, etc.	Cosmetics, etc.	Multiple, e.g. pharmaceuticals
Known catalytic activity	None	None	None	None	None
Production method	Precipitation	Precipitation	Flame hydrolysis / thermal process	Flame hydrolysis / thermal process	Precipitation

Table 4. Summary of the Physical-chemical Properties and Material Characterization Endpoints for all the SAS-NMs from the JRC Repository.

NANOMATERIAL / ENDPOINTS (method)	SiO_2 Principal Material	SiO_2 [Silicon Dioxide (SAS)] Alternate Materials			
	Silicon Dioxide (SAS) NM-200 (precipitated)	NM-201 (precipitated)	NM-202 (pyrogenic)	NM-203(pyrogenic)	NM-204 (precipitated)
PHYSICAL-CHEMICAL PROPERTIES					
1. Agglomeration/ Aggregation (DLS)	Results from 3 institutions and Ultra-pure water dispersion: Z-average (nm): 207.1 ± 11.9, PdI: 0.390±0.041(intra vial study) Z-average (nm): 181.5 ± 4.3, PdI: 0.238 ± 0.0.006 (inter vial study) Z-average (nm): 240.5 ± 2.3, PdI: 0.248±0.0.006(intra vial study)	Results from 1 institution and ultra-pure water dispersion: Z-average (nm): 208.1 ± 34.5, PdI: 0.352 ± 0.028 Z-average (nm): 197.0 ± 15.7, PdI: 0.337 ± 0.020	Results from 1 institution and ultra-pure water dispersion: Z-average (nm): 175.9 ± 4.5, PdI: 0.355 ± 0.001	Results from 3 institutions and Ultra-pure water dispersion: Z-average (nm): 172.9 ± 9.2. PdI: 0.427 ± 0.025 (intra vial study) Z-average (nm): 147.5 ± 4.5. PdI: 0.244 ± 0.017 (intra vial study) Z-average (nm): 146.8 ± 0.6, PdI: 0.229 ± 0.015 (inter vial study) Z-average (nm): 245.7 ± 37.2. PdI: 0.299 ± 0.024 (intra vial study)	-
(SAXS)	Measurement: Structure and size parameters from SAXS data.				
	Gyration radius of primary particles and aggregates 2xRg_1: 18 nm and 2xRg_2: 440 nm, fractal dimension D_f: 2.45 and number $N_{part/agg}$ of particles per aggregate: 3600	Gyration radius of primary particles and aggregates 2xRg_1: 20 nm and 2xRg_2: 180 nm, fractal dimension D_f: 2.45 and number $N_{part/agg}$ of particles per aggregate: 457	Gyration radius of primary particles and aggregates Rg_1: 16 nm and Rg_2: 100 nm, fractal dimension D_f: 2.5 and number $N_{part/agg}$ of particles per aggregate: 200	Gyration radius of primary particles and aggregates Rg_1: and Rg_2: fractal dimension D_f and number $N_{part/agg}$ of particles per aggregate could not be calculated as parameters could not be fitted.	-
(TEM)	Sub-rounded shape with a low to medium sphericity Mean diamater (nm): 31 ± 3. Feret min: 21.9 nm (median of 8001) Feret max: 34.5 nm (median of 8005) Morphology of aggregates/agglomerates:	Rounded to well rounded shapedwith a medium sphericity. Mean diamater (nm): 43 ± 4. Feret min: 25.4 nm (median of 5311) Feret max: 38.5 nm (median	Very angular to subangular shape with a low sphericity and complex and branched structure Mean diamater (nm): 53 ± 9. Feret min: 37.2 nm (median of 4248)	Very angular to subangular shape with a low sphericity and complex and branched structure Mean diamater (nm): 48 ± 4 Feret min: 33.5 nm (median of 4889) Feret max: 53.2 nm (median of	The number of particles smaller than 100 nm is 71.2 %

NANOMATERIAL / ENDPOINTS (method)	SiO_2 Principal Material	SiO_2 [Silicon Dioxide (SAS)] Alternate Materials			
	Silicon Dioxide (SAS) NM-200 (precipitated)	NM-201 (precipitated)	NM-202 (pyrogenic)	NM-203(pyrogenic)	NM-204 (precipitated)
	Low to medium sphericity, sub-angular to rounded.	of 5311) Morphology of aggregates/agglomerates: Medium sphericity, rounded to well--rounded. % of aggegates < 100 nm: 91 ± 2	Feret max: 58.4 nm (median of 4248) Morphology of aggregates/agglomerates: Low sphericity—very angular to sub-angular. % of aggregates <100 nm: 87 ± 2nm	4889). % of aggregates < 100nm: 88 ± 2. Morphology of aggregates/agglomerates: Low sphericity, angular.	
(TEM-tomography)	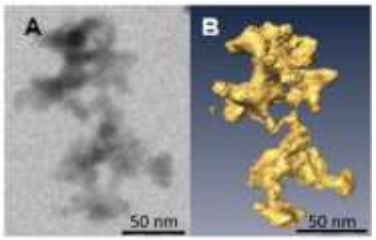 Aggregates of very complex morphology composed of a variable number of interconnected primary subunits.	-	-	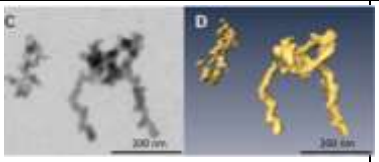 Aggregates of very complex morphology composed of a variable number of interconnected primary subunits.	-
AFM	median (of 1382): 21.9 nm	median (of 1275): 33.5 nm	median (of 1103): 38.2 nm	median (of 593): 24.2 nm.	
2. Water Solubility/ Dispersability (24-hour acellular *in vitro* incubation test)	Measurement: The 24-hour dissolution ratio was measured in three different media: 0.05% BSA in water, Gambles solution and Caco 2 media.				
	Both NM-200 and the Al impurities are partially soluble in all media but amounts vary considerably with medium, as does the relative amounts of dissolved Al impurities compared with dissolved Si, suggesting that the solubility behaviour of the Al impurity and NM-200 depends on	Both NM-201 and the Al impurities are partially soluble in Gambles Solution and Caco2 media but amounts vary considerably with the medium. In 0.05% BSA in water only the Al impurities are partially soluble; Si was	Both NM-202 and the Al impurities are partially soluble in all media but amounts vary considerably with medium as does the relative amounts of dissolved Al impurities and dissolved Si suggesting	Both NM-203 and the Al impurities are partially soluble in all media but amounts vary considerably with medium, as does the relative amounts of dissolved Al impurities compared with dissolved Si, suggesting that the solubility behaviour of the Al impurities and	Both NM-204 and the Al impurities are partially soluble in 0.05% BSA in water and Caco2 media but amounts vary considerably with medium. In Gambles solution only NM-204 is partially soluble. The relative

NANOMATERIAL / ENDPOINTS (method)	SiO_2 Principal Material	SiO_2 [Silicon Dioxide (SAS)] Alternate Materials			
	Silicon Dioxide (SAS) NM-200 (precipitated)	NM-201 (precipitated)	NM-202 (pyrogenic)	NM-203(pyrogenic)	NM-204 (precipitated)
	the medium.	below the detection limit. The relative amounts of dissolved Al impurities and dissolved Si are different depending on medium, which suggests different solubility behaviour of Al impurities and NM-201 depending on the medium.	different solubility behaviour of Al impurities and NM-202 depending on the medium.	NM-203 depend on the medium.	amounts of dissolved Al impurities and dissolved Si differ depending on medium, which suggests different solubility behaviour of Al impurities and NM-204 depending on the medium.
3. Crystalline phase (XRD)	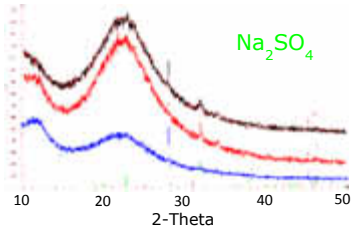 Measurements by 3 institutes: The SiO_2 phase is amorphous. Impurities: peaks consistent with the presence of Na_2SO_4 were observed.	Measurements by 3 institutes: The SiO_2 phase is amorphous. Impurities: peaks consistent with the presence of Na_2SO_4 were observed and then it is suggested that boehmite is present as well.	Measurements by 3 institutes: The SiO_2 phase is amorphous.	Measurements by 3 institutes: The SiO_2 phase is amorphous.	Measurements by 3 institutes: The SiO_2 phase is amorphous.
4. Dustiness (Small Rotating drum) (VORTEX shaker method)	Inhalable dustiness index (n=3) 6459 ±2 73 Respirable dustiness index (n=3) 293 ± 1 93	Inhalable dustiness index (n=3) 6034 ± 199 Respirable dustiness index (n=3) 218 ± 24	Inhalable dustiness index (n=3) 4988 ± 1866 Respirable dustiness index (n=3) 91 ± 11	Inhalable dustiness index (n=3) 5800 ± 1488 Respirable dustiness index (n=3) 354 ± 6	Inhalable dustiness index (n=3) 24969 ± 601 Respirable dustiness index (n=3) 1058±-
	Respirable dustiness index (n=1) 34000	Respirable dustiness index (n=1) 6500	Respirable dustiness index (n=1)17000	Respirable dustiness index (n=1) 51000	Respirable dustiness index (n=1) 14000

NANOMATERIAL / ENDPOINTS (method)	SiO_2 Principal Material	SiO_2 [Silicon Dioxide (SAS)] Alternate Materials			
	Silicon Dioxide (SAS) NM-200 (precipitated)	NM-201 (precipitated)	NM-202 (pyrogenic)	NM-203(pyrogenic)	NM-204 (precipitated)
5. Crystallite size (XRD)	Measurements by 3 institutes: The SiO_2 phase is amorphous.	Measurements by 3 institutes: The SiO_2 phase is amorphous.	Measurements by 3 institutes: The SiO_2 phase is amorphous.	Measurements by 3 institutes: The SiO_2 phase is amorphous.	Measurements by 3 institutes: The SiO_2 phase is amorphous.
6. Electron Microscopy (TEM) micrographs (TEM))	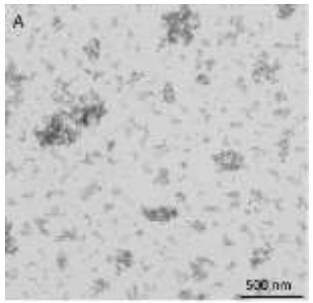 Aggregates with complex structure	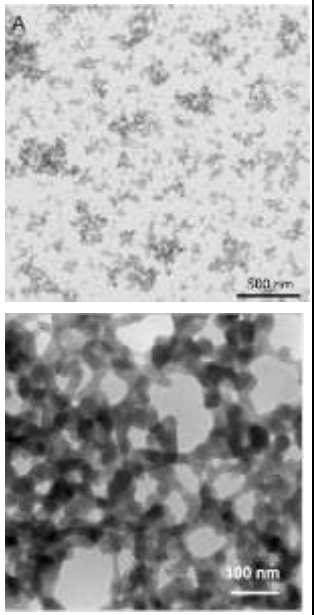 Aggregates with complex network structure.	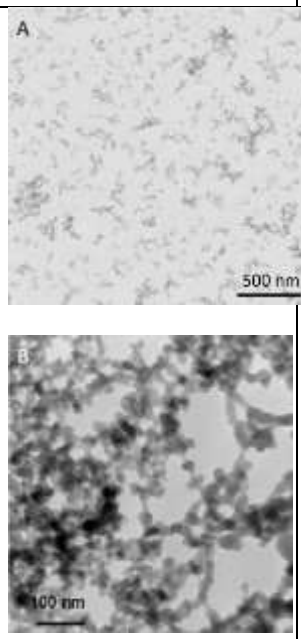 Aggregates with a complex and branched structure	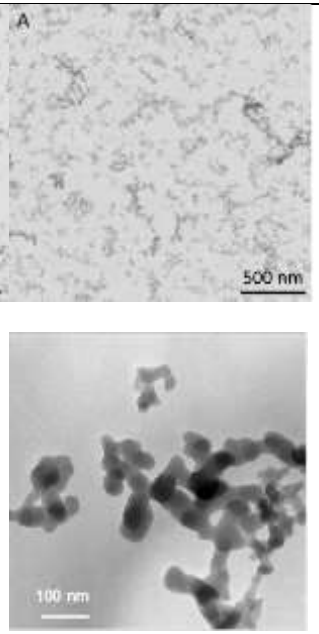 Aggregates with a complex and branched structure.	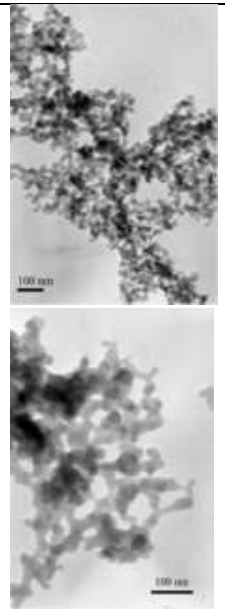 Aggregates with complex, open structure.
7. Particle size distribution	Primary particle size: Equivalent diameter for spheres: 22 nm	Primary particle size: Equivalent diameter for	Primary particle size: Equivalent diameter for	Primary particle size: Equivalent diameter for spheres: 16	Primary particle size: Equivalent diameter for

NANOMATERIAL / **ENDPOINTS** (method)	**SiO_2 Principal Material**	**SiO_2 [Silicon Dioxide (SAS)] Alternate Materials**			
	Silicon Dioxide (SAS) NM-200 (precipitated)	NM-201 (precipitated)	NM-202 (pyrogenic)	NM-203(pyrogenic)	NM-204 (precipitated)
(SAXS)	Gyration radius for primary particles $2xRg_1$ = 18 nm	spheres: 22 nm Gyration radius for primary particles $2xRg_1$ = 20 nm	spheres: 15 nm Gyration radius $2xRg_1$ = 16 nm	nm Parameters could not be fitted	spheres: 21 nm
(TEM)	Primary particle size measured by three institutions: 14 ± 7 nm, 23 ± 8 nm, 18 nm	Primary particle size measured by three institutions: 17 ± 8 nm, 19 ± 4 nm, 18 nm	Primary particle size measured by three institutions: 15 ± 7 nm, 18 ± 3 nm, 20 nm	Primary particle size measured by three institutions: 13 ± 6 nm, 16 ± 3 nm, 45 nm	Primary particle size 19 nm and by manual measurements 10 -15 nm.
(DLS)	The material is polydisperse. The intensity size distribution, which consists of two main peaks is very broad and revels the presence of large aggregates of few microns. The material is dispersed in ultra-pure water. The results from 3 institutes are: Z-average (nm): 207.1 ± 12.3, Pdl: 0.390 ± 0.041, FWHM peak width(nm): 159.8 ± 50.11 Z-average (nm): 181.5 ± 4.3, Pdl: 0.238 ± 0.006, main peak (nm): 116.7 ± 8.3 Z-average (nm): 240.5 ± 2.3, Pdl: 0.248 ± 0.006	The material is polydisperse. The intensity size distribution, which consists of two main peaks is very broad and revels the presence of large aggregates of few microns. The material is dispersed in ultra-pure water. The results from 1 institute are: Z-average (nm): 197.0 ± 15.7, PdI: 0.337 ± 0.020 FWHM peak width(nm): 105.6 ± 49.3	The material is polydisperse. The intensity size distribution, which consists of two main peaks is very broad and revels the presence of large aggregates of few microns. It display size distributions thinner and centred around slightly smaller values. The material is dispersed in ultra-pure water. The result from 1 institute is: Z-average (nm): 175.9 ± 4.5, PdI: 0.355 ± 0.001, FWHM peak width (nm): 56.2 ± 2.9	The material is polydisperse. The intensity size distribution, consisting of two main peaks is very broad and reveals the presence of large aggregates of few microns. It display size distributions thinner and centred around slightly smaller values. The material is dispersed in ultra-pure water. The results from 3 institutes are: Z-average (nm): 245.7 ± 37.2. PdI: 0.299 ± 0.024 Z-average (nm): 147.5 ± 4.5. PdI: 0.244 ± 0.017, FWHM: 84.4 ± 10.4 Z-average (nm): 146.8 ± 0.6 PdI: 0.229 ± 0.015, FWHM: 83.8 ± 0.6	

NANOMATERIAL / ENDPOINTS (method)	SiO_2 Principal Material	SiO_2 [Silicon Dioxide (SAS)] Alternate Materials			
	Silicon Dioxide (SAS) NM-200 (precipitated)	NM-201 (precipitated)	NM-202 (pyrogenic)	NM-203(pyrogenic)	NM-204 (precipitated)
8. Specific surface area (BET)	189.16 m^2/g	140.46 m^2/g	204.11 m^2/g	203.92 m^2/g	136.6 m^2/g
(SAXS)	123.3 ± 4.9 m^2/g	123.3 ± 8.3 m^2/g	184 ± 17.8 m^2/g	167.2 ± 13.4 m^2/g	131 ± 22.9 m^2/g
(TEM-tomography)	VSSA: 342 ± 36 m^2/cm^3	-	-	VSSA: 219 ± 23 m^2/cm^3	-
9. Zeta-Potential (Surface charge) (Zeta-potential/electrical mobility)	NM-200 forms a stable suspension, with negatively to neutral charged nanoparticles. The zeta potential varied greatly as function of pH and reached -45 mV around pH 7. IEP <2	NM-201 forms a stable suspension, with negatively to neutral charged particles. The zeta potential varied greatly as function of pH and reached -40 mV around pH 7. IEP <2	NM-202 forms a stable suspension, with negatively to neutral charged particles. The zeta potential varied greatly as function of pH and reached -40 mV around pH 7. IEP <2	NM-203 forms a stable suspension, with negatively to neutral charged particles. The zeta potential varied greatly as function of pH and reached -35 mV around pH 7. IEP 2-4	-
10. Surface chemistry (XPS)	The following elements were identified in the surface: O (70.8 at%), Si (24.1at%), C (4.1 at%), and Na (1 at%). The presence of C is considered to be due to surface contamination.	The following elements were identified in the surface of NM-201: O (70.3 at%), Si (23.6 at%), C (4.5 at%) and Na (1.5 at%). The presence of C is considered to be due to surface contamination.	The following elements were identified in the surface of NM-202: O (72.1 at%), Si (25 at%),and C (2.9 at%). The presence of C is considered to be due to surface contamination.	The following elements were identified in the surface of NM-203: O (71.7 at%), Si (26 at%) and C (2.3 at%). The presence of C is considered to be due to surface contamination.	The following elements were identified in the surface of NM-204: O (71.9 at%), Si (23.2 at%), Na (0.5 at%) and C (4.3 at%). Presence of C is considered to be due to surface contamination.
(TGA)	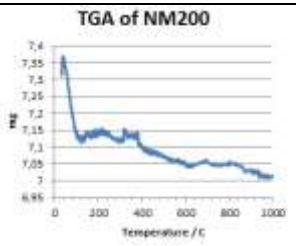 4% mass loss below 100°C (water). Gradual mass loss above 110°C, possibly a coating.	2% mass loss below 100°C (water). Gradual mass loss above 110°C., possibly a coating.	No mass loss observed	No mass loss detected. Phase transtion detected at 324°C (DTA)	2% mass loss below 100°C (water). Gradual mass loss above 110°C, more than 1% which may indicate organic coating.

NANOMATERIAL / ENDPOINTS (method)	SiO_2 Principal Material	SiO_2 [Silicon Dioxide (SAS)] Alternate Materials			
	Silicon Dioxide (SAS) NM-200 (precipitated)	NM-201 (precipitated)	NM-202 (pyrogenic)	NM-203(pyrogenic)	NM-204 (precipitated)
11. Photocatalytic activity	n/a	n/a	n/a	n/a	n/a
12. Pour density (Weighing)	0.12 g/cm^3 (8 wt% water content)	0.28 g/cm^3 (8 wt% water content)	0.13 g/cm^3 (1 wt% water content)	0.03 g/cm^3 (1 wt% water content)	0.16 g/cm^3 (6 wt% water content)
13. Porosity (BET)	Micropore volume (mL/g): 0.01181	Micropore volume (mL/g): 0.00916	Micropore volume (mL/g): 0.00084	Micropore volume (mL/g): 0.0	Micropore volume (mL/g): 0.00666
14. n-octanol-water partition coefficient	n/a	n/a	n/a	n/a	
15. Redox potential (OxoDish fluorescent sensor plate for O_2 detection)	The evolution of O_2 level during 24-hour incubation was measured in three different media. Different dO_2 values were observed for all applied media.				
	In Gambles solution the concentration of dO_2 increases together with concentration of NM-200. Conversely, for Caco 2 media dO_2 level decreases while the concentration of NM-200 increases. For 0.05% BSA water media almost no changes in the dO_2 levels were observed. The maximum O_2 changes observed for NM-200 are in the order of 40 µmol/ml, which suggests that the particle reactivity can exceed 1µmol/mg.	In Gambles solution and Caco 2 media the concentration of dO_2 peaked for 0.16mg/ml concentration of NM-201. In the 0.05% BSA in water the dO_2 level increases along with the concentration of NM-201. The maximum O_2 changes observed for NM-are in the order of 40 µmol/ml, which suggests that the particle reactivity can exceed 1µmol/mg.	In Caco 2 media the concentration of dO_2 peaked for 0.16 mg/ml concentration of NM-202. In Gambles solution and in 0.05% BSA in water the dO_2 level increased along with the concentration of NM-202. The maximum O_2 changes observed for NM-202 are in the order of 40 µmol/ml, which suggests that the particle reactivity can exceed 1µmol/mg.	In all three media the level of dO_2 increased along with the concentration of NM-203. The maximum O_2 changes observed for NM-203 are in the order of 40 µmol/ml, which suggests that the particle reactivity can exceed 1µmol/mg.	A slight reduction of dO_2 was observed for the 3 concentrations of NM-204 in 0.05% BSA in water and Gambles solution. For Caco2 media an increase in dO_2 level was observed only for the lowest concentration. The maximum O_2 changes observed for NM-204 are in the order of 40 µmol/ml, which suggests that the particle reactivity can exceed 1µmol/mg.
16. Radical formation potential	n/a	n/a	n/a	n/a	n/a
17. Other relevant information	-	-	-	-	-

2.2 Characterisation data for the material from Korea

Manufacturer: Synthesised in the test laboratory in KRISS (as alternative materials). The protocols and procedures are given in Annex VI.

Information on Particle size distribution – dry and in relevant media

Results

a) TEM size measurement results (size and distribution of particle size)

TEM images of SiO_2 nanoparticles on carbon-coated copper grids are shown in Figure 4. The nominal sizes of the synthetic SiO_2 nanoparticles were 30 and 40 nm, respectively, and the particles were spherical. The average SiO_2 nanoparticle sizes were 28.6 ± 0.67 nm and 39.4 ± 0.77 nm based on the analysis of 85 and 103 particles in TEM images for the 30 and 40 nm nanoparticles, respectively.

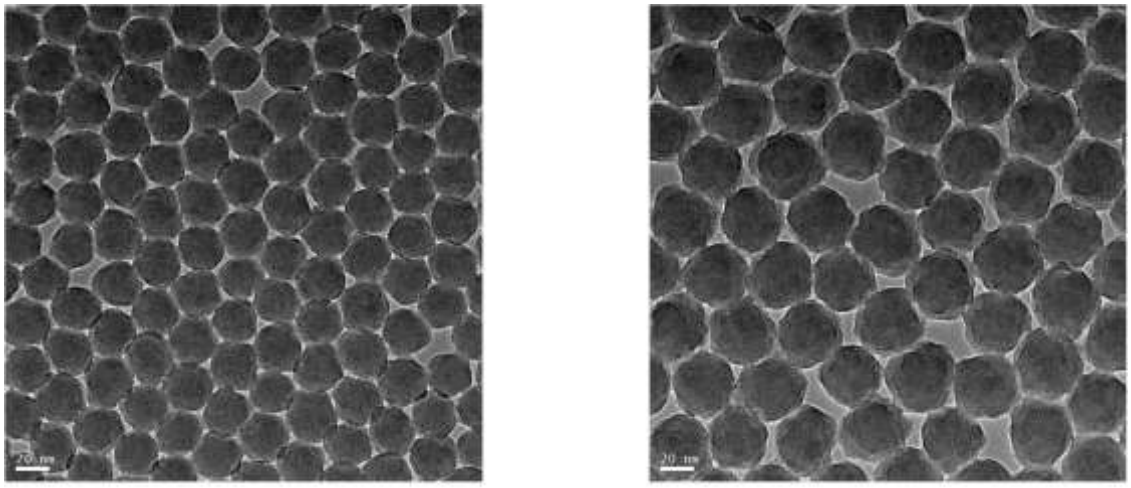

Figure 4. TEM images of 30 nm (left) and 40 nm (right) SiO_2 particles on carbon-coated copper TEM grids

As shown in Figure 5 the size distribution histogram fitted well with a normal distribution (R^2 = 0.8719). This result gave the standard deviation of the primary particle size as 3.1 ± 0.47 nm and 4.0 ± 0.55 nm for the 30 and 40 nm nanoparticles, respectively, meaning that 95 % of the particles were between 20.9 and 36.3 nm for 30 nm SiO_2 and between 29.7 and 49.1 nm for 40 nm SiO_2 [2].

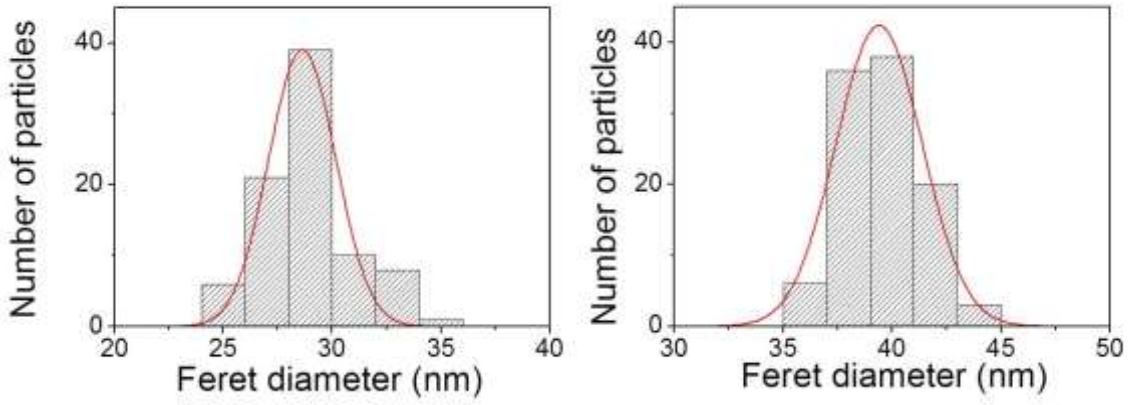

Figure 5. The particle size distribution estimated with the Feret diameters in the images for 30 nm (left) and 40 nm SiO_2 (right) nanoparticles. The Feret diameter is the longest distance between any two points in a particle image boundary.

The average particle size and size distribution was estimated with the Feret diameter, taken from particles identified on TEM images, as a function of storage time for both 30 nm and 40 nm SiO_2 nanoparticles, see Figure 6.

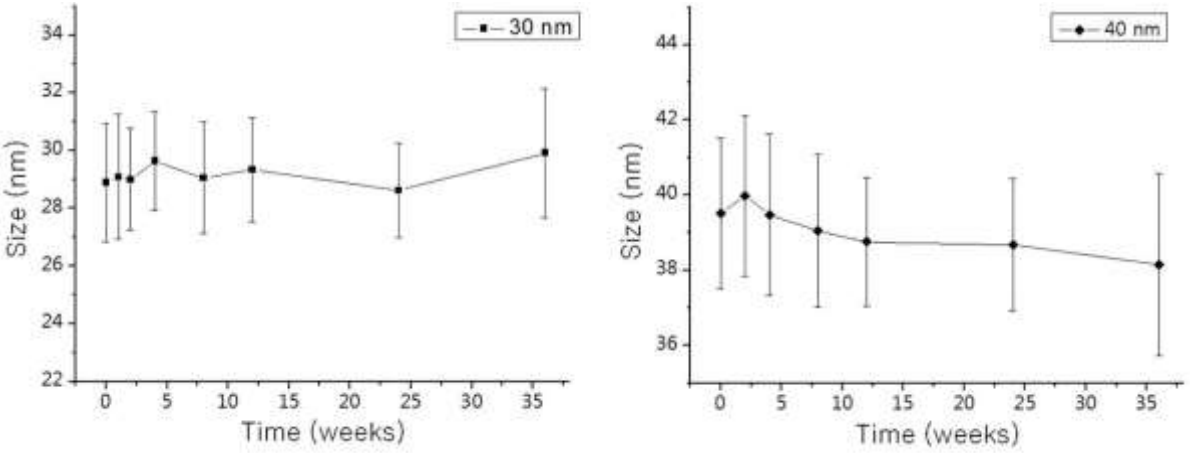

Figure 6. The average particle size and size distribution estimated with the Feret diameter in TEM images as a function of storage time for (left) 30 nm and (right) 40 nm SiO_2 nanoparticles.

b) The results of DLS size measurement

The DLS size of nominal 30 nm SiO_2 was 30.1 ± 0.7 (right-angle detection) and 37.2 ± 3.8 nm (backscatter mode detection). The DLS size of nominal 40 nm SiO_2 was 39.4 ± 1.2 (right angle detection) and 52.4 ± 0.5 nm (backscatter mode detection). The DLS size differed by up to 33 % depending on the detection angles. The suspension stability was investigated for 1 year by observing the UV-Vis absorption spectra and DLS size (Figure 7 and Figure 8). For the 30 nm SiO_2 nanoparticles in aqueous suspension, the UV-Vis absorption spectra were almost invariant, indicating

that the SiO_2 nanoparticles rarely underwent sedimentation. In addition, the DLS size of the SiO_2 nanoparticles was constant within 15 % of the average value for 1 year, see Figure 7. In contrast, the UV-Vis absorption spectra of 40 nm SiO_2 nanoparticles in aqueous suspension decreased slightly with storage time, showing that SiO_2 nanoparticles underwent slight sedimentation. The DLS size of 40 nm SiO_2 nanoparticles was constant within 33 % of the average value for 9 months (Figure 8).

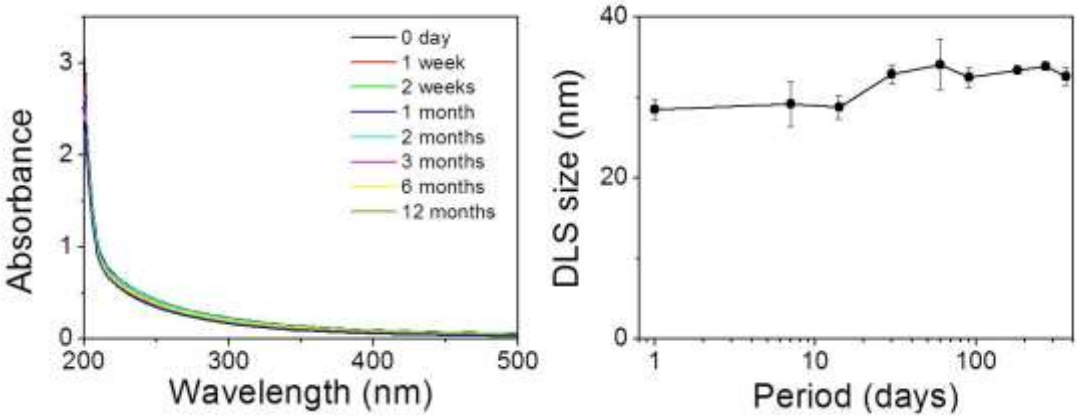

Figure 7. Time dependence of UV-Vis absorption spectra (left) and DLS size of 30 nm SiO_2 in aqueous suspension (right).

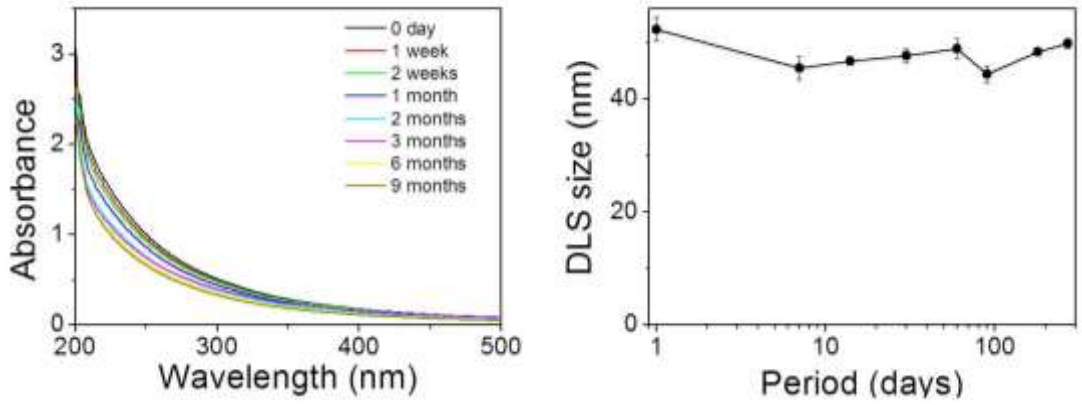

Figure 8. Time dependence of UV-Vis absorption spectra (left) and DLS size of 40 nm SiO_2 in aqueous suspension (right).

Conclusions

The alternate materials, SiO_2 nanoparticles synthesised at KRISS, have been characterised as spherical and have nominal diameters of 30 and 40 nm. The size and size distribution showed that the normalised standard deviation ($\sigma(d)/\langle d\rangle$, where $\sigma(d)$ is the standard deviation of particle size and $\langle d\rangle$ is average value of particle size) for the nanoparticles was 10 %. The DLS size of the 30 and 40 nm SiO_2 nanoparticles was 30.1 ± 0.7 and 39.4 ± 1.2 nm, respectively. The DLS size differed by up to 33 % depending on the detection angles. The DLS size of the 30 nm SiO_2 nanoparticles in aqueous suspension was constant within 15 % of the average value for 1 year. However, the DLS size of 40 nm SiO_2 nanoparticles in aqueous suspension was only constant within 33 % of the average value for

9 months. Based on the time-lapse observation of UV-visible spectra, 30 nm SiO_2 nanoparticles in aqueous suspension were stable for 1 year, while 40 nm SiO_2 nanoparticles in aqueous suspension showed partial sedimentation.

References

1. S.Y. Kwon, Y.-G. Kim, S.H. Lee and J.H. Moon "Uncertainty analysis of measurements of the size of nanoparticles in aqueous solutions using dynamic light scattering" *Metrologia*, **48** 417-425 **(2011)**.

2. N.W. Song, K.M. Park, I.-H. Lee, H. Huh, "Uncertainty estimation of nanoparticle size distribution from a finite number of data obtained by microscopic analysis" *Metrologia*, **46(5)** 480-488 **(2009)**.

3. Ministry of Education, Science and Technology, Korea, 2010. The Report on "Development of Nano-materials Safety and Characterization Techniques" (KRISS)

4. Ministry of Education, Science and Technology, Korea, 2011. The Report on "Development of Nano-materials Safety and Characterization Techniques" (KRISS).

ZETA POTENTIAL/SURFACE CHARGE

The methods are described in Annex IX.

Results

The zeta potential was - 81.4 ± 5.3 mV (pH = 8.47) and - 54.6 ± 1.4 mV (pH = 6.22) for 30 and 40 nm SiO_2 nanoparticles in Distilled Water (DW) suspension, respectively. When the suspensions were kept at ambient conditions, the zeta potential of these nanoparticles was maintained for 3 months. However, the zeta potential increased with slopes of 0.14 mV/day and 0.068 mV/day for 30 and 40 nm SiO_2 nanoparticle suspensions, respectively. The pH of the suspensions was stable for 2 weeks but converged to neutral (pH = 7) with increasing storage time.

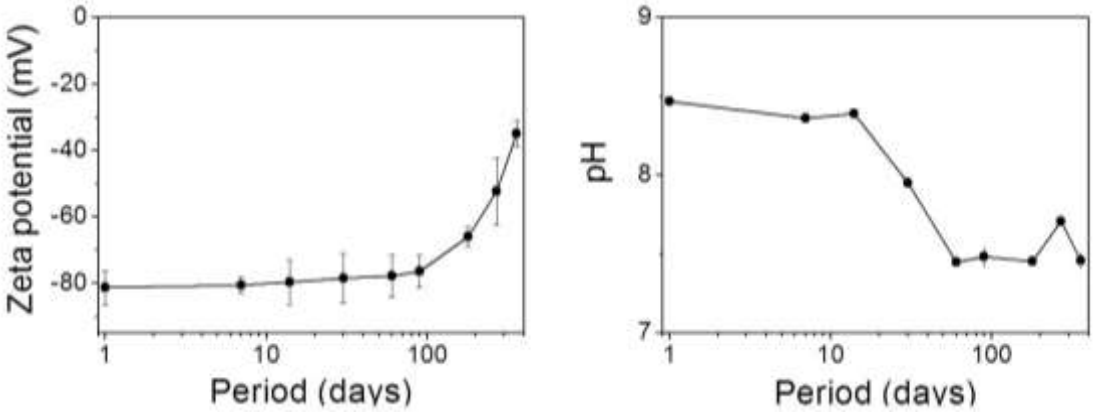

Figure 9. Time dependence of the zeta potential (left) and pH of 30 nm SiO_2 nanoparticles (right) in aqueous suspension

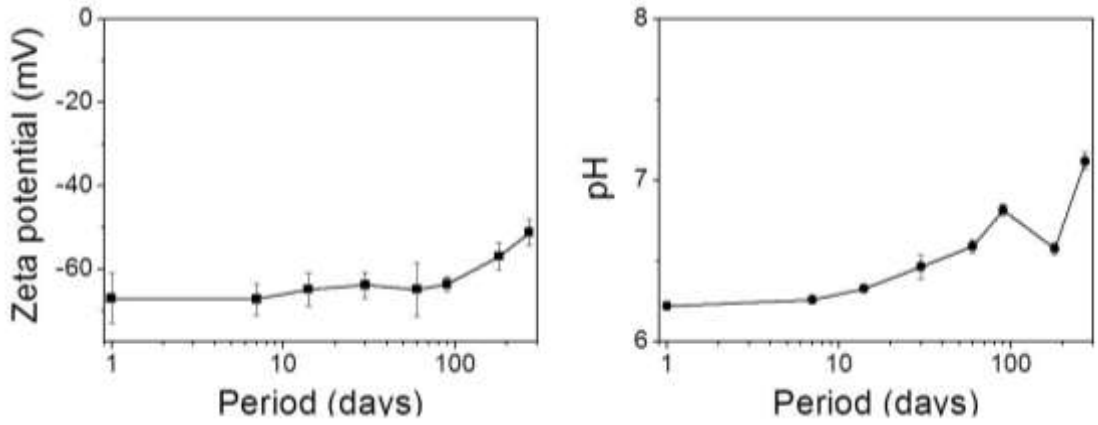

Figure 10. Time dependence of the zeta potential (left) and pH of 40 nm SiO_2 nanoparticles (right) in aqueous suspension.

Conclusions

The zeta potential was - 81.4 ± 5.3 mV (pH = 8.47) and - 54.6 ± 1.4 mV (pH = 6.22) for 30 and 40 nm SiO_2 nanoparticles in DW suspension, respectively. The zeta potential was stable up to 3 months but it increased with longer storage time.

References

1. Ministry of Education, Science and Technology, Korea, 2010. The Report on "Development of Nano-materials Safety and Characterization Techniques" (KRISS)

2. Ministry of Education, Science and Technology, Korea, 2011. The Report on "Development of Nano-materials Safety and Characterization Techniques" (KRISS)

3 ENVIRONMENTAL FATE AND PATHWAYS

The properties of synthetic amorphous silica have already been reviewed and assessed in several contexts, and three main review reports were identified, see 7b. in the Overview (OECD 2004, SASSI 2008, and ECETOC 2006); these report all pre-date the WPMN.

SAS is reported to be sparingly soluble in water (values given range from 15 to 68 mg/l, (OECD 2004) and has a vapour pressure of 13.3 hPa at 1732 ºC; its melting point is ca. 1700 ºC (OECD 2004). It is inorganic and fully oxidised, so biodegradation is not relevant. No further search for information was performed. Based on the chemical nature of SiO_2, i.e. the inorganic structure and chemical stability of the Si-O bond, which is highly stable, no photo degradation or chemical degradation is expected.

Based on the properties described above, it is expected that SiO_2 released to the environment will distribute to soil or sediment. One of the main components of any soil or sediment is silicon dioxide (in crystalline or amorphous form), and it evaluated that it is not possible to distinguish SAS from the amorphous SiO_2 naturally occurring in the environment, unless SAS is labelled.

In the first part, a brief description (General information, section 1.2) of SAS surface chemistry was given.

Siloxane groups (Figure 11) are functional groups, which are hydrophobic and little reactive. Siloxane groups could be formed at high temperature during a process of silica dehydration for example through condensation of two silanols:

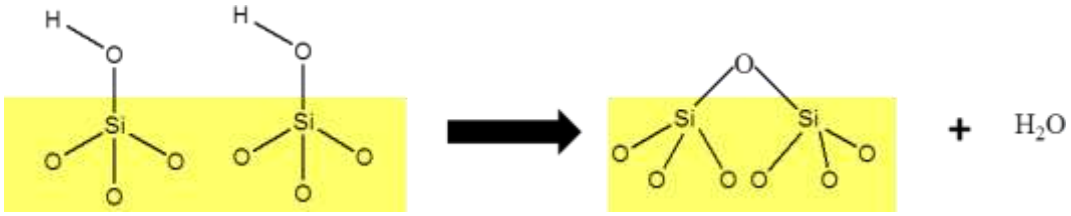

Figure 11: Siloxane group formed by the condensation of two silanol groups

Another chemical group present on the surface of syntetic amorphous silicon dioxide is the silanol group, which may exist in three different spatial arrangements that have different reactivity (Figure 12):

- Isolated group (free silanol) which consist of a silicon atom linked to three bonds in the bulk structure and the fourth one attached to a single OH group (Figure 12A).

- Vicinal group (bridged silanol) where 2 single groups are attached to different silicon atoms and are close enough to form an H-bond (Figure 12B).

- Germinal group which consist of two hydroxyl groups linked to one silicon atom. The germinal groups are too close to form a hydrogen bond, whereas the two groups are too far separated (Figure 12C).

The silanol group is more reactive than the siloxane group. The distribution of these active groups is depending on the silica type, and the method of synthesis chosen. The temperature and the hydration degree are also an important factor. Within the silanol the spatial arrangement, see Figure

12 A, B and C, also influences the reactivity with the Isolated (free) silanol being the most reactive species.

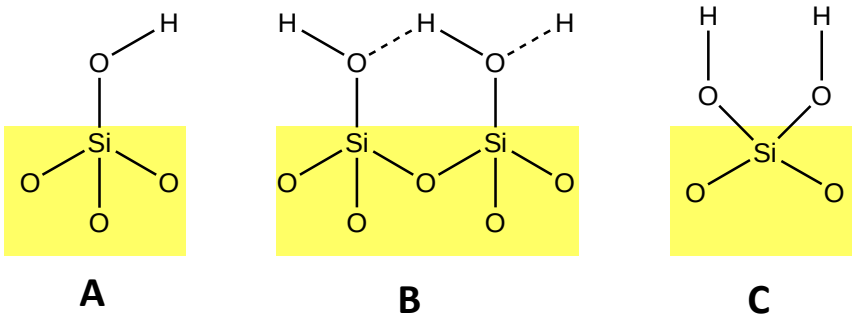

Figure 12: Scheme of main types of silanol. Isolated (free) silanol (A), Vicinal silanol (B) and germinal silanol (C)

The reactivity of the SAS depends on the degree and the accessibility of the silanol groups, especially the Isolated (free) ones. SAS is stable at pH values between 2 and 8, and at a pH above 8 these reactions occur at a much higher frequency.

$(SiO_2)_x + 2\ H_2O \rightleftharpoons (SiO_2)_{x-1} + Si(OH)_4$

$Si(OH)_4 \rightleftharpoons H_6Si_2O_7 + H_2O$

The chemisorption of the hydroxyl group enables release of a monosilicic acid molecule.

Above ph > 9, dissolution of silica increases quickly as silicate ions will be formed from the $Si(OH)_4$ monomer. When catalysed by hydroxide ions (OH^-) this dissolution occurs more rapidly.

$Si(OH)_4 \rightleftharpoons Si(OH)_5^- \rightleftharpoons H_3SiO_4^- + H_2O$

The SIDS assessment [OECD 2004] states: "The bioavailable form of synthetic amorphous silica and silicates is the dissolved form which exists exclusively as monosilicic [$Si(OH)_4$] acid under environmental pH. In analogy to the general chemical reaction of weak acids and salts of weak acids with water, the water-soluble fraction of silica acts as a weak acid and, therefore, will tend to lower the pH value, while that of a silicate acts as a base tending to bind protons and, thus, raise the pH value by forming hydroxyl ions (…). But pH shifts which are measurable at high loadings under laboratory conditions are not expected to occur from the anthropogenic deposition in the aquatic environment of synthetic amorphous silica and silicates due to low aquatic releases and sufficient natural buffer capacities.
Finally, these materials are supposed to combine indistinguishably with the soil layer or sediment due to its chemical similarity with inorganic soil matter.
Dissolved silica can be actively assimilated by some marine and terrestrial organisms as normal natural processes mainly related to structural function."

Thus, the relevance of testing for the environmental fate and behaviour end-points were evaluated to essentially not be relevant in view of the known information on SiO_2, see table 5.

Korea performed sewage treatment testing with SiO_2 from Sukgyung AT (Korea) and Aldrich (USA), whereas the materials from the NM-series were not tested for this.

3.1 Environmental information of SAS nanoparticles from JRC repository

Table 5. Summary of the Environmental Fate Endpoints.

NANOMATERIAL / ENDPOINTS	SiO_2 Principal Material	SiO_2 [Silicon Dioxide (SAS)] Alternate Materials			
	Silicon Dioxide (SAS) NM-200 (precipitated)	NM-201 (precipitated)	NM-202 (pyrogenic)	NM-203 (pyrogenic)	NM-204 (precipitated)
ENVIRONMENTAL FATE[4]					
1. Dispersion stability in water	A slight sedimentation is observed during the first hour and then the samples are very stable for the next 16 h (stationary state of Z average and mean count rate).	A slight sedimentation is observed during the first hour and then the samples are very stable for the next 16 h (stationary state of Z average and mean count rate).	A slight sedimentation is observed during the first hour and then the samples are very stable for the next 16 h (stationary state of Z average and mean count rate).	A slight sedimentation is observed during the first hour and then the samples are very stable for the next 16 h (stationary state of Z average and mean count rate).	A slight sedimenta-tion is observed during the first hour and then the samples are very stable for the next 16 h (stationary state of Z average and mean count rate).
2. Biotic degradability	n/a	n/a	n/a	n/a	n/a
• **Ready biodegradability**	n/a	n/a	n/a	n/a	n/a
• **Inherent biodegradability**	n/a	n/a	n/a	n/a	n/a
• **Simulation testing in surface water**	n/a	n/a	n/a	n/a	n/a
• **Soil simulation testing**	n/a	n/a	n/a	n/a	n/a
• **Sediment simulation testing**	n/a	n/a	n/a	n/a	n/a
• **Sewage treatment**	n/a	n/a	n/a	n/a	n/a

.

NANOMATERIAL / ENDPOINTS	SiO_2 Principal Material	SiO_2 [Silicon Dioxide (SAS)] Alternate Materials			
	Silicon Dioxide (SAS) NM-200 (precipitated)	NM-201 (precipitated)	NM-202 (pyrogenic)	NM-203 (pyrogenic)	NM-204 (precipitated)
simulation testing					
• **Anaerobic biodegradability**	n/a	n/a	n/a	n/a	n/a
3. Identification of degradation product	n/a	n/a	n/a	n/a	n/a
4. Further testing of degradation products	n/a	n/a	n/a	n/a	n/a
5. Abiotic degradability and fate	n/a	n/a	n/a	n/a	n/a
• **Hydrolysis**	The reactivity of the SAS depends on the degree and the accessibility of the silanol group, especially the free ones. NM-200 is synthesized by the precipitation process leading to relatively more –OH groups on the surface than the thermal process. Presence of large amounts of SiOH makes the material more hygroscopic, and it may readily adsorb water molecules from the air.	See NM-200	See NM-200. The pyrolysis synthesis process minimizes the presences of –OH groups, thus thermal SAS is relatively less hygroscopic than precipitated SAS.	See NM-202	See NM-200
• **Phototransformation**	n/a [Stable in water and Air]	n/a	n/a	n/a	n/a
6. Adsorption-desorption	n/a [OECD TG 106: the test substance is also a major component in soil, thus the method is not meaningful.]				
7. Adsorption to soil or sediment	n/a [OECD TG 106: the test substance is also a major component in soil, thus the method is not meaningful.]				
8. Bioaccumulation potential	n/a [SAS is not lipophilic. SAS is not bio-accumulating due to inherent substance properties.]				
• **Bioconcentration: Flow-through fish test**	n/a				

NANOMATERIAL / ENDPOINTS	SiO_2 Principal Material	SiO_2 [Silicon Dioxide (SAS)] Alternate Materials			
	Silicon Dioxide (SAS) NM-200 (precipitated)	NM-201 (precipitated)	NM-202 (pyrogenic)	NM-203 (pyrogenic)	NM-204 (precipitated)
• **Bioaccumulation is sediment-dwelling Benthic Oligochaetes**	n/a				
9. Other relevant information	n/a				

n/a : not applicable

3.2 *Environmental information on SAS nanoparticles tested by Korea (sewage treatment)*

Test substances

Nanomaterial name: Silicon dioxide (SiO_2), CAS number: 7631-86-9 (SiO_2)

Remarks: SiO_2 from Aldrich (USA) and Sukgyung AT (Korea)

Methods

Media: De-ionized water and synthetic sewage (Glucose 200 mg/L, yeast extract 10 mg/L, bactopeptone 10 mg/L, $(NH_4)_2SO_4$ 50 mg/L, $K_2H_2PO_4$ 30 mg/L, KH_2PO_4 30 mg/L, $MgSO_4$ 1.8 mg/L, $FeCl_3$ 0.04 mg/L, NaCl 1.4 mg/L, $CaCl_2$ 0.04 mg/L, $CoCl_2$ 0.48 mg/L, $NaHCO_3$ 30 mg/L)

Method/guideline followed: OECD Test Guideline 303, "Activated sludge process", OECD Test Guideline 106, "Adsorption test"

Type: Batch test

Year (study performed): 2011

GLP: No

Activated sludge: Gimpo sewage treatment plant

Analytical monitoring: ICP (Inductively Coupled Plasma)-Optical Emission Spectrometer (ICP-730 ES, VARIAN, Australia)

Exposure period (duration): 24 h

Doses/concentration levels: 10 mg/L

Test conditions

Dilution water source: De-ionized water

Stock and test solution and how they are prepared: SiO_2 suspension diluted with de-ionized water was exposed to activated sludge

Exposure vessel type: 50 mL polypropylene conical tube

Test temperature: 25℃

Results

Effect of exposure time on fate of SiO_2 in activated sludge process

The adsorption of both Aldrich and Sukgyung AT SiO_2 to activated sludge was affected by the exposure time. The effluent concentration and percent of SiO_2 were progressively decreased with time. The removed percent was increased from 8 h to 24 h exposure time by ca. 0.4% and 0.3% in the case of Aldrich and Sukgyung AT SiO_2, respectively. The results indicate that the retention time of the SiO_2 in activated sludge bioreactor is an important factor for the fate of the SiO_2 in the activated sludge process.

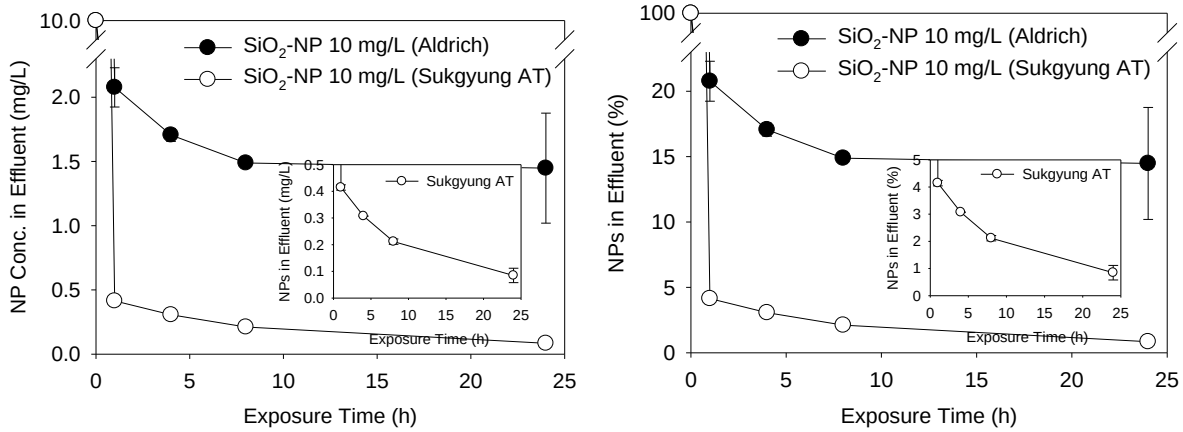

Figure 13. SiO_2 in effluent (deionised water condition); concentration (left) and % = effluent concentration/initial concentration x 100 (right)

Effects of synthetic sewage on SiO_2 concentration in effluent

SiO_2 was exposed to activated sludge in the presence or absence of synthetic sewage, and the concentrations in the effluent were compared. In the presence of synthetic sewage, more Aldrich SiO_2 (ca. 8%) were adsorbed to the activated sludge as compared with the absence of synthetic sewage (de-ionized water), resulting in a low concentration of SiO_2 (ca. 0.7 mg/L) in the effluent. On the other hand, synthetic sewage induced the reduction of Sukgyung AT SiO_2 adsorption (ca. 2.5%) to the activated sludge. The result suggests that sewage components may affect the fate of SiO_2 in the activated sludge process.

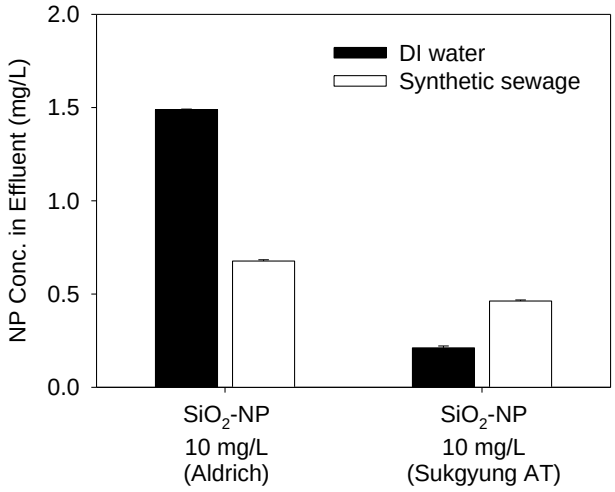

Figure 14. Effect of synthetic sewage on SiO_2 concentration in effluent (exposure time: 8 h)

Effects of SiO_2 in effluent water quality

The effluent COD and NH_4-N concentrations of the activated sludge process were monitored after 10 mg/L SiO_2 exposure, and the values were compared with control. There was no significant difference between the COD concentrations of control and both Aldrich and Sukgyung AT SiO_2 exposure, whereas nitrogen concentrations were slightly affected by both Aldrich and Sukgyung AT SiO_2 after 24 hrs.

Table 6. Water quality in the absence and presence of SiO_2 (mg/L)

	Synthetic sewage	8 h			24 h		
		Control	SiO_2 (Aldrich)	SiO_2 (Sukgyung)	Control	SiO_2 (Aldrich)	SiO_2 (Sukgyung)
COD	221 ± 7	116 ± 3	130 ± 39	75 ± 6	89 ± 6	90 ± 4	90 ± 14
NH_4-N	27 ± 1	26 ± 1	21 ± 0	22 ± 0	14 ± 0.4	19 ± 0	17 ± 3

Conclusions

The fate of both Aldrich and Sukgyung AT SiO_2 was affected by the exposure time and synthetic sewage. 10 mg/L of Aldrich and Sukgyung AT SiO_2 exposure respectively induced 0.7 and 0.5 mg/L of SiO_2 release to the effluent in the synthetic sewage condition for 8 h of exposure time. The effluent COD was not affected by both Aldrich and Sukgyung AT SiO_2 exposure, whereas the nitrogen concentration was slightly changed by both Aldrich and Sukgyung AT SiO_2 after 24 hrs.

References

OECD test guidelines 303 Simulation Test - Aerobic Sewage Treatment

OECD test guidelines 106 Adsorption and Desorption Using a Batch Equilibrium Method.

National Institute of Environmental Research, Ministry of Environment, Korea, 2011. Ecotoxicology and environmental fate for the manufactured nanomaterials.

4 ENVIRONMENTAL TOXICITY

The OECD WPMN testing programme lists the following end-points, see Table 7.

Table 7. End-points for environmental toxicology.

	Environmental toxicology
42	Effects on pelagic species (short/ long term)
43	Effects on sediment species (short/ long term)
44	Effects on soil species (short/ long term)
45	Effect on terrestrial species
46	Effect on micro-organisms
47	Other relevant information

For some of these end points, information from tests was submitted by BIAC. The substances tested were declared equivalent to the SAS from the JRC Nanomaterials Repository, but no characterisation data accompanied the test results. Furthermore, the test results were originally submitted with a view to supporting the description of silicon dioxide as an industrial high production volume chemical and the testing predates the WPMN programme. The results are summarised in the table below.

Silicon dioxide (in its several naturally occurring forms including crystalline quartz) is one of the most abundant chemical compounds in nature, so *a priori* only little monitoring data on SAS reported in literature was expected, and none was identified.

A few studies on environmental effects of SAS were identified as well as several review articles of nanoparticles that included SiO_2. Only one of these studies reported exactly which source of SAS was used; however some general conclusions can be drawn based on the studies. One additional study focuses on *Mytilus* haemocytes instead of the whole organism but can also be considered as an environmental study. Some of the studies have an element of comparison with "bulk" SiO_2 defined as having micron sized grains. In the six identified studies with SAS, the reported characterisation of SAS was limited, and 2 studies are performed using Ludox, which is colloidal SAS. The studies with colloid SiO_2 do not provide data on the characterisation of the composition of the suspension, though addition of a biocide would be expected to ensure shelf life of the commercial product, as biocides have anti-microbial properties.

Table 8. Short term effect on pelagic species

Material	Test Organism / System	Method	Exposure/ dose	Main findings	Contributor to WPMN Testing Programme	Comment
Substance declared equivalent to **NM-200** (precipitated) No Characterisation provided	*Brachydanio rerio*	OECD Guideline 203 (Fish, Acute Toxicity Test)	96 hours 1000 and 10,000 mg SiO_2/L	After 96 h of exposure all animals were alive and their conditions (swimming behaviour, colour, respiratory function or any other visually observable morphological or behavioural criterion) was equal to that of the control animals.	Data provided by BIAC. Tests performed by TNO Division of Nutrition and Food Research, Zeist (NL) in 1992	
Substance declared equivalent to **NM-201** (precipitated) No Characterisation provided	*Brachydanio rerio*	OECD Guideline 203 (Fish, Acute Toxicity Test)	96 hours 1000 and 10,000 mg SiO_2/L	After 96 h of exposure all animals were alive and their conditions (swimming behaviour, colour, respiratory function or any other visually observable morphological or behavioural criterion) was equal to that of the control animals.	Data provided by BIAC. Tests performed by TNO Division of Nutrition and Food Research, Zeist (NL) in 1992	
Substance declared equivalent to **NM- 202** (pyrogenic) No Characterisation provided	*Brachydanio rerio*	OECD Guideline 203 (Fish, Acute Toxicity Test)	96 hours 1000 and 10,000 mg SiO_2/	After 96 h of exposure all animals were alive and their conditions (swimming behaviour, colour, respiratory function or any other visually observable morphological or behavioural criterion) was equal to that of the control animals	Data provided by BIAC. Tests performed by TNO Division of Nutrition and Food Research, Zeist (NL) in 1992	
Substance declared equivalent to **NM- 203** (pyrogenic) No Characterisation provided	*Brachydanio rerio*	OECD Guideline 203 (Fish, Acute Toxicity Test)	96 hours 1000 and 10,000 mg SiO_2/	After 96 h of exposure all animals were alive and their conditions (swimming behaviour, colour, respiratory function or any other visually observable morphological or behavioural criterion) was equal to that of the control animals	Data provided by BIAC. Tests performed by TNO Division of Nutrition and Food Research, Zeist (NL) in 1992	

Table 9. Short term effect on crustacean species

Material	Test organism / System	Method	Exposure/ dose	Main findings	Contributor to WPMN Testing Programme	Comment
Substance declared equivalent to **NM-200** (precipitated) No Characterisation provided	*Daphnia magna*	OECD guideline 202, 24 h	24 hours 1000 and 10,000 mg SiO_2/L (nominal, loading)	0/40 of the control group were immobilised/dead. 3/40 (7.5 %) and 1/40 (2.5 %) were immobilised /dead at a loading of 1000 and 10000 mg/L respectively. The observed effects were not dose related, and it is likely that they are caused by physical hampering of the test animals.	Data provided by BIAC. Tests performed by TNO Division of Nutrition and Food Research, Zeist (NL) in 1992	Test duration 24 h (acc. to the valid guideline of 04 April 1984) instead of 48 h (today) / In one test, the oxygen content was 4.2 mg/L after 24 h, i.e. less than 60 % of saturation (not assumed to have affected the outcome).
Substance declared equivalent to **NM-201** (precipitated) No Characterisation provided	*Daphnia magna*	OECD guideline 202, 24 h	24 hours 1000 and 10,000 mg SiO_2/L (nominal, loading)	0/40 of the control group were immobilised/dead. 3/40 (7.5 %) and 1/40 (2.5 %) were immobilised/dead at a loading of 1000 and 10000 mg/L respectively. The observed effects were not dose related, and it is likely that they were caused by physical hampering of the test animals.	Data provided by BIAC. Tests performed by TNO Division of Nutrition and Food Research, Zeist (NL) in 1992	Test duration 24 h (acc. to the valid guideline of 04 April 1984) instead of 48 h (today). In one test, the oxygen content was 4.2 mg/L after 24 h, i.e. less than 60 % of saturation (not assumed to have affected the outcome).
Substance declared equivalent to **NM-202** (pyrogenic) No Characterisation provided	*Daphnia magna*	OECD guideline 202, 24 h	24 hours 1000 mg/L $_{SiO2}$ nominal	Overall 1/40 treated animal was found immobile after 24 h of exposure (2.5 %). Two parallel series using clear or slightly milky solutions of the water soluble fractions were achieved: 0/15 immobile animals (0 %) (assumed to relate to test medium microfiltrated 1.7 µm) 1/25 immobile animals (4 %) (assumed to relate to test medium microfiltrated 1.7 µm and 1.2 µm)	Data provided by BIAC. Tests performed by TNO Division of Nutrition and Food Research, Zeist (NL) in 1992	Test duration 24 h (acc. to the valid guideline of 04 April 1984) instead of 48 h (today) / In one test, the oxygen content was 4.2 mg/L after 24 h, i.e. less than 60 % of saturation (not assumed to have affected the outcome).
Substance declared equivalent to **NM-203** (pyrogenic) No Characterisation provided	*Daphnia magna*	OECD guideline 202, 24 h	24 hours 1000 mg/L $_{SiO2}$ nominal	Overall 1/40 treated animal was found immobile after 24 h of exposure (2.5 %). Two parallel series using clear or slightly milky solutions of the water soluble fractions were achieved: 0/15 immobile animals (0 %) (assumed to relate to test medium microfiltrated 1.7 µm) 1/25 immobile animals (4 %) (assumed to relate to test medium microfiltrated 1.7 µm and 1.2 µm)	Data provided by BIAC. Tests performed by TNO Division of Nutrition and Food Research, Zeist (NL) in 1992	Test duration 24 h (acc. to the valid guideline of 04 April 1984) instead of 48 h (today) / In one test, the oxygen content was 4.2 mg/L after 24 h, i.e. less than 60 % of saturation (not assumed to have affected the outcome).

Summary of published Environmental Toxicology studies

A literature review was performed and the publications identified are listed in Table 10 below presents a summary of the published environmental toxicology data identified for SAS. As numerous studies have been performed with crystalline silica, some of these had to be further checked before it was evident that the study concerned crystalline material(s), and these studies are also listed below. Amorphous silica appears to not have been studied much, and only few publications were identified. The table does not include a column for "derived effect value" as none was derived.

Table 10. Summary of published Environmental Toxicology studies.

Reference	Material / Size	Test Organism / System	Method	Exposure/ dose	Main findings
Effects on pelagic species (short/ long term)					
Fish					
F. Sharif et al. (2012)	Mesoporous sílica nanoparticles (Crystalline silica)	zebrafish embryos			Zebra fish embryos were exposed to synthesized mesoporous silica, whose inner structure was compared to MCM-41, i.e. Mobil Crystalline Materials. In addition the SiO_2 surface was functionalised, thus the information is not evaluated further here.
R. Ramesh et al. (2013)	SiO_2 nanoparticles Crystalline silica	zebra fish *(Danio rerio)*			Zebra fish were exposed to SiO_2, described as crystalline in the text and thus the information is not evaluated further here.
Crustaceans					
S.-W. Lee et al. (2009)	SiO_2 from Sigma Corp. St. Louis MO, USA. Primary particles of 7nm (fumed) and BET surface area of 644.44 m^2/g and 10nm (porous type) and BET surface area of 349.71 m^2/g	*Daphnia Magna and Chironomus riparius*	OECD Guideline 202 211	1 mg/L	*D. magna* and the larva of *C. riparius* were exposed to nanosilicas, one precipitated (primary particle size 10nm) and one pyrogenic silica (primary particle size 7nm) (Lee, 2008). No genotoxic effects, measured as DNA strand breaks by the comet assay, were observed on these two species. Exposure to SiO_2 had no genotoxic effect on either species. SiO_2 did not seem to affect DNA integrity whereas the mortality of the SiO_2 exposed *D. Magna* and *C. riparius* increased. mortality *D. magna* *C. riparius* 7 nm : 10% ± 8% 5% ± 4 10 nm : 15% ± 4% 20% ± 0 Control 5% ± 4.08 0
M. Casado	SiO_2 from Kisker Biotech	*Daphnia*	OECD	0.1 to 1000 µg/mL	Plain and fluorescently labelled silica NPs showed no significant toxicity in any of the

et al. (2013)	GmbH (amorphous) Amorphous and mono-disperse silica nanoparticles of 50 nm and 100 nm. Plain silica NPs and green fluorescently labelled silica NPs were tested	*Magna and* *Thamnocephalus platyurus*	Guideline 202 Kit from SDI Europe	0.1 to 1000 µg/mL	acute ecotoxicity tests performed on the different organisms for both diameters. Such a response may be expected as amorphous silica NPs are known for their low toxicity (Barnes et al. 2008; Rabolli et al. 2010), indicating their suitability as a good negative control for NP exposure. In the case of the cytotoxicity testing, both assays indicate a low dose and exposure time dependent response a slightly larger effect being observed for the 50 nm than the 100 nm silica NPs in both assays.
J.Mankiewicz-Boczek et al. (2009)	Ludox® SiO_2 CL-X nanoparticles (21 nm)	*Thamnocephalus Platyurus* *Heterocypris Incongruens*	Thamnotoxkit F™ Ostracodtoxkit F test.	50 to 1000 mg/L 300 to 1000 mg/L	Silica LUDOX® CL-X was not toxic to the tested crustaceans at the maximum concentration tested (1,000 mg/l).
Algae					
K. Fujiwara et al. (2008)	Silica nano-particles of 5, 26 and 78 nm from Shokubai Kasei Industrial Co.	*Chlorella kessleri*			No characterization data of the SiO_2 are provided. The conclusions state ".. . Other amorphous nano-silica should be inspected with regard to bio-toxicity. …" which indicate that the silica nanoparticles investigated are amorphous. The investigated silica nanoparticles show size dependent toxicity ("appearance of some amorphous structures on the cell, obstruction of cell division, and faint of chlorophyll colour").
K. van Hoecke et al. (2008)	Ludox® LS and TM 40 silica nanoparticles (12.5 nm and 27 nm) The specific surface areas of the particles are 236 and 135 m^2/g SiO2 for LUDOX LS and TM40, respectively. The particles in LUDOX are monodispersed, discrete uniform spheres of silica that have no internal surface area or detectable crystallinity.	*Pseudokirchneriella subcapitata*	OECD Guideline 201	2.2 to 460 mg/L.	Electron microscopy images of exposed algae cells did not provide evidence for the internalization of nanoparticles in the algal cells. No significant changes in shape or cell morphology were noted. However, considerable adsorption of the NPs to the outer surface of the cells was observed. When the results of the algal growth–inhibition test using Na2SiO3·5H2O were compared to the concentrations of reactive silica in the nanoparticle suspensions, it could be concluded that reactive silica (4.14 mg/L SiO_2) could not be responsible for the observed toxic effects of the LUDOX suspensions. Hence, it is clear the observed adverse effects to *P. subcapitata* were due to the SiO_2 nanoparticles. On a mass basis, the smaller particles were more toxic, although the difference in toxicity disappeared when concentration was expressed as a surface area. These conclusions support the importance of the total surface area for the toxicity of SiO_2 nanoparticles. The paper does not discuss possible effects from the dispersant and any antimicrobial agents in the colloid.

K. van Hoecke et al. (2011)	Ludox® SiO_2 CL-X nanoparticles (22 nm) specific surface area 102 m^2/g	*Pseudokirchneriella subcapitata*	OECD Guideline 201	4.6 to 1000 mg/l	*P. subcapitata* (green algae) was exposed to silica, Ludox®, which is a colloid amorphous silica. SiO_2 NPs were not toxic at pH 6.0 up to a conc. of 220 mg/l. Chlorophyll analysis of algae exposed to the SiO_2 NPs indicated a much more severe effect on algal growth rate compared to the cell count based data. In fact, at the highest test concentration, the algal cells almost completely lacked chlorophyll. It turned out that nanoparticles toxicity can be strongly pH dependent (from pH 6.8). These results suggest that breakdown of chlorophyll and/or chlorophyll synthesis inhibition was an important aspect of the mechanistic toxic response induced by the SiO_2 NPs. In fact, at the highest test concentration, the algal cells almost completely lacked chlorophyll. The paper does not discuss possible effects from the dispersant and any antimicrobial agents in the colloid.
C. Wei et al. (2010)	Silica nanoparticles from Sigma Aldrich (10-20 nm) with a purity of 99.5 %	*Scenedesmus obliquus*		25 to 200 mg/L.	*S. obliquus* was exposed to nanosilica particles from Sigma Aldrich and bulk silica from Shanghai Chemical Reagent Company of China. SEM micrographs of both silicas are provided, but no further characterisation; the SEM micrograph of bulk SiO_2 shows a very angular structure which could be crystalline – this is not discussed in the paper. The algal growth rate decreased as a function of the following exposure concentration (50, 100, and 200 mg/L) and time (48, 72, and 96 h). These results indicate that there is some degree of toxicity to S. obliquus when exposed to SiO_2 NPs in the aquatic environment but the inhibition rate of the highest concentration groups did not reach 50%. The algal cells did not change morphologically when observed under the optical microscope, which was consistent with the phenomenon observed by Van Hoecke et al. (2008)
M. Casado et al. (2013)	SiO_2 from Kisker Biotech GmbH (amorphous) Amorphous and Monodisperse silica nanoparticles of 50 nm and 100 nm. Plain silica NPs and green fluorescently labelled silica NPs were tested	*Pseudokirchneriella subcapitata*	OECD Guideline 201	100 µg/mL	For both diameters plain and fluorescently labelled silica NPs induced no significant toxicity in any of the acute ecotoxicity tests performed on the different organisms.
J. Ji et al. (2011)	SIO_2 from Zhejiang Hongsheng Material Technology Co. 4 types of nanoparticles were tested:	*Chlorella sp.*		0.5 to 1000 mg/L.	No significant toxicity was observed for nano-SiO_2 with concentration up to 1000 mg/L during the 6 days except that SS1 and SP1 inhibited the algal growth by ca. 20% ($p < 0.05$) at the 2nd day.

	- SS1 (20-50 nm) spherical with a specific surface area 102 m^2/g - DS1 (20-50 nm) spherical with a specific surface area 221 m^2/g - SP1 (20-50 nm) spherical with a specific surface area 570 m^2/g - DP1 (20-50 nm) spherical with a specific surface area 675 m^2/g				
D. M. Metzler et al. (2012)	4 types of nanoparticles from Degussa Corp: were tested: (produced by continuous flame hydrolysis) Aerosil 90 (35.6 nm) l with a specific surface area 76.5 m^2/g Aerosil 130 (26 nm) with a specific surface area 105.1 m^2/g Aerosil 200 (14.3 nm) with a specific surface area 190.6 m^2/g Aerosil 300 (9.6 nm) with a specific surface area 248.8 m^2/g	*Pseudokirchneriella subcapitata*		100 and 1000 mg/L.	Van Hoecke et al. found that SiO_2 at particle size of 12.5 and 27.0 nm had a 72 h specific growth rate EC_{20} of 20.0 ± 5.0 and 28.8 ± 3.2mg/L, respectively Of the NP concentrations used in the Van Hoecke et al. study, the highest concentration of dissolved Si was 4.1 mg/ L at pH 7.5. The measured dissolved Si at EC_{20} in the present study was 234 mg/L, which was adequate to affect the growth of algae. Therefore, dissolved Si was not considered a major actor in SiO_2 toxicity. The difference in EC values between this work and that of Van Hoecke et al. could be due to different initial algal densities. In this study, the initial cell density was 106 and Van Hoecke et al. used 105 cell/mL. SiO2 did not play a major role in the growth of P. subcapitata over the concentration range tested in our work, which agreed with Ji et al. who reported little effect on Chlorella sp. Growth at SiO_2 concentration of 1000 mg/L in the size range of 20–50 nm. SiO_2 caused an increase in lipid peroxidation. An increase in SiO2 caused an increased average normalized specific lipid peroxidation,. Although not considered a photocatalyst, SiO2 has been observed to produce similar photosensitive effects, including increased ROS levels and reduced glutathione levels, as a photocatalyst. SiO2 affected the chlorophyll content of the algal cells. Low NP concentration increased the concentration of chlorophyll, whereas high NP concentration decreased it. Results showed that limited light availability can affect the chlorophyll content in algae. The reduction in light availability would encourage the algae to produce more chlorophyll per cell. At low concentrations the algae will attempt to overcome the decreased light availability.
N. Oya San	Silica Nanoparticles produced	*Chlorella*			Silica NPs produced by laser ablation increased the growth of C. vulgaris. In the

et al. (2014)	by laser ablation (38–190 nm)	*vulgaris.*			article data on the concentration tested are missing as are graphs for the concentration-effect curves, no TEM pictures are available for showing if morphology is affected and if the nanoparticles were internalised in the cells.
Effects on sediment species (short/ long term)					
L. Canesi et al. (2010)	Nano-SiO_2 Aerosil 200 (12 nm) with a specific surface area 205 m^2/g from Degussa Evonik.	*Mytilus galloprovincialis*		0.05 to 5 mg/mL	Characterisation data provided. No mortality was observed in any condition of exposure. The nanoparticle did not induce lysosomal membrane destabilisation. Lysosomal lipofuscin and catalase activity were increased; whereas GST (glutathione-S-transferase) activity was not. The digestive gland appears to be the main target for nanoparticle toxicity.
L. Canesi et al. (2010)	Nano-SiO_2 Aerosil200 (12 nm) with a specific surface area 205 m^2/g from Degussa Evonik.	Mytilus hemocytes	In vitro	1, 5 and 10 µg/mL	Characterisation data provided. Test concentrations of 1, 5 and 10 µg/mL did not induce significant cytotoxicity, but stimulated lysozyme release, oxidative burst and NO production.
Effects on soil species (short/ long term)					
A. Pluskota et al. (2009)	Amorphous silica nano-particles 50nm from Kisker, Germany (both labelled and unlabelled) Amorphous bulk silica particles 500 nm from Kisker, Germany	*caenorhabditis elegans*		Concentrations of 0.25mg/ml – 7.1 µg/cm^2 0.5mg/ml – 14.2 µg/cm^2 2.5mg/ml – 71 µg/cm^2 5 mg/ml– 142 µg/cm^2 in aqueous suspension. 50 µl applied to bacterial lawn.	Fluorescently labelled nanoparticles are efficiently taken up by *caenorhabditis elegans* during feeding, and translocate to primary organs such as epithelial cells of the intestine, as well as secondary organs belonging to the reproductive tract. The life span of nanoparticle-fed worms remained unchanged whereas a reduction of progeny production was observed in silica nanoparticle exposed worms versus untreated controls. It is suggested that silica-nanoparticles induce an age-related degeneration of reproductive organs.
Effects on terrestrial species (short/ long term)					
Y. Liang et al. (2007)	silicon	higher plants Review			It is suggested that Si should be considered an essential element for higher plants. Silicon is known to effectively mitigate various abiotic stresses such as manganese, aluminium and heavy metal toxicity and salinity, drought, chilling and freezing stress. The review is about the mechanisms of this alleviation. The publication did not look into uptake of nano-silica.
H.A. Currie and C.C. Perry (2007)	Silica	plants Review			Currie et al. (2007) observed that plants take up silicic acid, and that the ".. presence of Si in plants has been found to alleviate many abiotic and biotic stresses, leading to the incorporation of silicates into many fertilizers…". The publication did not look into uptake of nano-silica.
M. H.	Nano-SiO_2 Aerosil 200 (12	Tomato		2-10 g/L	The present experiment was conducted to test the beneficial effects of nanosilicon

Siddiqui et al. (2014)	nm) with a specific surface area 200 m^2/g from Degussa Evonik.	(*Lycopersicum esculentum* Mill. cv Super Strain B)			dioxide ($nSiO_2$: size 12 nm) on the seed germination of tomato (Lycopersicum esculentum Mill. cv Super Strain B). Application of $nSiO_2$ significantly enhanced the characteristics of seed germination. It improved percent seed germination, mean germination time, seed germination index, seed vigour index, seedling fresh weight and dry weight. Therefore, it is very clear that $nSiO_2$ has a positive significant impact on the seed germination potential.
V. Shah et al.(2009)	3-aminopropyl functionalized silica nanoparticles from Sigma Aldrich chemical Co.	Lettuce seeds		0.013% and 0.066% (w/w)	Results show a statistically insignificant influence of the nanoparticles in the soil on the number of colony forming units, peak areas of methyl ester of fatty acids in the FAME profile or on the total soil community metabolic fingerprint ($P>0.05$). The nanoparticles tested in the study influenced the growth of lettuce seeds as measured through shoot/root ratios of the germinated plant ($P<0.05$).
M. Kalteh et al. (2014)	The particles were produced from rough rice. One gram of silicium particles with 7 nm diameter has absorption surface equal to 400 m^2	Basil (*ocimum basilicum*)		10 ml silica nanoparticles was dissolved in 1 L of distilled water and sprayed on plants.	Silica nanoparticles were found to reduce the pollution effects on Basil originating from salinity.
Effect on micro-organisms					
L.K. Adams et al. (2006)	nanoscale SiO_2 14 nm, 930 nm and 60 µm particles from Sigma Aldrich	*B. subtilis* *E. coli*			Publication unclear on the identity of the tested SiO_2 (characterization data missing, production method missing, no information on whether crystalline or amorphous, literature references to both crystalline and amorphous SiO_2). Although this article stated that the effects of particles could not be effectively measured in this study, it also noted a toxicity displayed by nanosized SiO_2 toward *B. subtilis*. The information was deemed of no further use for the report.
W. Jiang et al. (2009)	Ludox Cl, 20nm from Sigma Aldrich and micro-sized particles from Fisher Scientific Co.	*B. subtilis* *E. coli* *P. fluorescens*			Nano-SiO_2 showed highly significant ($p<0.01$) toxicity towards all three bacteria. The possible effects from antimicrobial agent(s) in the colloid are not discussed. Microsized particle SiO_2 showed no toxicity towards the three bacteria types.
C. Garcia-Saucedo et al. (2011)	SiO_2 nanoparticles 10- 20 nm from American Elements	*Saccharomyces cerevisiae*			Garcia-Saucedo et al. (2011) exposed the yeast *S. cerevisae* to silica nanoparticles. They conclude "Taken as a whole the results of this study demonstrate that nano-sized oxides evaluated … SiO_2, … are not expected to be toxic to *S. cerevisiae* cells at environmentally relevant concentrations."
Other information/background information					
K. Yang et al. (2009)	Nanosized Inorganic Oxides	Humic Acid			The interaction of humic acid with nanosized inorganic oxides, including SiO_2, was investigated (Yang et al., 2008). The SiO_2 is described as S or P form and it is not

					clear whether it is crystalline or not as the characterisation data are limited. According to the results, humic acid does not adsorb to SiO_2.
L. Reijnders (2009)	SiO_2 nanoparticles	release from nanocomposites			Noting that nanomaterials may be hazardous and may be released from composites this article review how to make safer composites
M.N. Moore (2006)	nanoparticles	review			This review addresses the potential ecotoxicological risks for the health of the aquatic environment and the effect that may result from exposure of aquatic animals to nanoparticles.
R.D.Handy et al. (2008)	nanoparticles and nanomaterials	review			This article reviews the current status, challenges and future needs for the ecotoxicological studies of nanoparticles, and is not especially addressing SAS nanoparticles. It points out that nanoparticles should be tested in different environments before drawing conclusions. For water environment, nanoparticles should be studied in freshwater and seawater.
B. Nowack and T.D. Bucheli (2007)	nanoparticles	review			These review present effects of nanoparticles (natural and manufacturers) on the environment. Very few studies about SAS nanoparticles were reported.
S.J. Klaine et al. (2008)	Nanomaterials	review			The review deals with NM in the environment (behaviour, fate and bioavailability). Nevertheless, little information about SAS nanoparticles was detailed. A lot of studies are reviewed, especially for carbon based material and titanium dioxide particles.
V. Stone et al. (2010)	Nanomaterials	review			This article gives an overview of the outcomes of an Environmental NanoImpactNet 2008 Workshop (NIN is a European Commission Framework Programme 7 (FP7) funded project that provides a forum for the discussion of current opinions on nanomaterials in relation to human and environmental issues). The focus was on three key questions: 1. What properties should be characterised for nanomaterials used in environmental and ecotoxicology studies? 2. What reference materials should be developed for use in environmental and ecotoxicological studies? 3. Is it possible to group different nanomaterials into categories for consideration in environmental studies? And the article reviews the (partial) answers.
P. Borm et al. (2006)	Nanoscale Particles				This article reviews dissolution, translocation, and disposition, which have been shown to play a key role in the fate and effects of inhaled particles and fibers.
M. Farré et al. (2009)		review:			This review addresses the ecotoxicity and analysis of nanomaterials in the aquatic environment. A lot of NMs are studied but little information about SAS is available.
M. Cassado et al. (2013)	SiO_2 from Kisker Biotech GmbH (amorphous) Amorphous and	*Vibrio Fischeri*	SDI Europe (MIcrot	0.1 to 1000 µg/mL	Plain and fluorescently labelled silica NPs showed no significant toxicity in any of the acute ecotoxicity tests performed on the different organisms for both diameters

	Monodisperse silica nanoparticles of 50 nm and 100 nm. Plain silica NPs and green fluorescently labelled silica NPs were tested		ox test)		

5 MAMMALIAN TOXICITY

Several studies have been identified reporting results of in vivo tests relevant for mammalian toxicology, emphasis given to studying inhalation effects to understand pulmonary toxicity. While the pulmonary toxicity effects of crystalline silica is abundantly described due to the wide occupational exposure and association with severe pulmonary pathologies like silicosis (Hamilton, Jr. *et al.*, 2008; Iyer *et al.*, 1996), the toxicity of SAS particles (micro-sized or nano-sized particles) has not been widely studied (Napierska *et al.*, 2009; Merget *et al.*, 2002b; Cho *et al.*, 2007).

According to current knowledge, the inhalation constitutes a major pathway for SAS to enter into the human body. Regarding epidemiological data on SAS, with the exception of a few case reports with poorly described exposure scenarios, there is no evidence of a fibrogenic effect of SAS to the human lung. As the available information on humans is not sufficient to exclude a fibrogenic effect of SAS in exposed workers, further epidemiological evidence should be obtained (Merget *et al.*, 2002). The digestive absorption of mineral compounds like SAS depends on their solubility and on the ingested amount. Ingested dust is stored in the intestinal mucous membrane. The non-assimilated fraction is eliminated directly in the faeces. The long-term retention is expected to be weak. However studies specific to SAS are lacking. The penetration of SAS in the organism by the dermal route seems also minimal but this point is only rarely discussed in any study.

In vivo animal studies show that SAS induces a strong inflammatory response in the lungs (Arts *et al.*, 2007; Cho *et al.*, 2007), the response being even higher with ultrafine particles of SAS (Kaewamatawong *et al.*, 2005), but the effect is transient and reversible after a 3-month recovery period in rats (Arts *et al.*, 2007) or even earlier in mice (Cho *et al.*, 2007). The recruitment number of leukocytes and neutrophils concentrations in bronchoalveolar lavage (BAL) fluid seems to be somewhat lower, and may decrease faster than for quartz (Ernst *et al.*, 2002; Chen *et al.*, 2004). The transient effect can be attributed to the rapid clearance of amorphous silica from the lungs to other organs (Nemmar *et al.*, 2006). However some studies describe a minor persistent interstitial collagen deposition (Merget *et al.*, 2002) or some remaining histopathological changes ((Arts *et al.*, 2007).

An animal inhalation study using SAS encapsulated TiO_2 has also shown reversible pulmonary inflammation, emphysema and alveolar hyperinflation (Warheit *et al.*, 2006), although these data are not further used as this report focus on pure SAS particles.

Although SAS is regarded as safe and has been approved for use as a food additive (E 551), no studies were identified that provide a thorough characterization of the fate of ingested SAS.

5.1 Toxicokinetics, Metabolism and Distribution

- In vitro studies

No in vitro toxicokinetics data is available for the NM-series.

- In vivo studies

BIAC provided data for toxico-kinetics via the inhalatory route, see Table 11, which contains a summary of NANOhub entries for Toxicokinetics (Inhalation). The data is generated before the WPMN set up its testing programme, and it is stated the the material tested is equivalent to the NM-series. The study in Table 11 performed in Essen compares the results to results obtained when studying Subcutaneous Toxicokinetics, however no detail are given for the Subcutaneous Toxicokinetics study.

Table 12 gives a summary of the NANOhub entries for toxicokinetics (oral route). Some of the data was generated in the Nanogenotox project using the materials in the NM-series; BIAC provided data pre-dating the WPMN testing programme and it is stated the the material tested is equivalent to the NM-series.

Table 13, which summarises the NANOhub entries for toxicokinetics (intravenous route). The data was generated in the Nanogenotox project using the materials in the NM-series.

Table 11. Summary of NANOhub entries for Toxicokinetics (Inhalation)

Material	Test Organism / System	Method	Exposure/ dose	Main findings	Contributor to WPMN Testing Programme	Comment
Substance declared equivalent to **NM-201** (precipitated) No Characterisation provided	Rat (male and female	Inhalation Subchronic Inhalation Toxicity: 90-day Study (OECD 413 guideline)	90 days 35 mg/m^3 Sampling: 1, 13, 29, 39, and 52 weeks post exposure	SILICA DEPOSITION: Silica could be detected in lungs of all exposed rats at the end of the exposure period: In all males, residual amounts were still present after half a year post-exposure, while only one female rat showed Si in the lung at that time. After exposure (one week post-exposure), in 3/10 males and 5/10 females Si was found in the lymph nodes, which slowly declined during recovery.	Data provided by BIAC. Tests performed by TNO Division of Nutrition and Food Research, Zeist (NL) in 1987	Special modifications as compared with standard study: Focus upon lung, respiratory tract, and regional lymph nodes. Post-exposure recovery period up to one year
Substance declared equivalent to **NM-201** (precipitated) No Characterisation provided	Rat (male and female)	Inhalation Subchronic Inhalation Toxicity: 90-day Study (OECD 413 guideline)	90 days 35 mg/m^3 Sampling: 1, 13, 29, 39, and 52 weeks post exposure	SILICA DEPOSITION: Silica could be detected in lungs of all exposed rats at the end of the exposure period: In all males, residual amounts were still present after half a year post-exposure, while only one female rat showed Si in the lung at that time. After exposure (one week post-exposure), in 3/10 males and 5/10 females Si was found in the lymph nodes, which slowly declined during recovery	Data provided by BIAC. Tests performed by TNO Division of Nutrition and Food Research, Zeist (NL) in 1987	Special modifications as compared with standard study: Focus upon lung, respiratory tract, and regional lymph nodes. Post-exposure recovery period up to one year
Substance declared equivalent to **NM-202** (pyrogenic) No Characterisation provided	Rat (female)	Inhalation	6 and 18 weeks and 12 months (Interim kill after 6 and 18 weeks) 5 h/d, 5x/wk initially, but later (time not stated) weekly frequency reduced to 2-3x/wk because suppurative bronchitis and severe inflammation caused losses.	No substantial increase in the SiO_2 deposition in the lung and the mediastinal lymph nodes were observed between exposure of 18 wks and of 12 months. About 90 % of the SiO2 was cleared from the lungs and 50 - 60 % from the mediastinal lymph nodes within 5 months. This corresponds to an approximate half-life time of 7 weeks, based on first-order elimination kinetics. 20 hours after the last exposure 0.25 mg SiO_2 were found in the lungs. After 3 months the SiO_2 content was 0.018 mg SiO_2. In the lymph node 0.018 mg SiO_2 was found after 1 month and 0.008 mg SiO_2 after 3 months.	Data provided by BIAC. Tests performed by Institut für Hygiene und Arbeitsmedizin, Klinikum Essen (DE) in 1969	

			Post exposure (recovery period): 5 months			
Substance declared equivalent to **NM-202** (pyrogenic) No Characterisation provided	Rat (male and female)	Inhalation Subchronic Inhalation Toxicity: 90-day Study (OECD 413 guideline)	90 days 1.3, 5.9 or 31 mg/m^3 (mean analytical values) Recovery period: 1, 13, 29, 39, and 52 weeks	Silica could be detected in lungs only in relatively small amounts one week after the end of the exposure period, on the average 0.2 mg in all animals of the 30-mg groups, in 10 male and 7 female rats of the 6-mg groups, and in 3 animals of each in the 1-mg groups. Only in one untreated male animal, a low level of Si was detected. Only one male exposed to 30 mg/m^3 showed a small amount of silica in the regional lymph node. No significant increased Si levels were observed at any other recovery interval	Data provided by BIAC. Tests performed by TNO Division of Nutrition and Food Research, Zeist (NL) in 1987	Special modifications as compared with standard study: Focus upon lung, respiratory tract, and regional lymph nodes. Post-exposure recovery period up to one year
Substance declared equivalent to **NM- 203** (pyrogenic) No Characterisation provided	Rat (male and female)	Inhalation Subchronic Inhalation Toxicity: 90-day Study (OECD 413 guideline)	90 days 1.3, 5.9 or 31 mg/m^3 (mean analytical values) Recovery period: 1, 13, 29, 39, and 52 weeks	Silica could be detected in lungs only in relatively small amounts one week after the end of the exposure period, on the average 0.2 mg in all animals of the 30-mg groups, in 10 male and 7 female rats of the 6-mg groups, and in 3 animals of each in the 1-mg groups. Only in one untreated male animal, a low level of Si was detected. Only one male exposed to 30 mg/m^3 showed a small amount of silica in the regional lymph node. No significant increased Si levels were observed at any other recovery interval	Data provided by BIAC. Tests performed by TNO Division of Nutrition and Food Research, Zeist (NL) in 1987	Special modifications as compared with standard study: Focus upon lung, respiratory tract, and regional lymph nodes. Post-exposure recovery period up to one year

Table 12. Summary of NANOhub entries for Toxicokinetics (oral route)

Material	**Test Organism / System**	**Method**	**Exposure/ dose**	**Main findings**	**Contributor to WPMN Testing Programme**	**Comment**
NM- 200 (precipitated)	Rat (male and female)	Oral (gavage) Sampled organs: liver, spleen, GI tract (small intestine), mesenteric lymph nodes	20 mg/kg bw/d (male and female) Cumulative dose: 100 mg/kg bw Administration: repeated (on 5 consecutive days, day 1-5) Sampling time: day 6 and day 14	Bioaccumulation negligible or absent of NM200 following repeated oral administration of 20 mg/ml Very low levels in the liver and spleen (< 2 mg/kg organ weight) near the LOQ and LOD	Data provided by Nanogenotox performed by ISS (I) in 2013	

			Blood sampling: day 5 t=30 min, t=60 min, t=2 h, t=4 h, t= 8 h, day 6	indicating a very low absorption from the gastro-intestinal tract.		
Substance declared equivalent to **NM-202** No Characterisation provided	Rat (female)	Oral (gavage)	100 mg/animal (approx. 500 mg/kg) 20 administrations	In 20 rats receiving 20 daily oral doses of 100 mg Silica per animal (about 500 mg/kg bw) each, tissue values apparently were very slightly increased in liver and kidney: in liver 4.2 µg (control value 1.8 µg), in the spleen 5.5 µg (7.2 µg) and in the kidneys 14.2 µg (7.8 µg).	Data provided by BIAC. Tests performed by institut für Hygiene und Arbeits-medizin, Klinikum Essen (DE) in 1969	
NM-203 (pyrogenic)	Rat (male and female)	Oral (gavage) Sampled organs: liver, spleen, GI tract (small intestine), mesenteric lymph nodes	20 mg/kg bw/d (male and female) Cumulative dose: 100 mg/kg bw Administration: repeated (on 5 consecutive days, day 1-5) Sampling time: day 6 and day 14 Blood sampling: day 5 t=30 min, t=60 min, t=2 h, t=4 h, t= 8 h, day 6	Bioaccumulation negligible or absent of NM203 following repeated oral administration of 20 mg/kg Very low levels in the liver and spleen (< 2 mg/kg organ weight) near the LOQ and LOD indicating a very low absorption from the gastro-intestinal tract.	Data provided by Nanogenotox performed by ISS (I) in 2013	

Table 13. Summary of NANOhub entries for Toxicokinetics (Intravenous)

Material	**Test Organism / System**	**Method**	**Exposure/ dose**	**Main findings**	**Contributor to WPMN Testing Programme**	**Comment**
NM-200 (precipitated)	Rat (male and female)	Intravenous Tissues sampled: liver, spleen, kidneys, heart, lungs, brain, testes/ovaries,	Single (day 1) or repeated (on 5 consecutive days) 20 mg/kg bw/d (male and female) Cumulative dose: 100 mg/kg bw Administration: Single (day 1) or repeated (on 5 consecutive days, day 1-5) Sampling time:	Bioaccumulation of Si in liver >spleen, lungs at day 2 and 6 which decreases at or below the limit of quantification at day 90 following single dose whereas it is still above the control in liver and spleen following repeated administrations Single administration: liver >spleen, lungs Decrease in Si level at or below LOQ in all organs at 90 days	Data provided by Nanogenotox performed by ISS (I) in 2013	

			- Single admin: day 2 and day 90 - Repeated admin: day 6, 14, 30 and 90 (day 6 and 90 for female) Blood sampling: - single and repeated admin (day 1): t=5, t=10, t=20, t=30, t=60 min, t=2 h, t=4h, t=8h, t=24h	Repeated administrations: day 6: liver> spleen and lungs. Si >LOQ in all other organs At day 90, Si still >LOQ in liver and spleen		
NM-203 (pyrogenic)	Rat (male and female)	Intravenous Tissues sampled: liver, spleen, kidneys, heart, lungs, brain, testes/ovaries,	Single (day 1) or repeated (on 5 consecutive days) 20 mg/kg bw/d (male and female) Cumulative dose: 100 mg/kg bw	Single administration: day 6, spleen >liver, lungs and levels of Si above background in heart, kidney, testis day 90 : level of Si still higher than control in spleen and liver Repeated administrations: day 6: concentrations very high liver> spleen and lungs. Si >LOQ in all other organs At day 90, Si still higher than the control in liver and spleen	Data provided by Nanogenotox performed by ISS (I) in 2013	

5.2 Acute toxicity

The tables below, Table 14 and Table 15, summarise the results for acute toxicity; Table 14 gives data for the alternate material supplied by Japan and Table 15 summarises the information from scientific literature of toxic response to a single dose of test material.

Table 16 provides an overview of acute toxicity testing results entered into NANOhub by BIAC. The data concerns the following exposure routes: inhalation, oral and dermal. The data is generated before the WPMN set up its testing programme, and it is stated the the material tested is equivalent to the NM-series.

Table 14. Data supplied by Japan on their alternate material

TEST ITEM	Nanomaterial Information	TEST ORGANISATION	TEST METHOD(S)	TEST RESULTS/ COMMENTS	ANY ISSUES IDENTIFIED
***In Vitro* tests**	Two different Amorphous SiO_2 nanoparticles: **UFP-80** primary particle size: 34 nm purity: >99.5 % from Denki Kagaku Kogyo Kabushiki Kaisha (Japan) http://www.denka.co.jp/eng/denzai/product/25.html **Nanotek** -primary particle size: 25 nm (TEM, average) -amorphous, -spherical shape, -specific surface area (BET): 86.0m^2/g, - purity: 99.9 % - from C. I. Kasei Co. Ltd. (Japan). Physical Vapor Synthesis (PVS) method http://www.cik.co.jp/product/nanotek/english/	Japan/AIST http://www.aist-riss.jp/projects/nedo-nanorisk/rd/iwahashi2009_e.html Contact: t-igarashi@aist.go.jp	Ten different cell lines including A549, HaCaT, and THP-1. Cell viability, oxidative stress, DNA injury, colony forming ability, gene expression of cytokine and apoptosis.	SiO_2 nanoparticles induced oxidative stress in cultured cells. The intracellular ROS level was elevated by SiO_2 exposure. Subsequently, cell viability was decreased. The MTT activity was slightly decreased (50 % of untreated cells) at conc. of approx. 50 µg/ml for 24 h exposure. Activity of apoptosis related enzyme caspase-3 was increased by 24 h exposure.	

Single dose toxicity

A/ *In vivo* Studies

Table 15. Summary of information from scientific literature. (The table does not include a column for "Derived effect value" as none was derived.)

Reference	Material / Size	Test Organism/ System	Method	Exposure/ dose	Main findings
Pulmonary route					
Arts, JHE, et al, 2007	Zeosil 45 Syloid 74 Cal-O-Sil M5	Wistar rats	Inhalation	6 h/day for 5 consecutive days 1, 5 or 25 mg/m^3 Sampling at day 6, 1 month and 3 months following exposure	Transient and reversible elevation of biomarkers of cytotoxicity in BAL fluids, during the 3 months recovery period. Slight histopathological lung changes at the higher exposure levels.
Chen et al. 2004	Unspecified nanosized silica (SAS?) provided by Zhoushan Mingri Nanomaterial Limited Company (Zhejiang, China)	Wistar rats	Inhalation	40 min/day for 4 weeks 24.1 mg/m^3	The fibrogenic effect of nanosized SiO2 might be milder than that of microsized SiO_2 in rats.
Sayes et al. 2007	Zeofree 80	Male Crl :CD(SD) IGS BR Rats	Intratracheal instillation	Single doses: 1 or 5 mg/kg Sampling at 24 h; 1 week; 1 month; 3 months post exposure	Pulmonary instilled SAS produced reversible and transient inflammatory response in rats.
Cho WS, 2007	14 nm SAS particles from Sigma Aldrich	A/J mice	Intratracheal instillation	Single doses: 2, 10 and 50 mg/kg Sampling at 24 h, and 1, 4 and 14 weeks following exposure	Increase in the lung weights, in total BAL cells and in several pro inflammatory mediators during the early stages. No changes were detected after week 1 or 4. Instillation of SAS induced transient, but very severe lung inflammation.
Kaewamatawong et al., 2005	14nm (UF SAS) / 213nm (Fine SAS) (manufacturer's specifications)	ICR mice	Intratracheal instillation	Single dose: 3 mg Sampling 30 min to 24 h post exposure	Ultrafine SAS causes more lung inflammation and tissue damages than Fine SAS Between 30 min and 24 hours post exposure

Kaewamatawong et al., 2006	14nm (Fuso Chemical Co.) Surface specific area 194 m^2/g (manufacturer specifications)	ICR mice (male)	Intratracheal instillation	Single doses: 0.3; 3; 10; 30 and 100 µg Sampling 3 days postexposure	Transient acute moderate lung inflammation and tissue damage. Oxidative stress and apoptosis may underlie the lung tissue injury induction. This study demonstrated the pulmonary biological and pathological responses after intratracheal instillation of low dose of SiO_2 NPs in mice during the acute and subacute stages. Low dose of SiO_2 NP produced moderate inflammation and tissue damage on the lungs of mice during the acute period, but these responses were not sustained through a 30-day period after instillation and almost recovery at the subacute stage. Furthermore, SiO_2 NP can induce oxidative damage and apoptosis, which may be underlying causes of the lung tissue injury. The data from the dose and time responses in this study may be useful in predicting the acute and subacute effects of SiO_2 NP on lungs.
Choi, M et al. 2008	Unspecified 14 nm SAS from Sigma Aldrich	A/J mice	Intratracheal instillation	Single doses: 2; 10; 50 mg/kg Sampling : 24 h, 1, 4 and 14 weeks after exposure	Transient signs of fibrosis
Park E-J et al., 2009	12 nm SAS particles from Degussa	ICR mice	Intratracheal instillation	Single dose	SiO_2 NPs increased the distribution of cytotoxic T cell, NK cell, and NKT cell, and induced subchronic inflammatory response
Other route					
Park E-J et al. 2011	12 nm SAS particles from Degussa	ICR mice	Intraperitoneal injection	Single dose: 50 mg/kg Sampling at 3 days post exposure	ROS and pro-inflammatory responses
Cho MJ et al., 2009	SiNPs from BITERIALS Co. Ltd. Korea	BALB/c mouse	Intravenous	Single dose: 50 mg/kg 12, 24, 48, and 72h, 7 days following injection	Incidence and severity of inflammatory response was transiently increased with injection of 200 and 100 nm SiNPs within 12 h. But there was no significant response related to injection of 50 nm particles. The SiNPs of 50, 100 and 200 nm were cleared via urine and bile. SiNPs were trapped by macrophages in the spleen and liver and remained there until 4 weeks after the single injection.
REVIEW	**Merget, R. et al., 2002: Health hazards due to the inhalation of amorphous silica**				
Gärtner, H, 1952 Klosterkötter, W,	Aerosil R972, Aerosil 200, R 974,	Rabbits, Rats, Guinea Pigs,			It was concluded that “there was no evidence for a fibrogenic effect of intentionally manufactured SAS to the human lung. Animal

1953 Schepers, GWH, Delahant, AB, 1957 Schepers, GWH, Durkan, TM, 1957 Schepers, GWH, Durkan, TM, 1957 Schepers, GWH, 1959 Schepers, GWH, 1962 Klosterkötter, W, 1965 Schepers, GWH, 1981 Groth, DH, 1981 Reuzel, PG, 1991 Lee, KP, 1993 Lewinson, J, 1994 Warheit, D, 1995	Aerosil n.s., Hi-Sil 233, Sipernat 22S, Zeofree 80, Ludox, S.gel and precipitated n.s., fumed n.s., pyrogenic n.s.	Monkeys			studies showed no persistent silicotic nodules even in long term inhalation experiments with high concentrations of SAS that are probably not encountered in workplace. This contrasts with inhalation experiments using crystalline silica which clearly demonstrated such effects. Although some collagen formation has been described in animals exposed to SAS, this is at least partially reversible after discontinuation of exposure. However, some studies described a minor persistent interstitial collagen deposition. Bronchitis, airway obstruction and emphysema were considered by few studies as outcome variables. Such effects in workers exposed to SAS have been described, but the importance of confounders cannot be quantifies sufficiently in these studies. Inflammatory responses and emphysema have been described in a number of animal studies, especially in rats and monkeys. Thus, parameters assessing bronchitis, airway obstruction and emphysema had to be considered in further epidemiological studies as primary outcome variable."

* it was not possible to verify what type of silicon dioxide was used from the information in the article, and consulting the web page of the listed company did not produce any information either.

Table 16. Summary of NANOhub entries for Acute Toxicity

Material	Test Organism / System	Method	Exposure/ dose	Derived effect value (dose descriptor)	Main findings	Contributor	Comment
Inhalation							
Substance declared equivalent to **NM-200** (precipitated) No Characterisation provided	Rat (male and female)	Acute Inhalation Toxicity (OECD Guideline 403)	4 h maximum attainable concentration: 691 mg/m^3 (range: 650 - 725 mg/m3) Nominal concentration: 36.7 g/m^3	LC0 ≥ 0.69 mg/L air (analytical) LD50 ≥ 0.69 mg/L air (analytical)	No clinical symptoms except some restlessness and eye closing. Body weight gain was not affected in males, but females hardly gained weight during two days after exposure, however, subsequently, showed normal development. No findings at autopsy after 14 d post-treatment.	Data provided by BIAC. Tests performed by TNO Division of Nutrition and Food Research, Zeist (NL) in 1983	Air exchange of the inhalation chamber was lower than recommended 0.8/h instead of 10 - 15/h.
Substance declared equivalent to **NM-201** (precipitated) No Characterisation provided	Rat (male and female)	Acute Inhalation Toxicity (OECD Guideline 403)	4 h maximum attainable concentration: 691 mg/m^3 (range: 650 - 725 mg/m3) Nominal concentration: 36.7 g/m^3	LD50 ≥ 0.69 mg/L air(analytical)	No clinical symptoms except some restlessness and eye closing. Body weight gain was not affected in males, but females hardly gained weight during two days after exposure, however, subsequently, showed normal development. No findings at autopsy after 14 d post-treatment.	Data provided by BIAC. Tests performed by TNO Division of Nutrition and Food Research, Zeist (NL) in 1983	Air exchange of the inhalation chamber was lower than recommended 0.8/h instead of 10 - 15/h.
Substance declared equivalent to **NM-202** (pyrogenic) No Characterisation provided	Rat (male and female)	Acute Inhalation Toxicity (OECD Guideline 403)	4 h maximum technically attainable analytical concentration: av. 139 mg/m^3 (range 110 - 190 mg/m^3) Nominal concentration: 16.7 g/m^3	LC0 ≥ 0.14 mg/L air LD50 ≥ 0.14 mg/L air (analytical)	Restlessness, half-closed eyes Slight decrease or stagnation on day 2, but not related to previous exposure (note: By mistake animals were deprived of water for 16 h directly after exposure. No clinical symptoms and no findings at autopsy after 14 d post-treatment.	Data provided by BIAC. Tests performed by TNO Division of Nutrition and Food Research, Zeist (NL) in 1983	Air exchange of the inhalation chamber was lower than recommended 0.8/h instead of 10 - 15/h.

Substance declared equivalent to **NM-202** (pyrogenic) No Characterisation provided	Rat (male and female)	Acute Inhalation Toxicity (OECD Guideline 403)	4 h Analytical concentration: 2.08 mg/L (average of 10 samples with a range from 1.63 to 2.70 mg/L, one outlier with 0.45 mg/L) Nominal concentration: 58.8 mg/L	LC0 ≥ 2.08 mg/L air (analytical) LD50 > 2.08 mg/L air (analytical) LC0 > 58.8 mg/L air (nominal) LD50 > 58.8 mg/L air (nominal)	No animals died. Nasal discharge during exposure, crusty eyes, crusty nose and alopecia at days post-exposure. No macroscopic organ lesions, but in one animal discoloration of the lung.	Data provided by BIAC. Tests performed by Toxigenics Inc., (USA) in 1981	The highest attainable exposure concentration was limited for technical reasons
Substance declared equivalent to **NM-203** (pyrogenic) No Characterisation provided	Rat (male and female)	Acute Inhalation Toxicity (OECD Guideline 403)	maximum technically attainable analytical concentration: av. 139 mg/m^3 (range 110 - 190 mg/m^3) Nominal concentration: 16.7 g/m^3	LC0 ≥ 0.14 mg/L air LD50 ≥ 0.14 mg/L air (analytical	Restlessness, half-closed eyes Slight decrease or stagnation on day 2, but not related to previous exposure (note: By mistake animals were deprived of water for 16 h directly after exposure. No clinical symptoms and no findings at autopsy after 14 d post-treatment.	Data provided by BIAC. Tests performed by TNO Division of Nutrition and Food Research, Zeist (NL) in 1983	
Substance declared equivalent to **NM-203** (pyrogenic) No Characterisation provided	Rat (male and female)	Acute Inhalation Toxicity (OECD Guideline 403)	4 h Analytical concentration: 2.08 mg/L Nominal concentration: 58.8 mg/L	LC0 ≥ 2.08 mg/L air (analytical) LD50 > 2.08 mg/L air (analytical) LC0 > 58.8 mg/L air (nominal) LD50 > 58.8 mg/L air (nominal)l	No animals died. Nasal discharge during exposure, crusty eyes, crusty nose and alopecia at days post-exposure. No macroscopic organ lesions, but in one animal discoloration of the lung.	Data provided by BIAC. Tests performed by Toxigenics Inc., (USA) in 1981	The highest attainable exposure concentration was limited for technical reasons
Oral							
Substance declared equivalent to **NM-200** (precipitated) No Characterisation provided	Rat (male and female)	Acute Oral Toxicity (OECD Guideline 401)	Oral (gavage) 1000, 2500, and 5000 mg/kg bw (pre-study); 5000 mg/kg bw (main study)	LD50 > 5000 mg/kg bw/	No signs of toxicity	Data provided by BIAC. Tests performed by IFT (F) in 1986	
Substance declared equivalent to **NM-200**	Rat (male and	Acute Oral Toxicity (OECD	Oral (gavage)	LD50 > 5000 mg/kg bw/	No signs of toxicity	Data provided by BIAC. Tests	

(precipitated) No Characterisation provided	female)	Guideline 401)	2000 and 5000 mg/kg bw			performed by Laboratorium für Pharmakologie und Toxikologie (LPT) (GER) in 1977	
Substance declared equivalent to **NM-201** (precipitated) No Characterisation provided	Rat (male and female)	Acute Oral Toxicity (OECD Guideline 401)	Oral (gavage) 1000, 2500, and 5000 mg/kg bw (pre-study); 5000 mg/kg bw (main study)	LD50 > 5000 mg/kg bw	No signs of toxicity	Data provided by BIAC. Tests performed by IFT (F) in 1986	
Substance declared equivalent to **NM -201** (precipitated) No Characterisation provided	Rat (male and female)	Acute Oral Toxicity (OECD Guideline 401)	Oral (gavage) 2000 and 5000 mg/kg bw	LD50 > 5000 mg/kg bw	No signs of toxicity	Data provided by BIAC. Tests performed by Laboratorium für Pharmakologie und Toxikologie (LPT) (GER) in 1977	
Substance declared equivalent to **NM-202** (pyrogenic) No Characterisation provided	Rat (male and female)	Acute Oral Toxicity (OECD Guideline 401)	Oral (gavage) 2000 and 3300 mg/kg bw.	LD50 > 3300 mg/kg bw	No signs of toxicity Body weight slight reduction of 4 - 8 %, measured at days 1, 2, and 14 Feed consumption reduced in the 2000 mg group (10 , 4, 6 % at day 1,2 and 14)	Data provided by BIAC. Tests performed by Laboratorium für Pharmakologie und Toxikologie (LPT) (GER) in 1977	
Substance declared equivalent to **NM-202** (pyrogenic) No Characterisation provided	Mouse (male)	Acute Oral Toxicity (OECD Guideline 401)	Oral (gavage) 178, 316, 562, 1000, 1780 and 3160 mg/kg The test substance was given by gavage at variable volumes, at maximum 10 ml/kg.	LD50 > 3160 mg/kg bw	No adverse signs of toxicity in any animal during the study, no macroscopic lesions upon necropsy after 14-d observation.	Data provided by BIAC. Tests performed by Hazelton Laboratories, (USA) in 1964	
Substance declared	Rat (male	Acute Oral	Oral (gavage)	LD50 > 3300 mg/kg	slight reduction of body weight of	Data provided by	

equivalent to **NM-203** (pyrogenic) No Characterisation provided	and female)	Toxicity (OECD Guideline 401)	2000 and 3300 mg/kg bw.	bw	4 - 8 %, measured at days 1, 2, and 14 Feed consumption reduced in the 2000 mg group (10, 4, 6 % at day 1,2 and 14)	BIAC. Tests performed by Laboratorium für Pharmakologie und Toxikologie (LPT) (GER) in 1977	
Substance declared equivalent to **NM-203** (pyrogenic) No Characterisation provided	Mouse (male)	Acute Oral Toxicity (OECD Guideline 401)	Oral (gavage) 178, 316, 562, 1000, 1780 and 3160 mg/kg The test substance was given by gavage at variable volumes, at maximum 10 ml/kg.	LD50 > 3160 mg/kg bw	No adverse signs of toxicity in any animal during the study, no macroscopic lesions upon necropsy after 14-d observation	Data provided by BIAC. Tests performed by Hazelton Laboratories, (USA) in 1964	
Substance declared equivalent to **NM-204** (precipitated) No Characterisation provided	Rat (male and female)	Acute Oral Toxicity (OECD Guideline 401)	Oral (gavage) Single administration 5110 mg/kg bw 237 mg/mL	LD50 > 5000 mg/kg bw	No signs of toxicity	Data provided by BIAC. Tests performed by ASTA Pharma AG in 1990	
Substance declared equivalent to **NM-204** (precipitated) No Characterisation provided	Rat (male and female)	Acute Oral Toxicity (OECD Guideline 401)	Oral (gavage) 10000, 12600, 15800, and 20000 mg/kg	LC0 > 2000 mg/kg bw	no clinical symptoms; after 1 day the stools were white coloured (reversible after 2 days)	Data provided by BIAC. Tests performed by Huntingdon Research Center (HRC) in 1978	

Dermal							
Substance declared equivalent to **NM-204** (precipitated) No Characterisation provided	Rabbit	Standard acute method under occlusive conditions	24 h 2000, 3000, 4000, and 5000 mg/kg	LD50 > 5000 mg/kg bw	Local effect: very slight erythema (score 1 of 4), reversible after 2 days or 5 d in one or a few animals. No systemic signs of toxicity or organ toxicity.	Data provided by BIAC. Tests performed by Huntingdon Research Center (HRC) in 1978	

5.3 Irritation

Table 17 lists the nanohub entries for skin and eys irritation studies. The data is generated before the WPMN set up its testing programme, and it is stated the the material tested is equivalent to the NM-series.

Table 17. Summary of NANOhub entries for Skin and Eye Irritation.

Material	Test Organism / System	Method	Exposure/ dose	Main findings	Contributor
Skin irritation					
Substance declared equivalent to **NM-200** (precipitated) No Characterisation provided	Rabbit	National standard protocol (No. IPC/05-92) corresponding to US EPA	24 h 190 mg/0.5 mL Observation period: 3 days intact and abraded skin	Slight erythemas were seen in 4/6 animals 0.5 h after 24 h exposure. No signs of irritation after 72 h.	Data provided by BIAC. Tests performed by Hazelton (F) in 1992
Substance declared equivalent to **NM-200** (precipitated) No Characterisation provided	Rabbit	Acute Dermal Irritation / Corrosion (OECD Guideline 404) Patch-Test; Hazardous Substances, Part 191, Section 11, FDA, Washington, 1965	24 h 0.5 g Observation period: 14 days 6 (intact skin) 6 (abraded skin)	No signs of irritation	Data provided by BIAC. Tests performed by Laboratorium für Pharmakologie und Toxikologie LPT (GER) in 1978
Substance declared equivalent to **NM-201** (precipitated) No Characterisation provided	Rabbit	Acute Dermal Irritation / Corrosion (OECD Guideline 404) Patch-Test; Hazardous Substances,	24 h 0.5 g Observation period: 14 days	No signs of irritation	Data provided by BIAC. Tests performed by Laboratorium für

		Part 191, Section 11, FDA, Washington, 1965	6 (intact skin) 6 (abraded skin)		Pharmakologie und Toxikologie LPT (GER) in 1978
Substance declared equivalent to **NM-202** (pyrogenic) No Characterisation provided	Rabbit	Acute Dermal Irritation / Corrosion (OECD Guideline 404) Patch-Test; Hazardous Substances, Part 191, Section 11, FDA, Washington, 1965	24 h 0.5 g Observation period: 14 days 6 (intact skin) 6 (abraded skin	No signs of irritation	Data provided by BIAC. Tests performed by Laboratorium für Pharmakologie und Toxikologie LPT (GER) in 1978
Substance declared equivalent to **NM-203** (pyrogenic) No Characterisation provided	Rabbit	Acute Dermal Irritation / Corrosion (OECD Guideline 404) Patch-Test; Hazardous Substances, Part 191, Section 11, FDA, Washington, 1965	24 h 0.5 g Observation period: 14 days 6 (Observation period: 3 days)	No signs of irritation	Data provided by BIAC. Tests performed by Laboratorium für Pharmakologie und Toxikologie LPT (GER) in 1978
Substance declared equivalent to **NM-204** (precipitated) No Characterisation provided	Rabbit	Acute Dermal Irritation / Corrosion (OECD Guideline 404)	24 h 0.5 g Observation period: 14 days	The single application (4 hours, occlusive patch) of 0.5 g test substance to the intact skin of three rabbits each caused no changes. During the observation period neither erythema nor endema could be detected. The irritation index is 0.0. The test substance therefore is classified as non-irritant in this test system	Data provided by BIAC. Tests performed by ASTA Pharma AG in 1991
Substance declared equivalent to **NM-204** (precipitated) No Characterisation provided	Rabbit	National standard protocol (No. IPC/05-92) corresponding to US EPA	24 h 190 mg Observation period: 3 days intact and abraded skin	Slight erythemas were seen in 4/6 animals 0.5 h after 24 h exposure. No signs of irritation after 72 h.	Data provided by BIAC. Tests performed by Hazelton (F) in 1992
Eye irritation					
Substance declared equivalent to **NM-200** (precipitated) No Characterisation provided	Rabbit	Draize-Test; Hazardous Substances, FDA	4 h 100 mg Observation period: 96 h	No irritating response at any time after exposure (24 - 96 h).	Data provided by BIAC Tests performed by Laboratorium für Pharmakologie und Toxikologie LPT (GER) in 1978

Substance declared equivalent to **NM-201** (precipitated) No Characterisation provided	Rabbit	Draize-Test; Hazardous Substances, FDA	24 h 100 mg Observation period: 96 h	No irritating response at any time after exposure (24 - 96 h)	Data provided by BIAC. Tests performed by Laboratorium für Pharmakologie und Toxikologie LPT (GER) in 1978
Substance declared equivalent to **NM-202** (pyrogenic) No Characterisation provided	Rabbit	Draize-Test; Hazardous Substances, FDA	24 h 100 mg Observation period: 96 h	No irritating response at any time after exposure (24 - 96 h	Data provided by BIAC. Tests performed by Laboratorium für Pharmakologie und Toxikologie LPT (GER) in 1978
Substance declared equivalent to **NM-203** (pyrogenic) No Characterisation provided	Rabbit	Draize-Test; Hazardous Substances, FDA	24 h 100 mg Observation period: 96 h	No irritating response at any time after exposure (24 - 96 h)	Data provided by BIAC. Tests performed by Laboratorium für Pharmakologie und Toxikologie LPT (GER) in 1978
Substance declared equivalent to **NM-204** (precipitated) No Characterisation provided	Rabbit	Acute Eye Irritation / Corrosion (OECD Guideline 405)	24 h 100 mg Observation period: 7 days	There were weakly irritating effects on the conjunctivae only: redness score 2 (of 4) in all animals after 1 h, score 2 and 1 after 24 h and reversible by 72 h. Chemosis and discharge was very slight only 1 h after application (score 1).	Data provided by BIAC. Tests performed by ASTA Pharma AG in 1991

5.4 Sensitisation

The OECD WPMN did not list this end-point for investigation and thus no testing under the WPMN was undertaken.

5.5 Repeated dose toxicity

The tables below summarises the available information. Table 18 summarises the information from scientific literature available for repeated dose toxicity; the exposure is Intratracheal instillation (1 study) and oral exposure (1 study).

Table 19 summarises the data for short term (repeated) dose toxicity for the following exposure routes: Oral) , IV route and Intratracheal instillation (For these three routes the data is from Nanogenotox and the test material from the NM-series). Furthermore, Inhalation exposure data was provided by BIAC and the data is generated before the WPMN set up its testing programme, and it is stated the the material tested is equivalent to the NM-series.

Results from sub-acute toxicity studies are reported in Table 20 (oral gavage exposure) and from sub-chronic toxicity studies in Table 21 (inhalation exposure) where the data is provided by BIAC and the data is generated before the WPMN set up its testing programme, and it is stated the the material tested is equivalent to the NM-series.

Outcomes for chronic toxicity study (inhalation route) are reported in Table 22, the data is generated before the WPMN set up its testing programme, and it is stated the the material tested is equivalent to the NM-series.

Table 18. Repeated dose toxicity. Summary of information from scientific literature.

Reference	Material/ Size	Test Organism / System	Method	Exposure/ dose	Main findings
Ernst et al. 2002	Aerosil 150 (fumed SiO_2) particles 14 nm surface specific area 300 m^2/g	Wistar WU female rats	Intratracheal instillation	2 groups: 20 and 30 instillations at intervals of 2 weeks 0.5 mg	After repeated Intratracheal instillation exposure, elevation of biomarkers of cytotoxicity in BAL fluids were observed, but it did not affect the ability of the lung cells to respond to LPS (>< quartz and carbon black). This can be attributed to the rapid elimination of amorphous SiO_2 from lungs that was detected in a separate experiment mentioned in the article. Following intratracheal instillation, about 85% of the SAS was removed within 2 days, followed by a half-time of 11 days. It was concluded for the carcinogenicity study that chronic inflammation without persistent dust particles could be induced by 20 instillations at intervals of two weeks with low single doses of 0.5 mg. Intratracheal instillation of SiO_2 produced marked inflammatory lesions in the lungs of all treatment groups. The inflammation caused by amorphous SiO_2 was characterized by a lack of alveolar lipoproteinosis and relatively low numbers of intra-alveolar macrophages. The majority of the macrophages were foamy but not necrotizing. Amorphous SiO_2 also produced a pronounced but very localized interstitial fibrosis (interstitial fibrotic granulomas). These are believed to develop from acute alveolitis observed after a single administration of amorphous SiO_2.
So SJ et al., 2008	Nano- : 30 nm Micro-: 30 µm obtained by rice husk	BALB/c mouse C57BL/6J mouse	Oral route (food)	10 weeks 1 % SiO_2 in diet	Nano-sized Si particles had a toxic effect on the liver even though there was no significant different on the health in total fed amount of 140 g Si/kg mouse.

Table 19. Summary of NANOhub entries for Repeated Dose Toxicity (short-term)

Material	Test Organism / System	Method	Exposure/ dose	Derived effect value (dose descriptor)	Main findings	Contributor	Comment
Oral							
NM-200 (precipitated)	Rat (male and female)	Oral route (on 5 consecutive days, day 1-5)	6.0 mg/ml was prepared in sterile normal saline (NaCl 0.9% w/v). Groups received daily a dose of 20 mg/kg bw. The repeated dose groups received a total cumulative dose of 100 mg/kg bw after 5 days treatment,		Tissue deposition following repeated oral administration to a total dose of 100 mg SAS / kg bw was negligible or absent. Slight differences in gender/material investigated are apparent, though the limited absorption makes it difficult to draw any conclusions. In terms of effects, at sacrifice at day 6, altered organ weight (e.g. liver, lungs, uterus) was observed. Preliminary histopathological examinations; increased ratio between white and red pulp of the spleen and altered vascularisation in NM-200 treated female group.	Data provided by Nanogenotox performed by ISS (I) in 2013	
NM-203 (pyrogenic)	Rat (male and female)	Oral route (on 5 consecutive days, day 1-5)	6.0 mg/ml was prepared in sterile normal saline (NaCl 0.9% w/v). Groups received daily a dose of 20 mg/kg bw. The repeated dose groups received a total cumulative dose of 100 mg/kg bw after 5 days treatment,		Tissue deposition following repeated oral administration to a total dose of 100 mg SAS /kg bw was negligible or absent. Slight differences in gender/material investigated are apparent, though the limited absorption makes it difficult to draw any conclusions. In terms of effects, at sacrifice at day 6, altered organ weight (e.g. liver, lungs, uterus) was observed. Preliminary histopathological examinations showed increased ratio between white and red pulp of the spleen and apoptosis in NM-203 treated male and female groups; increased ratio between white and red pulp of the spleen and altered vascularisation in liver in NM-203 treated female group.	Data provided by Nanogenotox performed by ISS (I) in 2013	
IV route							
NM-200 (precipitated)	Rat (male and female)	IV route (on 5 consecutive days, day 1-5)	6.0 mg/ml was prepared in sterile normal saline (NaCl 0.9% w/v). Groups received daily a dose of 20 mg/kg bw. The repeated dose groups		After repeated dose IV administration, Si peaked in blood at 20 min in females and at 30 min in males. At day 6, Si concentrations were very high in liver, spleen and lungs, with marked particle and gender-related differences, and above the LOQ in other organs as well. At days 14 and 30 considerable amounts of Si were still present in liver,	Data provided by Nanogenotox performed by ISS (I) in 2013	

			received a total cumulative dose of 100 mg/kg bw after 5 days treatment,		spleen and lungs of male rats. In female rats, the highest concentra-tion was present in the liver both at day 6 and day 90. In male rats the highest concentration was in the liver. At day 90 Si concentration in liver and spleen tissues of males and females were still distinctly higher than those in controls. Gross observation at sacrifice at day 90 showed specific effects on liver and spleen. Furthermore after repeated IV exposure, NM-200 treated male animals showed a slight reduction in weight gain compared to control animals.	IT)	
NM-203 (pyrogenic)	Rat (male and female)	IV route (on 5 consecutive days, day 1-5)	6.0 mg/ml was prepared in sterile normal saline (NaCl 0.9% w/v). Groups received daily a dose of 20 mg/kg bw. The repeated dose groups received a total cumulative dose of 100 mg/kg bw after 5 days treatment,		After repeated dose IV administration, Si peaked in blood at 20 min in females and at 30 min in males. At day 6, Si concentrations were very high in liver, spleen and lungs, with marked particle and gender-related differences, and above the LOQ in other organs as well. At days 14 and 30 considerable amounts of Si were still present in liver, spleen and lungs of male rats. In female rats, similar concentrations were observed in liver and spleen both at day 6 and day 90 for NM-203, while for NM-200 the highest concentration was present in the liver both at day 6 and day 90. In male rats NM-203 showed the highest concentration in the spleen, while for NM-200 the highest concentration was in the liver. For NM-203 male rats a much higher distribution was noted compared to female rats at day 6 after the repeated administrations. At day 90 Si concentration in liver and spleen tissues of males and females were still distinctly higher than those in controls for both NM-200 and NM-203, suggesting a longer time required for complete elimination of administered NMs from the body. Following both single and repeated dose administration, gross observation at sacrifice at day 90 showed specific effects on liver and spleen. Furthermore after repeated IV exposure, NM- 200 treated male animals showed a slight reduction in weight gain compared to control animals	Data provided by Nanogenotox performed by ISS (I) in 2013	Only 5 exposure days; histopathology and organotoxicology limited; no clinical chemistry + haematology, but lung lavage cytology + biochemistry instead
Intratracheal instillation							
NM-200 (precipitated)	Rat (male)	Intratracheal instillation	1 administration at 0, 24 and 45 h 1.15; 2.3; 4.6 mg/kg bw/d		Dose-dependent increase in the number of neutrophils in BAL	Data provided by Nanogenotox performed by	

						NRCWE (DK) in 2013	
Inhalation							
Substance declared equivalent to **NM-200** (precipitated) No Characterisation provided	Rat (male and female)	Inhalation Toxicity: Method: in accordance with OECD Guide-line 412, 12 May 1981 and directive 92/69/EEC, 29 Dec. 1992, but focus on the respiratory tract (lung and lymph nodes).	6 h/day for 5 days 1.16 (± 0.36), 5.39 (± 0.58), 25.2 (± 1.5) mg/m^3 Post-exposure period: 1 or 3 months	NOEC (acute/sub-acute) is at 1.16 mg/m3. The NOAEC could be defined as 5.39 mg/m^3	There are slight increases in lung weight of the high dose group, statistically significant absolute weights in male and relative in females and an increase in relative weights of tracheobronchial lymph nodes in females of the high dose group. After 5 days, the absolute numbers of neutrophils increase significantly in the high dose groups of both genders. The relative number of macrophages decreased concomitantly. In the mid dose group, neutrophils slightly increased. After recovery of one month, the cell stimulating effect passed away and were also absent after 3 months recovery for females, but noted in males without changes. Slights trends were also seen in the mid dose group, but only reflected on the relative neutrophil increase. Significant increases in enzymes and proteins were found only at the high dose exposure, which completely reverse after recovery. Hypertrophy and hyperplasia of the bronchiolar epithelium (high dose) were noticed in 1/5 males and in 2/5 females. Because of the very rare occurrence in the rats of that age, this lesion was considered treatment relative. A very slight to slight polymorphonuclear leukocytes infiltration (inflammation response) was noted at all dose levels. The incidence and the severity was not clearly dose-related, 1/5 very slight case at the low dose level in the male and in the female group respectively. This effect was occasionally observed in the recovery group (as well in the recovery control group). In recovery of the high dose group, a tendency of accumulation of alveolar macrophages and hyperemic capillary unusual type II hyperplasia in 1/5 males were noted.	Data provided by BIAC. Tests performed by TNO Division of Nutrition and Food Research, Zeist (NL) in 2003	Only 5 exposure days; histopathology and organotoxicology limited; no clinical chemistry + haematology, but lung lavage cytology + biochemistry instead
Substance declared equivalent to **NM-201** (precipitated)	Rat (male and female)	Inhalation Toxicity: Method: in accordance with OECD Guide-line 412, 12 May 1981	6 h/day for 5 days 1.16 (± 0.36), 5.39 (± 0.58), 25.2 (± 1.5) mg/m^3 Post-exposure	NOEC (acute/sub-acute) is at 1.16 mg/m3. The NOAEC could be defined as	There are slight increases in lung weight of the high dose group, statistically significant absolute weights in males and relative in females and an increase in relative weights of tracheobronchial lymph nodes in females of the high dose group. After 5 days, the absolute numbers of neutrophils increase significantly in the high dose groups of both genders. The relative number of macrophages decreased concomitantly. In the mid dose group, neutrophils slightly increased.	Data provided by BIAC. Tests performed by TNO Division of Nutrition and Food Research, Zeist (NL) in	Only 5 exposure days; histopathology and organotoxicology

No Characterisation provided		and directive 92/69/EEC, 29 Dec. 1992, but focus on the respiratory tract (lung and lymph nodes).	period: 1 or 3 months	5.39 mg/m^3	After recovery of one month, the cell stimulating effect passed away and were also absent after 3 months recovery on females, but noted in males without changes. Slights trends were also seen in the mid dose group, but only reflected on the relative neutrophil increase. Significant increases in enzymes and proteins were found only at the high dose exposure, which completely reverse after recovery. Hypertrophy and hyperplasia of the bronchiolar epithelium (high dose) were noticed in 1/5 males and in 2/5 females. Because of the very rare occurrence in the rats of that age, this lesion was considered treatment relative. A very slight to slight polymorphonuclear leukocytes infiltration (inflammation response) was noted at all dose levels. The incidence and the severity was not clearly dose-related, 1/5 very slight case at the low dose level in the male and in the female group respectively. This effect was occasionally observed in the recovery group (as well in the recovery control group). In recovery of the high dose group, a tendency of accumulation of alveolar macrophages and hyperemic capillary unusual type II hyperplasia in 1/5 males were noted.	2003	limited; no clinical chemistry + haematology, but lung lavage cytology + biochemistry instead
Substance declared equivalent to **NM-202** (pyrogenic) No Characterisation provided	Rat (male and female)	Inhalation Toxicity: Method: in accordance with OECD Guide-line 412, 12 May 1981 and directive 92/69/EEC, 29 Dec. 1992,) but focus on the respiratory tract (lung and lymph nodes) Test substance was examined only in males	6 h/day for 5 days 1.39 (± 0.15), 5.41 (± 0,34), 25.3 (0.9) mg/m^3 Post-exposure period: 1 or 3 months	LOAEC 5.41 mg/m^3 air (analytical) NOEC 1.39 mg/m^3 air (analytical)	Significant mean increases in relative and absolute lung weights of the mid- and high-dose groups. No increases in weight of the tracheobronchial lymph nodes were noticed. Very slight hypertrophy of the bronchiolar epithelium in 3/5 animal (mid-dose) and slight hypertrophy in 4/5 (high dose) were observed. No case occurred in the recovery group. Accumulation of alveolar macrophages by a few granulocytes/neutrophils in 3/5 animal (mid dose) and 5/5 (high dose) were noted. In 3/5 high dose animals, alveolar accumulation of macrophages was accompanied by an infiltration of polymorphonuclear leukocytes. Following recovery of one month, very slight macrophage accumulation was still present in the lungs in 3/5 high-dose animals, but without epithelial changes and leukocytes infiltrations. At that time, lymph nodes also contained aggregates of macrophages (1/5 mid-dose), 5/5 high dose). Following recovery of 3 months, local accumulation of macrophages was still present in the lungs of 2/5 high-dose animals. The lymph nodes of 1/5 mid-dose and 5/5 high dose animals still contained macrophages aggregates. After 5 days, absolute and relative number of neutrophils increased	Data provided by BIAC. Tests performed by TNO Division of Nutrition and Food Research, Zeist (NL) in 2003	Only 5 exposure days; histopathology and organotoxicology limited; no clinical chemistry + haematology, but lung lavage cytology + biochemis

		because they had proven to be more sensitive than females, as observed in the first study.			significantly in both the mid- and the high-dose groups, the relative number of macrophage decreases concomitantly. After 1 month recovery, the cell stimulating effects passed away, there were still slight but statistically significant increase of the percentages of the neutrophils counts with concomitant decrease in relative macrophage units but no longer after 3 months. Significant increases in enzymes, proteins and the TNF –α levels were found at the mid- and high dose exposure.		try instead
Substance declared equivalent to **NM-203** (pyrogenic) No Characterisation provided	Rat (male and female)	Inhalation Toxicity: Method: in accordance with OECD Guide-line 412, 12 May 1981 and directive 92/69/EEC, 29 Dec. 1992,) but focus on the respiratory tract (lung and lymph nodes). Test substance was examined only in males because they had proven to be more sensitive than females, as observed in the first study.	6 h/day for 5 days 1.39 (± 0.15), 5.41 (± 0,34), 25.3 (0.9) mg/m^3 Post-exposure period: 1 or 3 months	LOAEC 5.41 mg/m^3 air (analytical) NOEC 1.39 mg/m^3 air (analytical)	Significant mean increases in relative and absolute lung weights of the mid- and high-dose groups. No increases in weight of the tracheobronchial lymph nodes were noticed. Very slight hypertrophy of the bronchiolar epithelium in 3/5 animal (mid-dose) and slight hypertrophy in 4/5 (high dose) were observed. No case occurred in the recovery group. Accumulation of alveolar macrophages by a few granulocytes/neutrophils in 3/5 animal (mid dose) and 5/5 (high dose) were noted. In 3/5 high dose animals, alveolar accumulation of macrophages was accompanied by an infiltration of polymorphonuclear leukocytes. Following recovery of one month, very slight macrophage accumulation was still present in the lungs in 3/5 high-dose animals, but without epithelial changes and leukocytes infiltrations. At that time, lymph nodes also contained aggregates of macrophages (1/5 mid-dose), 5/5 high dose). Following recovery of 3 months, local accumulation of macrophages was still present in the lungs of 2/5 high-dose animals. The lymph nodes of 1/5 mid-dose and 5/5 high dose animals still contained macrophages aggregates. After 5 days, absolute and relative number of neutrophils increased significantly in both the mid- and the high-dose groups, the relative number of macrophage decreases concomitantly. After 1 month recovery, the cell stimulating effects passed away, there were still slight but statistically significant increase of the percentages of the neutrophils counts with concomitant decrease in relative macrophage units but no longer after 3 months. Significant increases in enzymes, proteins and the TNF –α levels were found at the mid- and high dose exposure.	Data provided by BIAC. Tests performed by TNO Division of Nutrition and Food Research, Zeist (NL) in 2003	Only 5 exposure days; histopathology and organotoxicology limited; no clinical chemistry + haematology, but lung lavage cytology + biochemistry instead
Substance declared	Rat (male and	Inhalation Toxicity:	6 h/day for 5 days	NOEC mean 1.16 mg/m³ air	There are slight increases in lung weight of the high dose group, statistically significant absolute weights in male and relative in females	Data provided by BIAC. Tests	

equivalent to **NM-204** (precipitated) No Characterisation provided	female)	Method: in accordance with OECD Guide-line 412, 12 May 1981 and directive 92/69/EEC, 29 Dec. 1992, but focus on the respiratory tract (lung and lymph nodes).	1.16 (± 0.36), 5.39 (± 0.58), 25.2 (± 1.5) mg/m^3 Post-exposure period: 1 or 3 months	(analytical) (Histopathology: based on the absence of substance-related effects, in particular absence of a pulmonary response (inflammation reaction) NOAEC mean 5.39 mg/m³ air (analytical)(Histopathology: based on the pulmonary response (inflammation reaction)) LOAEC mean 25.2 mg/m³ air (analytical)	and an increase in relative weights of tracheobronchial lymph nodes in females of the high dose group. After 5 days, the absolute numbers of neutrophils increase significantly in the high dose groups of both genders. The relative number of macrophages decreased concomitantly. In the mid dose group, neutrophils slightly increased. After recovery of one month, the cell stimulating effect passed away and were also absent after 3 months recovery for females, but noted in males without changes. Slights trends were also seen in the mid dose group, but only reflected on the relative neutrophil increase. Significant increases in enzymes and proteins were found only at the high dose exposure, which completely reverse after recovery. Hypertrophy and hyperplasia of the bronchiolar epithelium (high dose) were noticed in 1/5 males and in 2/5 females. Because of the very rare occurrence in the rats of that age, this lesion was considered treatment relative. A very slight to slight polymorphonuclear leukocytes infiltration (inflammation response) was noted at all dose levels. The incidence and the severity was not clearly dose-related, 1/5 very slight case at the low dose level in the male and in the female group respectively. This effect was occasionally observed in the recovery group (as well in the recovery control group). In recovery of the high dose group, a tendency of accumulation of alveolar macrophages and hyperemic capillary unusual type II hyperplasia in 1/5 males were noted.	performed by TNO Division of Nutrition and Food Research, Zeist (NL) in 2003	

Table 20. Summary of NANOhub entries for Repeated Dose Toxicity (subacute)

Material	Test Organism / System	Method	Exposure/ dose	Derived effect value (dose descriptor)	Main findings	Contributor	Comment
Substance declared equivalent to **NM-200**	Rat (male)	Oral (gavage) OECD Guideline	1/day for 28 days 100, 300, 1000	NOEL = 1000 mg/kg bw/d (actual dose	No death occurred during the study and no adverse clinical symptoms were observed. No effects on food consumption or body weight were seen. The measurements of the spontaneous locomotor activity and the functional observational battery displayed no influence by the	Data provided by BIAC. Tests performed by Fraunhofer	

(precipitated) No Characterisation provided		407 (Repeated Dose 28-Day Oral Toxicity in Rodents)	mg/kg bw/d Rats were treated daily either with the vehicle (0.5% methylhydroxypropyl cellulose, control groups) or with Synthetic Amorphous Silica suspended in the vehicle for 28 consecutive days.	received)	treatment. Evaluation of haematological and clinical chemistry parameters did not reveal any treatment related effects. Decreases of the partial thromboplastin time (PTT), white blood cell count (WBC) and lymphocyte count (LYMC) as well as cholinesterase (CHE) and glucose (GLUC) in group 3 (mid dose) after 28 d of exposure were considered not treatment-related. Creatinin kinase (CK) and blood urea (UREA) concentration were mildly decreased in group 6 (high dose recovery) after a two week recovery period. During necropsy, no substance-related findings were observed. No effects were seen on organ weights or the organ weight to bodyweight ratio. During histopathological examination, no substance-related findings were observed in the examined organs of males of the control and high dose group. Toxicological analysis of silica ion concentration (non-GLP) in blood, kidney and liver tissue did not reveal differences between the control and the high dose group. This result is most likely due to the naturally occurring high background values of silica. Transmission electron microscopy (non-GLP) found electron dense structures composed of irregular homogenous to fine granular material in the cytoplasm of mesenteric lymph nodes cells, liver cells and kidney cells of all animals from the control and from the high dose group. The granular structures measured only few nanometers. However, these structures did not have the shape or appearance of amorphous material such as amorphous silica.	Institute for Toxicology and Experimental Medicine (ITEM) (GER) in 2011	

Table 21. Summary of NANOhub entries for Repeated Dose Toxicity (subchronic)

Material	Test Organism / System	Method	Exposure/ dose	Derived effect value (dose descriptor)	Main findings	Contributor	Comment
Inhalation							
Substance declared equivalent to	Rat (male and	Subchronic Inhalation Toxicity: 90-	90 days 6 hours/day, 5	no NOAEC identified (Test substance at a	A slight decrease of body weight (- 5 %) by 13 weeks exposure was observed (still at – 4 % after 52 weeks post exposure). No significant effects in haematology were detected but white blood cells count	Data provided by BIAC. Tests performed by TNO	

NM-200 (precipitated) No Characterisation provided	female)	Day (OECD Guideline 413)	days/week 35 mg/m^3 (mean analytical values) Basis analytical conc. 30 mg/m^3 (target concentration	level of 30 mg/m^3 induced generally mild changes, which quickly recovered during the exposure period.)	elevated in both males and females groups at the end of exposure period, but it wasn't clearly attributable to the increase in the number of neutrophilic leukocytes. After 13 weeks recovery, neutrophil count still tended to be higher in males and females, and normalised by 28 weeks of recovery. No changes in heart, thyroids, adrenals, testes, brain, spleen and kidneys weights were observed, but the relative mean of lungs weighs slightly increased (≈ x 1.3). Thymus weight increased as well. Swollen lungs and enlarged mediastinal lymph nodes were noted. The effects gradually subsided after the exposure period. Lung weights were normalised after 13 weeks recovery in males and females. In the lung, accumulation of alveolar macrophage, intra-alveolar polymorphonuclear leukocytes and increased septal cellularity in males and females were noted. Treatment related microscopic changes in the nasal region were found at the end of the exposure, such as very slight local necrosis and slight atrophy of the olfactory epithelium, intracystoplasmic proteinaeceous droplets. Accumulation of macrophages was seen in the mediastinal lymph nodes (disappearing after 39 week post exposure). Collagen content in the lungs slightly increased at the end of the exposure, During the recovery period, all changes disappeared mostly within 13 to 26 weeks post exposure. Silica could be detected in lungs only in relatively small amounts at the end of the exposure periods. On the average 0.5 mg per lung in male animal group, 0.35 mg per lung of female groups, decreasing over time and no longer measurable after 39 weeks post exposure were found.	Division of Nutrition and Food Research, Zeist (NL) in 1987	
Substance declared equivalent to **NM-201** (precipitated) No Characterisation provided	Rat (male and female)	Subchronic Inhalation Toxicity: 90-Day (OECD Guideline 413)	90 days 6 hours/day, 5 days/week 35 mg/m^3 (mean analytical values) Basis analytical conc.	no NOAEC identified (Test substance at a level of 30 mg/m3 induced generally mild changes, which quickly recovered during the	A slight decrease of body weight (- 5 %) by 13 weeks exposure was observed (still at – 4 % after 52 weeks post exposure). No significant effects in haematology were detected but white blood cells count elevated in both males and females groups at the end of exposure period, but it wasn't clearly attributable to the increase in the number of neutrophilic leukocytes. After 13 weeks recovery, neutrophil count still tended to be higher in males and females, and normalised by 28 weeks of recovery. No changes in heart, thyroids, adrenals, testes, brain, spleen and kidneys weights were observed, but the relative mean of lungs weighs slightly	Data provided by BIAC. Tests performed by TNO Division of Nutrition and Food Research, Zeist (NL) in 1987	Special modifications as compared with standard study: Focus upon lung, respiratory tract, and lymph nodes.

			30 mg/m^3 (target concentration	exposure period.)	increased (≈ x 1.3). Thymus weight increased as well. Swollen lungs and enlarged mediastinal lymph nodes were noted. The effects gradually subsided after the exposure period. Lung weights were normalised after 13 weeks recovery in males and females. In the lung, accumulation of alveolar macrophage, intra-alveolar polymorphonuclear leukocytes and increased septal cellularity in males and females were noted. Treatment related microscopic changes in the nasal region were found at the end of the exposure, such as very slight local necrosis and slight atrophy of the olfactory epithelium, intracystoplasmic proteinaeceous droplets. Accumulation of macrophages were seen in the mediastinal lymph nodes (disappeared after 39 week post exposure). Collagen content in the lungs slightly increased at the end of the exposure, During the recovery period, all changes disappeared mostly within 13 to 26 weeks post exposure. Silica could be detected in lungs only in relatively small amounts at the end of the exposure periods. On the average 0.5 mg per lung in male animal group, 0.35 mg per lung of female groups, decreasing over time and no longer measurable after 39 weeks post exposure were found.		Post-exposure recovery period up to one year. One high exposure level only within a combined study
Substance declared equivalent to **NM-202** (pyrogenic) No Characterisation provided	Rat (male and female)	Subchronic Inhalation Toxicity: 90-Day (OECD Guideline 413)	90 days 6 hours/day, 5 days/week 1.3, 5.9 or 31 mg/m^3 (mean analytical values) 1, 6 and 30 mg/m^3 (target concentrations)	NOAEC = 1.3 mg/m³ air (analytical) NOEC < 1.3 mg/m³ air (analytical) LOAEC = 5.9 mg/m³ air (analytical)	The respiration rate was increased (concentration related). No effect in female weights in aldose levels was detected. Depressive effects on males weight were found (1 mg/m^3 slightly at day 14 (- 5 %), 6 mg/m^3 slightly from day 49 to 77 (- 6 to -5 %), 30 mg/m^3 significant throughout exposure (-10 to -7 %)). No difference from control at day 45 observed. No haematology effects were found for 1 mg/m^3 group. For the 6 mg/m^3 group, white blood cell count elevated in males and females due to increase in the number of neutrophilic leukocytes but concentration response relation was poor. After 3 month recovery, these bloods parameters were normalised. For 30 mg/m^3 group, red blood and cellules and haemoglobins were statistically higher in males, but not in females. White blood cells count elevated in males and females due to increase on the number of neutrophilic leukocytes at 3 months of recovery. In females, a slight increase above the control group still existed after 6 month of recovery. Swollen lungs and enlarged mediastinal lymph nodes at the end of	Data provided by BIAC. Tests performed by TNO Division of Nutrition and Food Research, Zeist (NL) in 1987)	Special modifications as compared with standard study: Focus upon lung, respiratory tract, and lymph nodes. Post-exposure recovery period up to one year. One high exposure

					recovery was found (treatment related degrees of severity). No lung weight effect was found for 1 mg/m^3 group, but an increase was observed for the 6 (1.7 x for males and 1.4 x for females)and 30 mg/m^3 (2.3 x for males and 2.0 x for females) groups. For the 6 and 30 mg/m^3 groups, collagen content in the lungs was clearly increased, most pronounced in males. The above mentioned effects gradually subsided after the exposure period. But inn males exposed to6 to 30 mg/m^3, the collagen content was still above control values at the end of the study. Granuloma-like lesions were seen in animals at the end of exposure period and after the 13 weeks of recovery. They did not show fibroblastic activity and hyanilisation and regressed during recovery. Accumulation of macrophages was seen in the mediational lymph nodes (disappeared week 39). Treatment related microscopic changes in the nasal region were occasionally found at the end of exposure period such as focal necrosis and slight atrophy of the olfactory epithelium. Interstitial fibrosis was not noted directly after the exposure period, but appeared with a delay. It was observed for the first time after 13 weeks post exposure, increasing incidence especially for 30 mg/m^3 and less for 6 mg/m^3. It decreased in severity and frequency until the end of the study. All types of pulmonary lesions were more marked in males than in females. The level of 1.3 mg/m^3 induced only slight changes after 13 weeks post exposure which generally recovered quickly. Morphological changes after 13 weeks exposure are considered statistically significant at 1.3 mg/m^3. Silica could be detected in lungs only in relatively small amounts at the end of exposure period. Only one male exposed to 30 mg/m^3 show a small amount of silica in the regional lymph nodes. 90 days after termination of exposure, no silica could be recovered from any animal.		level only within a co mbined stu dy
Substance declared equivalent to **NM-203** (pyrogenic) No Characterisati	Rat (male and female)	Subchronic Inhalation Toxicity: 90-Day (OECD Guideline 413)	90 days 6 hours/day, 5 days/week 1.3, 5.9 or 31 mg/m^3 (mean analytical values)	NOAEC = 1.3 mg/m³ air (analytical) NOEC < 1.3 mg/m³ air (analytical)	The respiration rate was increased (concentration related). No effect in female weights in aldose levels was detected. Depressive effects on males weight were found (1 mg/m^3 slightly at day 14 (- 5 %), 6 mg/m^3 slightly from day 49 to 77 (- 6 to -5 %), 30 mg/m^3 significant throughout exposure (-10 to -7 %)). No difference from control at day 45 observed. No haematology effects were found for 1 mg/m^3 group. For the 6 mg/m^3 group, white blood cell count elevated in males and females	Data provided by BIAC. Tests performed by TNO Division of Nutrition and Food Research, Zeist (NL) in 1987)	Special mo difications as compare d with stand ard study: Focus upon lung, r espiratory tr

on provided			1, 6 and 30 mg/m^3 (target concentrations)	LOAEC = 5.9 mg/m³ air (analytical)	due to increase in the number of neutrophilic leukocytes but concentration response relation was poor. After 3 month recovery, these bloods parameters were normalised. For 30 mg/m^3 group, red blood and cellules and haemoglobins were statistically higher in males, but not in females. White blood cells count elevated in males and females due to increase on the number of neutrophilic leukocytes at 3 months of recovery. In females, a slight increase above the control group still existed after 6 month of recovery. Swollen lungs and enlarged mediastinal lymph nodes at the end of recovery was found (treatment related degrees of severity). No lung weight effect was found for 1 mg/m^3 group, but an increase was observed for the 6 (1.7 x for males and 1.4 x for females)and 30 mg/m^3 (2.3 x for males and 2.0 x for females) groups. For the 6 and 30 mg/m^3 groups, collagen content in the lungs was clearly increased, most pronounced in males. The above mentioned effects gradually subsided after the exposure period. But in males exposed to 6 to 30 mg/m^3, the collagen content was still above control values at the end of the study. Granuloma like lesions were seen in animals at the end of exposure period and after the 13 weeks of recovery. They did not show fibroblastic activity and hyanilisation and regressed during recovery. Accumulation of macrophages was seen in the mediational lymph nodes (disappeared week 39). Treatment related microscopic changes in the nasal region were occasionally found at the end of exposure period such as focal necrosis and slight atrophy of the olfactory epithelium. Interstitial fibrosis was not noted directly after the exposure period, but appeared with a delay. It was observed for the first time after 13 weeks post exposure, increasing incidence especially for 30 mg/m^3 and less for 6 mg/m^3. But it decreased in severity and frequency until the end of the study. All types of pulmonary lesions were more marked in males than in females. The level of 1.3 mg/m^3 induced only slight changes after 13 weeks post exposure which generally recovered quickly. Morphological changes after 13 weeks exposure are considered statistically significant at 1.3 mg/m^3. Silica could be detected in lungs only in relatively small amounts at the end of exposure period. Only one male exposed to 30 mg/m^3 show a small amount of silica in the regional lymph nodes. 90 days after termination		act, and lymph nodes. Post-exposure recovery period up to one year. One high exposure level only within a combined study

					of exposure, no silica could be recovered from any animal.		
Substance declared equivalent to **NM-204** (precipitated) No Characterisation provided	Rat (male and female)	Subchronic Inhalation Toxicity: 90-Day (OECD Guideline 413)	90 days 6 hours/day, 5 days/week 35 mg/m^3 (mean analytical values) Basis analytical conc. 30 mg/m^3 (target concentration	no NOAEC identified (Test substance at a level of 30 mg/m3 induced generally mild changes, which quickly recovered during the exposure period.)	A slight decrease of body weight (- 5 %) by 13 weeks exposure was observed (still at – 4 % after 52 weeks post exposure). No significant effects in haematology were detected but white blood cells count elevated in both males and females groups at the end of exposure period, but it wasn't clearly attributable to the increase in the number of neutrophilic leukocytes. After 13 weeks recovery, neutrophil count still tended to be higher in males and females, and normalised by 28 weeks of recovery. No changes in heart, thyroids, adrenals, testes, brain, spleen and kidneys weights were observed, but the relative mean of lungs weighs slightly increased (≈ x 1.3). Thymus weight increased as well. Swollen lungs and enlarged mediastinal lymph nodes were noted. The effects gradually subsided after the exposure period. Lung weights were normalised after 13 weeks recovery in males and females. In the lung, accumulation of alveolar macrophage, intra-alveolar polymorphonuclear leukocytes and increased septal cellularity in males and females were noted. Treatment related microscopic changes in the nasal region were found at the end of the exposure, such as very slight local necrosis and slight atrophy of the olfactory epithelium, intracystoplasmic proteinaeceous droplets. Accumulation of macrophages was seen in the mediastinal lymph nodes (disappeared after 39 week post exposure). Collagen content in the lungs slightly increased at the end of the exposure, During the recovery period, all changes disappeared mostly within 13 to 26 weeks post exposure. Silica could be detected in lungs only in relatively small amounts at the end of the exposure periods. On the average 0.5 mg per lung in male animal group, 0.35 mg per lung of female groups, decreasing over time and no longer measurable after 39 weeks post exposure were found.	Data provided by BIAC. Tests performed by TNO Division of Nutrition and Food Research, Zeist (NL) in 1987	Special modifications as compared with standard study: Focus upon lung, respiratory tract, and lymph nodes. Post-exposure recovery period up to one year. One high exposure level only within a combined study
Oral							
Substance declared equivalent to **NM-200**	Rat (male and female)	OECD Guideline 408 (Repeated	Oral (feed) Continuous 13 weeks exposure	NOEL 6.7 in feed NOEL highest dose ca. 4000 ≤	No clinical symptoms or other findings including haematological, blood-chemical and urinary parameters. Mean food intake was slightly increased in the female top-dose group (some +5 % after 4 wks) with no corresponding body-weight gain, but barely seen in males. The	Data provided by BIAC. Tests performed by TNO Division of	

(precipitated) No Characterisation provided		Dose 90-Day Oral Toxicity in Rodents)	Approx. 0.5, 2 and 6.7 % Si in the diet	4500 mg/kg bw/day (nominal)	reduced food efficiency may be due to the rather high amount of inert test substance. Water consumption was normal throughout. Gross and microscopical examinations did not reveal any (histo-)pathological changes that could be attributed to the feeding of the test substance.	Nutrition and Food Research, Zeist (NL) in 1981	
Substance declared equivalent to **NM-201** (precipitated) No Characterisation provided	Rat (male and female)	90-Day Oral Toxicity in Rodents (OECD Guideline 408)	Oral (feed) Continuous 13 weeks exposure Approx. 0.5, 2 and 6.7 % Si in the diet	NOEL 6.7 % in feed NOEL highest dose ca. 4000 ≤ 4500 mg/kg bw/day (nominal)	No clinical symptoms or other findings including haematological, blood-chemical and urinary parameters. Mean food intake was slightly increased in the female top-dose group (some +5 % after 4 wks) with no corresponding body-weight gain, but barely seen in males). The reduced food efficiency may be due to the rather high amount of inert test substance. Water consumption was normal throughout. Gross and microscopical examinations did not reveal any (histo-)pathological changes that could be attributed to the feeding of the test substance.	Data provided by BIAC. Tests performed by TNO Division of Nutrition and Food Research, Zeist (NL) in 1981	
Substance declared equivalent to **NM-204** (precipitated) No Characterisation provided	Rat (male and female)	90-Day Oral Toxicity in Rodents (OECD Guideline 408)	Oral (feed) Continuous 90 day exposure Approx. 0.5, 2 and 6.7 % Si in the diet	NOEL 6.7 % in feed NOEL highest dose ca. 4000 ≤ 4500 mg/kg bw/day (nominal)	No clinical symptoms or other findings including haematological, blood-chemical and urinary parameters. Mean food intake was slightly increased in the female top-dose group (some +5 % after 4 wks) with no corresponding body-weight gain, but barely seen in males. The reduced food efficiency may be due to the rather high amount of inert test substance. Water consumption was normal throughout. Gross and microscopical examinations did not reveal any (histo-)pathological changes that could be attributed to the feeding of the test substance.	Data provided by BIAC. Tests performed by TNO Division of Nutrition and Food Research, Zeist (NL) in 1981	

Table 22. Summary of NANOhub entries for Repeated Dose Toxicity (chronic)

Material	**Test Organism / System**	**Method**	**Exposure/ dose**	**Derived effect value (dose descriptor)**	**Main findings**	**Contributor**
Substance declared equivalent to **NM-202**	Rat (female)	Inhalation	6 and 18 weeks and 12 months 5 h/d, 5x/wk initially, but later (time not stated) weekly	no NOAEC identified	RETENTION of silica: After 12-months exposure, about 1 % of administered total respirable dust was estimated to be still retained in the lung. The increase in lung deposition was low from 18 weeks to 12 months of exposure (18 wk: 1.2 mg SiO_2, 12 months: 1.37 mg SiO_2). Mediastinal lymph nodes contained about 0.13 mg SiO_2 after	Data provided by BIAC. Tests performed by

(pyrogenic) No Characterisation provided			frequency reduced to 2-3x/wk because suppurative bronchitis and severe inflammation caused losses. Frequency of treatment: 5 h/d, 5x/wk, after unspecified time: 2 - 3x/wk 50 - 55 mg/m^3 (total dust) = approx. 30 mg/m^3 (respirable)		12 months. After 5 months post-exposure, mean levels of SiO_2 were 0.16 mg/lung and 0.047 mg/lymph node, i.e. a reduction at some 88 % in the lung and more than 50 % in the lymph nodes. PATHOLOGY: Microscopically visible small dust foci could be observed under the pulmonary pleura, mediastinal lymph nodes were moderately enlarged. In the interior of alveoles, numerous macrophages accumulated, partially normal, partially destroyed, associated with deposition of cell debris ("desquamation catarrh"). Perivascular and peribronchiolar small dust foci of macrophages, associated with mild and moderate formation of connective tissue (ranked as grade I to II, based on a ranking system according to Belt&King). In the alveolar septa the collagen formation was increased. In some cases, collagenic fibrosis was detected. There were no signs of typical silicosis. In the mediastinal lymph nodes, foci and clusters of phagocytes, partially normal, partially showing decay, were observed.	Institut für Hygiene und Arbeitsmedizin, Klinikum Essen (GER) in 1969

5.6 Mutagenicity

Table 23 below summarises the outcomes of in vitro mutagenicity studies as reported in literature. Table 24 sumarises the NANOhub entries for in vitro mutagenicity. Data is provided in bacterial tests by BIAC, [generated before the WPMN set up its testing programme, and it is stated the the material tested is equivalent to the NM-series], mammalian cells [from the Nanogenox project testing the NM-series materials, and from BIAC who submitted data generated before the WPMN set up its testing programme, and it is stated the the material tested is equivalent to the NM-series].

Table 23. Genotoxicity, in vitr testing. Summary of information from scientific literature

Reference	Material / Size	Test Organism / System	Method	Exposure/ dose	Main findings
Genotoxicity – in vitro					
Barnes CA, 2008	Commercial colloidal and laboratory synthesized silica	Mouse embryonic fibroblast cells	Comet assay	3; 6; 24h 4 and 40 µg/ml	No significant genotoxicity (results were independently validated in two separate laboratories)

Gonzales L., 2010	Purposely synthesized SAS (2): Stöber SAS (16, 60 and 104 nm)	Human bronchoalveolar carcinoma (A549)	Micronucleus assay (OECD guideline 487) Comet assay	40 h (cyto B at t=4h) 45,9 (16 nm SAS) 48,9 (60 nm SAS); 165,3 (104 nm SAS) µg/ml	At non-cytotoxic doses the smallest particles showed a slightly higher fold induction of micronuclei. The authors show that particle number and total surface area appeared to account for micronuclei induction as they both correlated significantly with the amplitude of the effect. Using nominal or cellular dose did not show statistically significant differences. Likewise, alkaline comet assay and FISH-centromeric probing of micronuclei indicated a weak and not statistically significant induction of oxidative DNA damage, chromosome breakage and chromosome loss.

Table 24. Summary of NANOhub entries for genotoxicity in vitro

Material	Test Organism / System	Method	Exposure/dose	Main findings	Contributor	Comment
Bacterial tests						
Substance declared equivalent to **NM-202** (pyrogenic) No Characterisation provided	S. typhimurium TA 1535, TA 1537, TA 98 and TA 100	Bacterial Reverse Mutation Assay (OECD Guideline 471)	Exposure duration: no data 667, 1000, 3333, 6667, and 10000 µg/plate ± S9 mix	Negative	Data provided by BIAC. Tests performed by Microbiological Associates, Inc.(USA) in 1989	
Substance declared equivalent to **NM-203** (pyrogenic) No Characterisation provided	S. typhimurium TA 1535, TA 1537, TA 98 and TA 100	Bacterial Reverse Mutation Assay (OECD Guideline 471)	Exposure duration: no data 667, 1000, 3333, 6667, and 10000 µg/plate ± S9 mix	Negative	Data provided by BIAC. Tests performed by Microbiological Associates, Inc.(USA) in 1989	
Mammalian cells						
NM-200 (precipitated)	Primary rat alveolar macrophage	Comet assay	4 h and 24 h 10, 50, 250 ng/cm² (19, 95, 475 ng/ml) Additionally: 4h at 10 µg/cm² (19 µg/ml) and 24 h at 2.5 µg/cm² (4.75 µg/ml)	No cytotoxic effect except for 10 µg/cm² No genotoxic effect at the tested doses. Slight increase in the tail intensity over the control at 10 µg/cm² more likely due to a particle effect.	Data provided by BIAC. Tests performed by Fraunhofer Institute for Toxicology and Experimental Medicine (ITEM) (GER) in 2012	No oxidative DNA damage detected with DNA-glycosylase 1 (hOGG1)

NM-200 (precipitated)	Human bronchial 16-HBE cells	Comet assay	3 h and 24 h 5; 20; 40; 80; 100 µg/ml (1.31; 5.26;10.5; 21; 26.3 µg/cm²)	Positive at 3 h: dose-dependent increase Negative at 24 h	Data provided by Nanogenotox performed by UAB (SP) in 2013	FpG-modified comet assay: negative at 3 h and 24 h
NM-200 (precipitated)	Human bronchial 16-HBE cells	Micronucleus assay (OECD guideline 487)	41 h 8; 16; 32 µg/ml	Negative	Data provided by Nanogenotox performed by IPL (F) in 2013	Micronucleus assay without cytochalasin B
NM-200 (precipitated)	Human bronchial BEAS-2B cells	Comet assay	3 h 2.56; 25.6; 256; 512 µg/ml (1.42; 14.2;142; 284 µg/cm²)	Positive at 25.6 and 256 µg/ml	Data provided by Nanogenotox performed by IPH (B) in 2013	FpG-modified comet assay: equivocal response (positive at one dose)
NM-200 (precipitated)	Human bronchial BEAS-2B cells	Micronucleus assay (OECD guideline 487)	48 h 8; 16; 32; 64;128 µg/ml (4; 8; 16; 32; 64 µg/cm²)	Negative	Data provided by Nanogenotox performed by FIOH (FL) in 2013	Cytochalasin B added 6 h after NM
NM-200 (precipitated)	Human pulmonary A549 cells	Comet assay	3 h and 24 h 2.56; 25.6; 256 ; 512 µg/ml (1.42; 14.2;142; 284 µg/cm²)	Equivocal at 3h Negative at 24 h	Data provided by Nanogenotox performed by IPH (B) in 2013	FpG-modified comet assay: negative at 3 h and 24 h
NM-200 (precipitated)	Human pulmonary A549 cells	Micronucleus assay (OECD guideline 487)	48 h 32; 64; 128; 256; 512 µg/ml (6.1; 12.2; 24.4; 48.8; 97.6 µg/cm²)	Negative (experiment 1 and 2)	Data provided by Nanogenotox performed by INRS (F) in 2013	Cytochalasin B added 6 h after NM
NM-200 (precipitated)	Human intestinal Caco-2 cells	Comet assay	3 h and 24 h 2.56; 25.6; 256 ; 512 µg/ml (1.42; 14.2;142; 284 µg/cm²)	Positive at 3h: 2 doses (25.6 and 256 µg/ml) Positive at 24h: 2 doses (256 and 512 µg/ml)	Data provided by Nanogenotox performed by IPH (B) in 2013	FpG-modified comet assay: equivocal at 3 h and positive at 24 h
NM-200 (precipitated)	Human intestinal Caco-2 cells	Micronucleus assay (OECD guideline 487)	52 h 9.5; 28; 85; 128; 256 µg/ml (2.5 ; 7.5 ; 22 ; 34 ; 67 µg/cm²)	Positive in 2 out 3 experiments: dose-dependent increase (85, 128, 256 µg/ml)	Data provided by Nanogenotox performed by Anses (F) in 2013	Cytochalasin B added 24 h after NM
NM-200 (precipitated)	Human primary peripheral blood lymphocytes	Micronucleus assay (OECD guideline 487)	30 h 64; 128; 256 µg/ml	Negative	Data provided by Nanogenotox performed by INSA (PT) in 2013	Cytochalasin B added 6 h after NM
NM-200	L5178Y TK +/-	In vitro mammalian	24 h	Negative	Data provided by	

(precipitated)	mouse lymphoma cells	cell gene mutation tests (OECD Guideline 476)	32; 64; 128; 256/ 625; 1250; 2500; 5000 µg/ml		Nanogenotox performed by IPL (F) in 2013	
NM-200 (precipitated)	L5178Y TK +/- mouse lymphoma cells	In vitro mammalian cell gene mutation tests (OECD guideline 476)	4 h ± S9 mix 10; 100; 300; 900; 2700; 5000 µg/ml	Negative	Data provided by BIAC. Tests performed by Fraunhofer Institute for Toxicology and Experimental Medicine (ITEM) (GER) in 2012	Incipient toxicity at 2700 µg/ml, marked at 5000 µg/ml
NM-200 (precipitated)	Chinese hamster lung fibroblasts (V79)	In Vitro Mammalian Chromosome Aberration Test (OECD guideline 473)	4 h + S9 mix: 600; 1000; 1500 µg/ml 4 h –S9 mix: 100; 200; 600; 1800 µg/ml 24 h –S9 mix: 2; 5; 16; 48 µg/ml	Negative	Data provided by BIAC. Tests performed by Fraunhofer Institute for Toxicology and Experimental Medicine (ITEM) (GER) in 2012	Marked cytotoxicity: ≥ 500 mg/ml (4 h – S9 mix) > 1000 µg/ml (4 h – +S9 mix) ≥ 10 µg/ml (24 h – S9 mix)
NM-201 (precipitated)	Human bronchial 16-HBE cells	Comet assay	3 h and 24 h 5; 10; 20; 40; 60 µg/ml (1.3; 2.63; 5.3; 10.4; 15.8 µg/cm²)	Negative at 3 h and 24 h	Data provided by Nanogenotox performed by UAB (SP) in 2013	FpG-modified comet assay: negative at 3 h and 24 h
NM-201 (precipitated)	Human bronchial 16-HBE cells	Micronucleus assay (OECD guideline 487	41 h 32; 64; 128; 256 µg/ml	Negative	Data provided by Nanogenotox performed by IPL (F) in 2013	Micronucleus assay without cytochalasin B
NM-201 (precipitated)	Human bronchial BEAS-2B cells	Comet assay	3 h 2.56; 25.6; 256; 512 µg/ml (1.42; 14.2;142; 284 µg/cm²)	Equivocal at 3 h: increase in the % Tail DNA at 1 dose (256 µg/ml)	Data provided by Nanogenotox performed by IPH (B) in 2013	
NM-201 (precipitated)	Human bronchial BEAS-2B cells	Micronucleus assay (OECD guideline 487	48 h 4; 8; 16; 32; 64 µg/ml (2; 4; 8; 16; 32 µg/cm²)	Negative	Data provided by Nanogenotox performed by FIOH (FL) in 2013	Cytochalasin B added 6 h after NM
NM-201 (precipitated)	Human pulmonary A549 cells	Comet assay	3 h and 24 h 2.56; 25.6; 256 ; 512 µg/ml (1.42; 14.2;142; 284 µg/cm²)	Positive at 3h: at 2 doses (256 and 512 µg/ml) Equivocal at 24h: increase at the lowest dose (2.56 µg/ml)	Data provided by Nanogenotox performed by IPH (B) in 2013	FpG-modified comet assay: negative at 3 h and equivocal at 24 h

NM-201 (precipitated)	Human pulmonary A549 cells	Micronucleus assay (OECD guideline 487	48 h 32; 64; 128; 256; 512 µg/ml (6.1; 12.2; 24.4; 48.8; 97.6 µg/cm²)	Positive: (32, 64, 128 and 256 µg/ml), 1st experiment) 256 and 512 µg/ml (2nd experiment)	Data provided by Nanogenotox performed by INRS (F) in 2013	Cytochalasin B added 6 h after NM
NM-201 (precipitated)	Human intestinal Caco-2 cells	Comet assay	3 h and 24 h 2.56; 25.6; 256 ; 512 µg/ml (1.42; 14.2;142; 284 µg/cm²)	Negative at 3 h Equivocal at 24 h: one dose (25.6 µg/ml)	Data provided by Nanogenotox performed by IPH (B) in 2013Nanogenotox	FpG-modified comet assay: negative at 3 h and positive at 24 h
NM-201 (precipitated)	Human intestinal Caco-2 cells	Micronucleus assay (OECD guideline 487	52 h 9.5; 28; 85; 128; 256 µg/ml (2.5 ; 7.5 ; 22 ; 34 ; 67 µg/cm²)	Positive in 2 out 3 experiments: dose-dependent increase (128, 256 µg/ml exp 1; 28, 85; 128; 256 exp 2)	Data provided by Nanogenotox performed by Anses (F) in 2013	Cytochalasin B added 24 h after NM
NM-201 (precipitated)	Human primary peripheral blood lymphocytes	Micronucleus assay (OECD guideline 487	30 h 64; 128; 256 µg/ml	Negative	Data provided by Nanogenotox performed by INSA (PT) in 2013	Cytochalasin B added 6 h after NM
NM-201 (precipitated)	L5178Y TK +/- mouse lymphoma cells	In vitro mammalian cell gene mutation tests (OECD guideline 476)	24 h 32; 64; 128; 256/ 625; 1250; 2500; 5000 µg/ml	Negative	Data provided by Nanogenotox performed by IPL (F) in 2013	
NM-202 (pyrogenic)	Human bronchial 16-HBE cells	Comet assay	3 h and 24 h 5; 10; 20; 40; 80 µg/ml (1.31; 2.63; 5.3; 10.4; 21 µg/cm²)	Negative at 3 h and 24 h	Data provided by Nanogenotox performed by UAB (SP) in 2013	FpG-modified comet assay: negative at 3 h and 24 h
NM-202 (pyrogenic)	Human bronchial 16-HBE cells	Micronucleus assay (OECD guideline 487	41 h 32; 64; 128 µg/ml	Negative	Data provided by Nanogenotox performed by IPL (F) in 2013	Micronucleus assay without cytochalasin B
NM-202 (pyrogenic)	Human bronchial BEAS-2B cells	Comet assay	3 h 2.56; 25.6; 256; 512 µg/ml (1.42; 14.2;142; 284 µg/cm²)	Positive at 3 h: at 3 doses (2.56, 25.6 and 256 µg/ml)	Data provided by Nanogenotox performed by IPH (B) in 2013	FpG-modified comet assay: positive at 3 h
NM-202 (pyrogenic)	Human bronchial BEAS-2B cells	Micronucleus assay (OECD guideline 487	48 h 4; 8; 16; 32; 64 µg/ml (2; 4; 8; 16; 32 µg/cm²)	Negative	Data provided by Nanogenotox performed by FIOH (FL) in 2013	Cytochalasin B added 6 h after NM
NM-202 (pyrogenic)	Human pulmonary	Comet assay	3 h and 24 h 2.56; 25.6; 256 ; 512 µg/ml	Positive at 3h: increase in at 2 doses (25.6 and 256 µg/ml)	Data provided by Nanogenotox performed by	FpG-modified comet assay: positive at 3 h

	A549 cells		(1.42; 14.2;142; 284 µg/cm²)	Equivocal at 24h: increase at one dose	IPH (B) in 2013	and negative 24 h
NM-202 (pyrogenic)	Human pulmonary A549 cells	Micronucleus assay (OECD guideline 487	48 h 32; 64; 128; 256; 512 µg/ml (6.1; 12.2; 24.4; 48.8; 97.6 µg/cm²)	Positive: 64, 128, 256 and 512 µg/ml (1st experiment) 128,256 and 512 (2nd experiment)	Data provided by Nanogenotox performed by INRS (F) in 2013	Cytochalasin B added 6 h after NM
NM-202 (pyrogenic)	Human intestinal Caco-2 cells	Comet assay	3 h and 24 h 2.56; 25.6; 256 ; 512 µg/ml (1.42; 14.2;142; 284 µg/cm²)	Equivocal at 3 h: one dose (25.6 µg/ml) Equivocal at 24 h: one dose (25.6 µg/ml)	Data provided by Nanogenotox performed by IPH (B) in 2013	FpG-modified comet assay: positive at 3 h and negative at 24 h
NM-202 (pyrogenic)	Human intestinal Caco-2 cells	Micronucleus assay (OECD guideline 487)	52 h 9.5; 28; 85; 128; 256 µg/ml (2.5 ; 7.5 ; 22 ; 34 ; 67 µg/cm²)	Positive in 2 out 3 experiments: dose-dependent increase	Data provided by Nanogenotox performed by Anses (F) in 2013	Cytochalasin B added 24 h after NM
NM-202 (pyrogenic)	Human primary peripheral blood lymphocytes	Micronucleus assay (OECD guideline 487)	30 h 64; 128; 256; 312.5; 625; 1250 µg/ml	Negative	Data provided by Nanogenotox performed by INSA (PT) in 2013	Cytochalasin B added 6 h after NM
NM-202 (pyrogenic)	L5178Y TK +/- mouse lymphoma cells	In vitro mammalian cell gene mutation tests (OECD guideline 476)	24 h 32; 64; 128; 256/ 625; 1250; 2500; 5000 µg/ml	Negative	Data provided by Nanogenotox performed by IPL (F) in 2013	
Substance declared equivalent to **NM-202** (pyrogenic) No Characterisation provided	Chinese hamster Ovary (CHO)	In vitro mammalian cell gene mutation Test (OECD guideline 476)	5 h -S9 : 10, 50, 100, 150 and 250 µg/ml + S9 : 100, 200, 300, 400 and 500 µg/ml	Negative	Data provided by BIAC performed by Microbiological Associates, Inc., (USA) in 1990	
Substance declared equivalent to **NM-202** (pyrogenic) No Characterisation provided	Chinese hamster Ovary (CHO)	In vitro mammalian cell gene mutation Test (OECD guideline 473)	-S9: 18 h 38, 75, 150, 300 µg/ml +S9: 2 h 250, 500, 750, 1000 µg/ml	Negative Cell proliferation began to be inhibited at 30 µg/L (-S9) and 300 µg/L (+S9). Simultaneously, the cell cycle became retarded with an accumulation of cells in the M1 phase. Neither in the control nor in the treated cultures, cells were observed in the M3	Data provided by BIAC performed by Microbiological Associates, Inc., (USA) in 1990	

				phase (except 1 instance in the DMSO control).		
Substance declared equivalent to **NM-202** (pyrogenic) No Characterisation provided	Primary rat hepatocytes	DNA Damage and Repair, Unscheduled DNA Synthesis in Mammalian Cells (OECD guideline 482)	18 h to 20 h 10, 30, 100, 300 and 1000 µg/ml	Negative	Data provided by BIAC performed by Microbiological Associates, Inc., (USA) in 1889	
NM-203 (pyrogenic)	Human bronchial 16-HBE cells	Comet assay	3 h and 24 h 5; 10; 20; 50; 80 µg/ml (1.31; 2.63; 5.3; 10.4; 21 µg/cm²)	Negative at 3 h and 24 h	Data provided by Nanogenotox performed by UAB (SP) in 2013	FpG-modified comet assay: negative at 3 h and 24 h
NM-203 (pyrogenic)	Human bronchial 16-HBE cells	Micronucleus assay (OECD guideline 487)	41 h 8; 12; 16 µg/ml	Negative	Data provided by Nanogenotox performed by IPL (F) in 2013	Cytochalasin B added 6 h after NM
NM-203 (pyrogenic)	Human bronchial BEAS-2B cells	Comet assay	3 h 2.56; 25.6; 256; 512 µg/ml (1.42; 14.2;142; 284 µg/cm²)	Positive at 3 h: at 3 doses (2.56, 25.6 and 256 µg/ml)	Data provided by Nanogenotox performed by IPH (B) in 2013	FpG-modified comet assay: positive
NM-203 (pyrogenic)	Human bronchial BEAS-2B cells	Comet assay	24 h 8; 32; 64 µg/ml (4; 16; 32 µg/cm²)	Negative in 3 experiments Positive in 3 experiments	Round robin test Data provided by Nanogenotox in 2013	
NM-203 (pyrogenic)	Human bronchial BEAS-2B cells	Micronucleus assay (OECD guideline 487)	48 h 4; 8; 16; 32; 64 µg/ml (2; 4; 8; 16; 32 µg/cm²)	Equivocal: increase at one dose (8 µg/ml)	Data provided by Nanogenotox performed by FIOH (FL) in 2013	Cytochalasin B added 6 h after NM
NM-203 (pyrogenic)	Human bronchial BEAS-2B cells	Micronucleus assay (OECD guideline 487	48 h 8; 32; 64 µg/ml (4; 16; 32 µg/cm²)	Negative in 3 experiments Positive in 2 experiments Equivocal in 1 experiment	Round robin test Data provided by Nanogenotox in 2013	Cytochalasin B added 6 h after NM
NM-203 (pyrogenic)	Human pulmonary A549 cells	Comet assay	3 h and 24 h 2.56; 25.6; 256 ; 512 µg/ml (1.42; 14.2;142; 284 µg/cm²)	Negative at 3h Positive at 24h: increase at 2 doses (25.6 and 256 µg/ml	Data provided by Nanogenotox performed by IPH (B) in 2013	FpG-modified comet assay: negative at 3 h and positive at 24 h
NM-203 (pyrogenic)	Human pulmonary	Micronucleus assay (OECD guideline	48 h 32; 64; 128; 256; 512 µg/ml	Negative (1st experiment) Equivocal (2nd experiment)	Data provided by Nanogenotox performed by	Cytochalasin B added 6 h after NM

	A549 cells	487)	(6.1; 12.2; 24.4; 48.8; 97.6 µg/cm²)		INRS (F) in 2013	
NM-203 (pyrogenic)	Human intestinal Caco-2 cells	Comet assay	3 h and 24 h 2.56; 25.6; 256 ; 512 µg/ml (1.42; 14.2;142; 284 µg/cm²)	Positive at 3h: 2 doses (2.56 and 25.6 µg/ml) Positive at 24h: 2 doses (25.6 and 512 µg/ml)	Data provided by Nanogenotox performed by IPH (B) in 2013	FpG-modified comet assay: positive at 3 h and equivocal at 24 h
NM-203 (pyrogenic)	Human intestinal Caco-2 cells	Comet assay	24 h 64; 128; 256 µg/ml (32; 64; 128 µg/cm²)	Negative in 3 experiments Positive in 2 experiments	Round robin test Data provided by Nanogenotox in 2013	
NM-203 (pyrogenic)	Human intestinal Caco-2 cells	Micronucleus assay (OECD guideline 487)	52 h 9.5; 28; 85; 128; 256 µg/ml (2.5 ; 7.5 ; 22 ; 34 ; 67 µg/cm²)	Positive in 2 out 3 experiments: dose-dependent increase	Data provided by Nanogenotox performed by Anses (F) in 2013	Cytochalasin B added 24 h after NM
NM-203 (pyrogenic)	Human intestinal Caco-2 cells	Micronucleus assay (OECD guideline 487)	48 h 64; 128; 256 µg/ml (32; 64; 128 µg/cm²)	Negative in 3 experiments Positive in 3 experiments	Round robin test Data provided by Nanogenotox in 2013	Cytochalasin B added 24 h after NM
NM-203 (pyrogenic)	Human primary peripheral blood lymphocytes	Micronucleus assay (OECD guideline 487)	30 h 256; 312.5; 625; 1250 µg/ml	Negative	Data provided by Nanogenotox performed by INSA (PT) in 2013	Cytochalasin B added 6 h after NM
NM-203 (pyrogenic)	L5178Y TK +/- mouse lymphoma cells	In vitro mammalian cell gene mutation tests (OECD Guideline 476)	24 h 32; 64; 128; 256/ 625; 1250; 2500; 5000 µg/ml	Negative	Data provided by Nanogenotox performed by IPL (F) in 2013	
Substance declared equivalent to **NM-203** (pyrogenic) No Characterisation provided	Chinese hamster Ovary (CHO)	In vitro mammalian cell gene mutation Test (OECD guideline 476)	5 h -S9 : 10, 50, 100, 150 and 250 µg/ml + S9 : 100, 200, 300, 400 and 500 µg/ml	Negative	Data provided by BIAC performed by Microbiological Associates, Inc., (USA) in 1990	
Substance declared equivalent to **NM-203** (pyrogenic) No Characterisation	Chinese hamster lung fibroblasts (V79)	In Vitro Mammalian Chromosome Aberration Test	-S9: 18 h 38, 75, 150, 300 µg/ml	Negative Cell proliferation began to be inhibited at 30 µg/L (-S9) and 300 µg/L (+S9). Simultaneously, the cell cycle became	Data provided by BIAC performed by Microbiological Associates, Inc., (USA) in 1990	

provided		(OECD Guideline 473)	+S9: 2 h 250, 500, 750, 1000 µg/ml	retarded with an accumulation of cells in the M1 phase. Neither in the control nor in the treated cultures, cells were observed in the M3 phase (except 1 instance in the DMSO control).		
Substance declared equivalent to **NM-203** (pyrogenic) No Characterisation provided	Primary rat hepatocytes	DNA Damage and Repair, Unscheduled DNA Synthesis in Mammalian Cells (OECD guideline 482)	18 h to 20 h 10, 30, 100, 300 and 1000 µg/ml	Negative	Data provided by BIAC performed by Microbiological Associates, Inc., (USA) in 1889	

Below is given an overview of the scientific literature reporting on in vivo genotoxicity testing of amorphous silicon dioxide, see Table 25, and the testing performed with the NM-series materials in the Nanogenotox project for this end-point, see Table 26.

Table 25. Genotoxicity, in vivo testing. Summary of information from scientific literature

Reference	Material / Size	Test Organism / System	Method	Exposure/ dose	Main findings
Genotoxicity – in vivo					
Johnston CJ, Driscoll KE, Finkelstein JN et al., 2000	NM-203	Rat (male)	Inhalation ex-vivo / in-vitro HPRT assay in alveolar epithelial	6 h/d, 5 d/wk for 90 days 50 mg/m^3 Basis nominal conc.	No cytotoxic effects Negative Alveolar type-II cells isolated from the 50-mg/m3 rat group showed no increased mutation frequency as compared to the control.

			cells.	50.4 +-19 mg/m^3 Basis analytical conc.	
Downs et al., 2012	Colloidal silica Levasil from HC Stark Lev 50 – diameter 55nm, specific surface area 50 m^2/g Lev 200-15 nm, specific surface area 200 m^2/g	Rat (male)	Intravenous 1- Comet assay 2- Micronucleus assay in bone marrow (OECD guideline 474) 3- Inflammation	3 injections on 3 consecutive days Sampling 4 h after the last injection 25, 50, 125 mg/kg	DNA damage in liver and increase in the % MN-RETs with Lev 15 nm at 50 mg/kg, inflammation (cytokine release in plasma). ”Intravenous injection of a 50 mg/kg dose of the 15 nm silica NPs resulted in a small increase in DNA damage in liver and lung tissue, and in white blood cells. No such effect was observed at the lower dose of the same particles or for the 55 nm silica particles, both of which also demonstrated lower acute toxicity than the high dose of the 15 nm silica NPs, which was the maximal dose the animals would tolerate. The small increase in DNA damage for the 50 mg/kg dose of the 15 nm silica NPs was reproduced in an independent second study, in which we also increased the dose of the larger 55 nm silica particles from 25 mg/kg to 125 mg/kg. At this higher dose, now representing the MTD, a 1.5–1.7-fold increase in DNA damage in the liver was also now measured in the 55 nm silica particle treatment group. Very good insight into the toxicity triggered by intravenous treatment of the rats with silica NPs came from histopathological analysis of the livers of the treated animals. Whereas vehicle control animals harboured minimal mononuclear cell infiltration and neutrophilic infiltration, an induction of mononuclear cell infiltrate, increase in Kupffer cell mitotic figures, hepatocellular necrosis, and haemorrhage were observed in the silica NP dose groups showing genotoxic activity. These findings demonstrate an inflammatory reaction of variable degree. Silica NP treatment resulted in an increase in the plasma levels of both markers; the effect was most pronounced for the 15 nm particles, but the 55 nm silica NPs and the quartz particles also caused an induction. These data suggest that there is a size-dependent induction of inflammatory markers, whereby it is possible that the smaller NPs may be penetrating tissues to a greater degree than the larger NPs, promoting an inflammatory response”

Table 26. Summary of NANOhub entries for genotoxicity in vivo

Material	Test Organis	Method	Exposure/dose	Main findings	Contributor	Comment

	m / System					
NM-200 (precipitated)	Rat (male)	Intratracheal instillation 1- Comet assay 2- Micronucleus assay in bone marrow (OECD guideline 474)	1 administration at 0, 24 and 45 h 3; 6; 12 mg/kg bw/d	1-Changes in BAL fluid cell number and composition may be associated with a toxicological process and an inflammatory response (especially granulocytes influx). Whatever the dose considered, a significant increase of influx of neutrophilic granulocytes was observed in BAL fluid from exposed animals with a dose-dependent trend. An increase of the total cell number was also noticed for all the SAS, but this change was not significant for the lowest dose of NM-200. Main cell types observed in BAL fluid were macrophages and neutrophilic granulocytes, some lymphocytes were also observed but their frequency and number in SAS exposed animals were not significantly different from the control group. In addition, in this study, the percentage of neutrophilic granulocytes in control (vehicle) group appears higher than that is usually obtained following a single intratracheal instillation and may be considered as an experimental artefact due to repeated animal exposure. Increase in lactate dehydrogenase (LDH), alkaline phosphatase (ALP) and N-acetyl-β-Dglucosaminidase (NAG) activities and protein content are often signs of pulmonary toxicity following pulmonary exposure to particulate matter. A significant increase in the broncho-alveolar fluid of LDH and NAG activities was observed. No change in alkaline phosphatase (ALP) was however observed (Figure 17). 2-In conclusion, intratracheal instillation did not induce any significant increase of DNA damages in all the organs tested. In all the experiments performed, positive controls (MMS Or ENU) always induced significant DNA strand breaks in the tissues analysed.	Data provided by Nanogenotox performed by INRS (F) in 2013	Sacrifice 3 h after the last administration FpG-modified comet assay: Negative in all the tested organs except from spleen (equivocal result)
NM-200 (precipitated)	Rat (male)	Oral 1- Comet assay 2- Micronucleus assay in bone marrow (OECD guideline 474) 3- Micronucleus assay in	1 administration at 0, 24 and 45 h 5, 10, 20 mg/kg bw/d	1-Negative in duodenum, colon, blood, bone marrow, liver, kidney, spleen 2-Negative 3-Negative	Data provided by Nanogenotox performed by Anses (F) in 2013	Sacrifice 3 h after the last administration FpG-modified comet assay: negative

		colon				
NM-201 (precipitated)	Rat (male)	Intratracheal instillation 1- Comet assay 2- Micronucleus assay in bone marrow (OECD guideline 474)	1 administration at 0, 24 and 45 h 3; 6; 12 mg/kg bw/d	1- Changes in BAL fluid cell number and composition may be associated with a toxicological process and an inflammatory response (especially granulocytes influx). Whatever the dose considered, a significant increase of influx of neutrophilic granulocytes was observed in BAL fluid from exposed animals with a dose-dependent trend. An increase of the total cell number was also noticed. Main cell types observed in BAL fluid were macrophages and neutrophilic granulocytes, some lymphocytes were also observed but their frequency and number in SAS exposed animals were not significantly different from the control group. In addition, in this study, the percentage of neutrophilic granulocytes in control (vehicle) group appears higher than that is usually obtained following a single intratracheal instillation and may be considered as an experimental artefact due to repeated animal exposure. Increase in lactate dehydrogenase (LDH), alkaline phosphatase (ALP) and N-acetyl-β-Dglucosaminidase (NAG) activities and protein content are often signs of pulmonary toxicity following pulmonary exposure to particulate matter. For all SAS, a significant increase in the broncho-alveolar fluid of LDH and NAG activities was observed. No change in alkaline phosphatase (ALP) was however observed. 2- Intratracheal instillation did not induce any significant increase of DNA damages in all the organs tested. In all the experiments performed, positive controls (MMS or ENU) always induced significant DNA strand breaks in the tissues analysed.	Data provided by Nanogenotox performed by INRS (F) in 2013	Sacrifice 3 h after the last administration FpG-modified comet assay: negative
NM-201 (precipitated)	Rat (male)	Oral 1- Comet assay 2- Micronucleus assay in bone marrow (OECD guideline 474) 3- Micronucleus assay in colon	1 administration at 0, 24 and 45 h 5, 10, 20 mg/kg bw/d	1-Negative in duodenum, colon, blood, bone marrow, liver, kidney, spleen 2-Negative 3-Negative	Data provided by Nanogenotox performed by Anses (F) in 2013	Sacrifice 3 h after the last administration FpG-modified comet assay: negative
NM-202	Rat	Intratracheal instillation	1 administration at 0,	1- Changes in BAL fluid cell number and composition may be	Data	Sacrifice 3 h after the

(pyrogenic)	(male)	1- Comet assay 2- Micronucleus assay in bone marrow (OECD guideline 474)	24 and 45 h 3; 6; 12 mg/kg bw/d	associated with a toxicological process and an inflammatory response (especially granulocytes influx). Whatever the dose considered, a significant increase of influx of neutrophilic granulocytes was observed in BAL fluid from exposed animals with a dose-dependent trend. An increase of the total cell number was also noticed, but this change was not significant for the lowest dose of NM- 202. Main cell types observed in BAL fluid were macrophages and neutrophilic granulocytes, some lymphocytes were also observed but their frequency and number in SAS exposed animals were not significantly different from the control group. In addition, in this study, the percentage of neutrophilic granulocytes in control (vehicle) group appears higher than that is usually obtained following a single intratracheal instillation and may be considered as an experimental artefact due to repeated animal exposure. Increase in lactate dehydrogenase (LDH), alkaline phosphatase (ALP) and N-acetyl-β-Dglucosaminidase (NAG) activities and protein content are often signs of pulmonary toxicity following pulmonary exposure to particulate matter. A significant increase in the broncho-alveolar fluid of LDH and NAG activities was observed. A significant increase in the BAL fluid of protein content was only observed for NM-202. No change in alkaline phosphatase (ALP) was however observed. 2- Intratracheal instillation did not induce any significant increase of DNA damages in all the organs tested. In all the experiments performed, positive controls (MMS or ENU) always induced significant DNA strand breaks in the tissues analysed.	provided by Nanogenotox performed by INRS (F) in 2013	last administration FpG-modified comet assay: negative
NM-202 (pyrogenic)	Rat (male)	Oral 1-Comet assay 2-Micronucleus assay in bone marrow (OECD guideline 474) 3-Micronucleus assay in colon	1 administration at 0, 24 and 45 h 5, 10, 20 mg/kg bw/d	1-Negative in duodenum, colon, blood, bone marrow, liver, kidney, spleen 2-Negative 3-Equivocal: increase at 1 dose (5 µg/ml)	Data provided by Nanogenotox performed by Anses (F) in 2013	Sacrifice 3 h after the last administration FpG-modified comet assay: negative
NM-203	Rat	Intratracheal instillation	1 administration at 0,	1- Changes in BAL fluid cell number and composition may be associated with a toxicological process and an inflammatory	Data provided by	Sacrifice 3 h after the

(pyrogenic)	(male)	1- Comet assay 2- Micronucleus assay in bone marrow (OECD guideline 474)	24 and 45 h 3; 6; 12 mg/kg bw/d	response (especially granulocytes influx). whatever the dose considered, a significant increase of influx of neutrophilic granulocytes was observed in BAL fluid from exposed animals with a dose-dependent trend. An increase of the total cell number was also noticed. Main cell types observed in BAL fluid were macrophages and neutrophilic granulocytes, some lymphocytes were also observed but their frequency and number in SAS exposed animals were not significantly different from the control group. In addition, in this study, the percentage of neutrophilic granulocytes in control (vehicle) group appears higher than that is usually obtained following a single intratracheal instillation and may be considered as an experimental artefact due to repeated animal exposure. Increase in lactate dehydrogenase (LDH), alkaline phosphatase (ALP) and N-acetyl-β-Dglucosaminidase (NAG) activities and protein content are often signs of pulmonary toxicity following pulmonary exposure to particulate matter. A significant increase in the broncho-alveolar fluid of LDH and NAG activities was observed. A significant increase in the BAL fluid of protein content was only observed for NM-203 (highest dose). No change in alkaline phosphatase (ALP) was however observed. 2- Intratracheal instillation did not induce any significant increase of DNA damages in all the organs tested. In all the experiments performed, positive controls (MMS or ENU) always induced significant DNA strand breaks in the tissues analysed.	Nanogenotox performed by INRS (F) in 2013	last administration FpG-modified comet assay: negative
NM-203 (pyrogenic)	Rat (male)	Oral 1- Comet assay 2- Micronucleus assay in bone marrow (OECD guideline 474) 3- Micronucleus assay in colon	1 administration at 0, 24 and 45 h 5, 10, 20 mg/kg bw/d	1-Negative in duodenum, colon, blood, bone marrow, liver, kidney, spleen 2-Negative 3- Equivocal: increase at 1 dose (5 µg/ml)	Data provided by Nanogenotox performed by Anses (F) in 2013	Sacrifice 3 h after the last administration FpG-modified comet assay: negative
NM-203 (pyrogenic)	Rat (male)	Intravenous 1- Comet assay	1 administration at 0, 24 and 45 h	The highest dose of intravenous (20 mg/kg) induced animal death (3 out of 6). NM-203 induced a dose dependent: increase of spleen weight, increase of liver damage as determined by liver enzymes (glutamic pyruvic transaminase (GPT) and glutamic oxaloacetic	Data provided by Nanogenotox performed by	Sacrifice 3 h after the last administration

		2- Micronucleus assay in bone marrow (OECD guideline 474)	5, 10, 20 mg/kg bw/d	transaminase (GOT)) released into plasma, thrombocytopenia. In both regular and FpG-modified comet assays, no increase of the percentage of tail DNA intensity was noticed in all the organs tested following intravenous NM-203 treatment. Only a significant induction of micronucleus was obtained at the highest dose (20 mg/kg) However, the induction is weak and the results were obtained only from 3 animals due to the lethality induced at this concentration.	INRS (F) in 2013	FpG-modified comet assay: negative

5.7 Carcinogenicity

Table 27 below summarises the information in scientific literature on studies of carcinogenicity of amorphous silicon dioxide.

Table 27. Carcinogenicity of amorphous silicon dioxide: Summary of information from scientific literature

Reference	Material/ Size	Test Organism / System	Method	Exposure/ dose	Derived effect value (dose descriptor)	Main findings
Takizawa Y et al, 1988	NM-204	B6C3F1 Mice (male and female)	Oral (feed) OECD guideline 453 (Combined Chronic Toxicity / Carcinogenicity Studies)	93 weeks continuous exposure with interim kill after 6 and 12 months 1.25, 2.5 and 5 % (nominal conc.)	NOAEL (highest dose level tested: 5 % in the diet) Effect level ca. 5000 — ca. 7000 mg/kg bw/day (actual dose received)	Negative
Takizawa Y et al, 1988	NM- 204	Fischer 344 rat (male and female)	Oral (feed) OECD Guideline 453 (Combined Chronic Toxicity / Carcinogenicity Studies)	103 weeks continuous exposure with interim kill after 6 and 12 months (10 animals each) 1.25, 2.5 and 5 %	NOAEL (highest dose level tested: 5 % in the diet) Effect level ca. 1800 — ca. 3000 mg/kg bw/day (actual dose received)	Negative

5.8 Toxicity for reproduction

Table 28 below summarises the test data available for toxicity to reproduction. The data is provided by BIAC and results are provided both for the NM-series as well as data generated before the WPMN set up its testing programme, for which it is stated the the material tested is equivalent to the NM-series.

Table 28. Summary of NANOhub entries for toxicity for reproduction

Material	Test Organism / System	Method	Exposure/dose		Main findings	Contributor	Comment
NM-200 (precipitated)	Rat (male and female)	Two-Generation Reproduction Toxicity Study (OECD 416)	Oral (gavage) 1x/day F0-Generation: The female animals were dosed during a 10-week premating period and during mating, gestation and lactation up to postnatal day 21. F1-Generation: Selected F1-generation pups were dosed from postnatal day 22 until the day prior to sacrifice.	NOAEL= 1000 mg/kg bw/d (highest tested dose)	No adverse effect on the reproductive performance of rats or on the growth and development of the offspring into adulthood, examined over two consecutive generations.	Data provided by BIAC performed by TNO Triskelion, Zeist (NL) in 2012	
Substance declared equivalent to **NM-202** (pyrogenic) No Characterisation provided	Rat (male and female	OECD Guideline 415 (One-Generation Reproduction Toxicity Study)	Oral (gavage) Exposure period: 6 months Premating exposure period (males and females): 4.5 months Duration of test: 6 months 497 mg/kg bw (m); 509 mg/kg bw (f)	NOAEL (P) 497 mg/kg bw/day NOAEL(F1) 497 mg/kg bw/day	Parents: No clinical symptoms; no mortality, no abnormalities in body-weight gain and feed consumption, no haematological findings. In pups during lactation [total: 45 and 37 (control), resp.], no behavioural or developmental or structural abnormalities.	Data provided by BIAC performed in 1963	no complete one generation study according to current standards: too low number of animals and examinations, one dose only, dose selection unclear (relatively low dose selected).
Substance declared	Rat (male and female)	One-Generation Reproduction Toxicity Study	Oral (feed) 1x/day	Generation P NOAEL = 497 mg/kg	No adverse effect in parents	(Data provided by BIAC performed in	no complete one generation study according to current

equivalent to **NM-203** (pyrogenic) No Characterisation provided		(OECD Guideline 415)	Exposure period: 6 months Premating exposure period (males and females): 4.5 months Duration of test: 6 months 497 mg/kg bw (male); 509 mg/kg bw (female)	bw/day Generation F1 NOAEL = 497 mg/kg bw/day		1963	standards: too low number of animals and examinations, one dose only, dose selection unclear (relatively low dose selected)

5.9 Toxicity in vitro

In vitro Mammalian Toxicology

The in vitro cytotoxicity of SAS is strongly influenced by the chemistry of the surface and in particular by the presence of two types of very reactive surface functional groups: the silanols (Si-OH) and siloxanes (Si-O-Si). The larger the number of silanols and siloxanes groups on the surface of SAS, the greater is the SAS reactivity and thus cytotoxicity. The covering of these active sites by ions will modify the properties of the surface of silicas and can thus lead to a change, and in particular to a reduction, of biological activity. The specific surface of SAS also influences their cellular toxicity. (Chang *et al.*, 2007; Jin *et al.*, 2007; Lin *et al.*, 2006; Lison *et al.*, 2008; Napierska *et al.*, 2009; Sayes *et al.*, 2007). Importantly, one study question the correlation of the results obtained *in vivo* and *in vitro* (Sayes et al., 2007). Although, looking at all the studies collected in the table I.3., some themes common to what is seen in vivo are emerging: even if SAS is not always shown to be cytotoxic it is quite potent to induce an inflammatory response, most probably mediated via oxidative stress (Lin, W., 2006; Park, EJ, 2009; Choi, SJ, 2009). In one reference various epithelial cells are exposed to dye doped SAS without significant genotoxic effects (Jin *et al.*, 2007). In another study the Comet assay was shown to be reproducibly used to study SAS nanoparticles and no significant genotoxicity on fibroblasts was detected (Barnes *et al.*, 2008), but one study shows also that silica nanoparticles can enter the cell and impair nuclear functions (Chen, 2005).

Table 29. In vitro toxicity testing. Summary from scientific literature

Reference	Material/ Size	Test Organism/ System	Method	Exposure/ dose	Main findings
Toxicity – in vitro					
Lison D, 2008	Ludox HS-40 Stöber silica nanoparticles 29.3+-4. nm (TEM), 35nm (DLS)	Mouse monocytes (J774), human bronchoalveolar carcinoma (A549), human endothelial cells (EAHY926)	Cytotoxicity (MTT, LDH release, LDH cell content, MTT, and crystal violet staining)	24 h Increasing concentrations of SiO_2 NP in a fixed volume of 200 ll per well or 37 µg/ml dispersed in increasing volumes of DMEM or fixed mass/SA/number of nanoparticles (7.5 µg) dispersed in increasing volumes of DMEM	The cellular response was determined by the total mass/number/SA of particles as well as their concentration and it was concluded that the nominal dose remains the most appropriate metric for in vitro toxicity testing of insoluble SiO_2 NP dispersed in aqueous medium.
Napierska D, 2009	Ludox L-14/L-15 (13.8 nm and 14.7 nm) Stöber silica nanoparticle of 16.4 , 19.4, 60.4 , 104.4 and 335 nm 14, 15, 16, 19, 60, 104 and 335 nm (checked by TEM and DLS)	Human endothelial cells (EAHY926)	Cytotoxicity (MTT, LDH)		It was concluded that that the cytotoxicity of monodisperse amorphous silica nanoparticles with the same morphology was strongly related to particle size. Smaller particles showed significantly higher toxicity than the bigger ones when dose was expressed in mass concentration. The surface area of tested particles was an important parameter determining toxicity of monodisperse amorphous SiO_2 nanoparticles.
Sayes et al., 2007	Zeofree 80 Aggregates of 1-3 µm (DLS)	Rat lung epithelial cells (L2), rat alveolar macrophages, cocultures of the two	Cytotoxicity (MTT, LDH) Inflammation	1 h to 48 h 0.0052–520lg/cm²	SAS was slightly cytotoxic and induced an inflammatory response in macrophages.
Lin W, et al., 2006	15 and 46 nm particles from Degussa TEM measurements: 15±5nm 46±12nm	Human bronchoalveolar carcinoma (A549)	Cytotoxicity Oxidative stress (fluorescence)	24; 48; 72h 10, 50, 100 µg/ml	It was concluded that 15-nm and 46-nm SiO_2 nanoparticles significantly reduce cell viability in a dose dependent and time-dependant manner in bronchoalveolar carcinoma-derived cells at 10–100 µg/ml dosage. Both of the SiO_2 nanoparticles showed higher cytotoxicity than the positive control material (Min-U-Sil 5). The ROS generated by exposure to 15-nm SiO_2 nanoparticles

					produce oxidative stress in these cells as reflected by reduced GSH levels and the elevated production of MDA and LDH, indicative of lipid peroxidation and membrane damage.
Park E-J, 2009	12 nm SAS particles from Degussa Unspecified	Mouse macrophages (RAW264,7)	Inflammation Oxidative stress (fluorescence)	24 h 5; 10; 20; 40 µg/ml	ROS and pro-inflammatory responses
Chang J.S., Chang L.B., 2007	Precipitated from Na silicate SEM analysis: 10-15 nm	Human fibroblasts (WS1, CCD-966sk, MRC-5, A549, MKN-28, HT-29)	Cytotoxicity (MTT, LDH)	48 h 667 µg/ml	The cytotoxicity of silica to human cells depends strongly on their metabolic activities but it could be significantly reduced by synthesizing silica with chitosan.
Jin Y, 2007	Purpose-made dye doped silica 50 nm nanoparticles (from TEOS)	Human bronchoalveolar carcinoma (A549)	Cytotoxicity (MTT)	48 h; 72 h 0.1 µg/ml to 0.5 mg/ml	No significant toxic effects induced by luminescent nanoparticles at the molecular and cellular levels below a concentration of 0.1 mg/mL
Wahl, B, 2008	Aerosil 200 and unspecified 15 nm silica nanoparticles from Merck	Human intestinal epithelial cells(CaCo-2)	Cytotoxicity (LDH, luminescence assay)		LDH assay showed strong interactions with the tested silica particles. These findings suggest that even well characterized assay systems need a careful evaluation of the particle assay interactions when working with nanoparticles. Furthermore, particles based on the same material exhibit different biological properties depending on whether the material is used in micro- or nanometer range.
Ye, 2010	SAS colloids from the Center of Analysis and Test Research (Shangai, China) 21, 48 and 86 nm	Human hepatic cells (L-02)	Cytotoxicity (MTT, LDH) Apoptosis Oxidative stress	12, 24, 36 and 48 h 0.2, 0.4 and 0.6 mg/ml	Cytotoxicity in was investigated for size, dose and time dependence. Oxidative stress and apoptosis were induced by exposure to 21 nm SiO_2.
Yang, 2010	SAS from Wang Jung New Material Co. 13+-3.8 nm 20±3.5 nm 50±9.2 nm 365±79 nm (DLS)	Human keratinocyte cell line (HaCaT)	Proteomic analysis	24 h 2.5 to 80 µg/ml	Size dependent effects on the expression of proteins involved in oxidative stress, cytoskeleton, chaperones, apoptosis, tumour and metabolism is demonstrated

Eom, 2009	Fumed silica (7 nm) Porous silica (5-15 nm) From Sigma	Human bronchial epithelial cell (Beas-2B)	ROS production (fluorescence analysis) Expression of HO-1, Nrf2, NFkB, ikB, ERK, p38 et JNK with western blot	24 h 40 mg/ml	Toxicity via oxidative stress was investigated. Cells exposed to porous silica nanoparticles showed a more sensitive response than those exposed to fumed silica.
Choi SJ, 2009	Aerosil200 (14 nm)	Human lung epithelial cells (A549 and L-132), human epithelial cells (HeLa) and human osteocarcoma cells (MNNG/HOS)	Cytotoxicity ROS measurement Cytokine expression	72 h 125, 250, 500 µg/ml	Small toxic effects on the proliferation or viability of the cells from the 4 cell lines were observed, but, silica significantly generated ROS, induced release of LDH release and IL-8 production from A549 cells.
Brown SC, 2007	SAS synthesized for the study (100 and 200 nm spheres and rods)	Human pleural mesothelial *cells* (*Met5A*)	Cytotoxicity (LDH) Inflammation		Increased LDH release and IL-8 expression in the presence of physiological stretch regardless of shape. Moreover, it is evident that shape-induced aggregation may play a significant role in mitigating particle clearance
Lu, 2009	Purposely prepared mesoporous silica, 30, 50, 110, 170 and 180 nm	Human epithelial cells (HeLa)	Cytotoxicity (MTT) Uptake		Uptake of mesoporous silica by HeLa cells is particle-size-dependent and the maximum uptake by cells occurs at a nanoparticle size of 50 nm. It is expected that the size effect on cell uptake would lead to size-dependent biochemical responses.
Slowing II, 2009	Purposely prepared mesoporous silica (MSN) and unspecified SAS from Sigma Aldrich MSN : 100-300 nm (TEM), ~300nm (DLS) SAS from Sigma: centred at 459 and 1720 nm (DLS)	Rabbit red blood cells	Haemolysis assay Spectroscopy		The authors show that, contrary to the known cytotoxicity of amorphous silica towards RBCs, MSNs exhibit a high biocompatibility at concentrations adequate for potential pharmacological applications. We demonstrated that the haemolytic properties of MSNs are related to the number of silanol groups accessible to the cell membranes of RBCs

Park YH et al., 2010	SAS particles from Degussa7 nm and 10-20 nm (SEM)	Human keratinocytes, human skin equivalent model	Cytotoxicity Irritation		Reduced cell viability no acute cutaneous irritation.
Rabolli V., 2010	Purposely synthesized SAS (2): - Stöber SAS - Lysin Silica Sols and Ludox HS-40, Ludox LS-30, Ludox SM-30	Mouse monocytes (J774), human endothelial cells (EAHY926), mouse fibroblasts (3T3) and human erythrocytes	Cytotoxicity (MTT and WST1 assay)		In J774 macrophages, the cytotoxic activity increased with external surface area and decreased with micropore volume; in EAHY926 and 3T3 cells, the cytotoxic activity increased with surface roughness and small diameter; in erythrocytes, the haemolytic activity increased with the diameter of the SAS nanoparticle. We conclude that it is possible to predict with good accuracy the in vitro

5.10 Summary of in vitro testing by Japan on alternate SiO_2 material

Table 30 below summarises the in vitro test results of the alternate material provided by Japan.

Table 30. Summary of in vitro testing by Japan on alternate SiO2 material

NANOMATERIAL INFORMATION/ IDENTIFICATION	**Nanomaterial name:** Silicon Dioxide (SAS) **Nanotek** **CAS Number:** (CAS no. general for SiO2: 7631-86-9) **Structural formula/ molecular structure:** SiO_2, strong, directional covalent bonds, and has a well-defined local structure: four oxygen atoms are arrayed at the corners of a tetrahedron around a central silicon atom **Composition of nanomaterial being tested:** purity: >99.9 % **Basic morphology:** Amorphous, Spherical shape, Specific surface area (BET): 86.0m^2/g, primary particle size (TEM, average): 25 nm **Description of surface chemistry:** Neither coated nor modified. **Major commercial uses:** as it is a High Production Volume (HPV) chemical; car tires (rubber), printing inks, pharmaceuticals, cosmetics, etc. **Known catalytic activity:** None 1. **Method of production:** Physical Vapor Synthesis (PVS) method 2. **Method of detection:**			
***In Vitro* tests**	- Nanotek primary particle size: 25 nm purity: 99.9 % from C. I. Kasei Co. Ltd. (Japan)	Japan/AIST http://www.aist-riss.jp/projects/nedo-nanorisk/rd/iwahashi2009	Ten different cell lines including A549, HaCaT, and THP-1. Cell viability, oxidative stress, DNA injury, colony	SiO_2 NP induced oxidative stress in cultured cells. The intracellular ROS level was elevated by SiO_2 exposure. Subsequently, cell viability was decreased. The MTT activity was slightly decreased (50 % of untreated cells) at conc. of approx. 50 µg/ml for 24 h exposure. Activity of

	http://www.cik.co.jp/product/nanotek/english/	e.html Contact: t-igarashi@aist.go.jp	forming ability, gene expression of cytokine and apoptosis.	apoptosis related enzyme caspase-3 was increased by 24 h exposure.

6 REFERENCES

[] http://timedomaincvd.com/CVD_Fundamentals/films/SiO2_properties.html

[] http://www.inchem.org/documents/sids/sids/SolubleSilicates.pdf

[] http://www.cdc.gov/niosh/npg/npgd0552.html, consulted 24 Nov. 2009

Introduction, Silica in the Environment and Annexes

[] Adams L. (2006). Adams, L.K., Lyon, D.Y. and Alvarez, P.J.J. "Comparative eco-toxicity of nanoscale TiO_2, SiO_2 and ZnO water suspensions". Water Research, vol. 40, (2006), pp. 3527-3532.

[] Borm P. (2006). Borm, P., Klaessig, F.C., Landry, T.D., Moudgil, B., Pauluhn, J., Thomas, K., Trottier, R. and Wood, S. "Research Strategies for Safety Evaluation of Nanomaterials, Part V: Role of Dissolution in Biological Fate and Effects of Nanoscale Particles". Tox. Sci., vol.90, iss. 1 (2006), pp. 23-32.

[R] Canesi L. (2010a). Canesi, L., Ciacci, C., Vallotto, D., Gallo, G., Marcomini, A. and Pojana, G. (2010) In vitro effects of suspensions of selected nanoparticles (C60 fullerene, TiO_2, SiO_2) on Mytilus hemocytes. *Aquat Toxicol* **96**: 151-158.

[] Canesi L. (2010b). Canesi, L., Fabbri, R., Gallo, G., Vallotto, D. and Marcomini, A. (2010) Biomarkers in *Mytilus galloprovincialis* exposed to suspensions of selected nanoparticles (C60 fullerene, Nano-TiO_2, Nano-SiO_2). *Aquat Toxicol* **100**: 168-177.

[] Casado (2013). Casado M. Macken A. and Byrne H.J. "Ecotoxicological Assessment of Silica and Polystyrene Nanoparticles Assessed by a Multitrophic Test Battery". Environmental International, Vol. 51 (2013) pp. 97-105

[R] Currie (2007). Currie, H.A. and Perry, C.C. (2007) Silica in plants: Biological, biochemical and chemical studies. Annals of Botany **100:** 1383-1389

[] EC (EC, 2006). "Regulation (EC) No 1907/2006 of the European Parliament and of the Council of 18 December 2006 concerning the Registration, Evaluation, Authorisation and Restriction of Chemicals (REACH), establishing a European Chemicals Agency, amending Directive 1999/45/EC and repealing Council Regulation (EEC) No 793/93 and Commission Regulation (EC) No 1488/94 as well as Council Directive 76/769/EEC and Commission Directives 91/155/EEC, 93/67/EEC, 93/105/EC and 2000/21/EC." Official Journal of the European Union (L396/1): 1-849.

[] EC (EC, 2007) Integrated Pollution Prevention and Control. Reference Document on Best Available Techniques for the Manufacture of Large Volume Inorganic Chemicals - Solids and Others industry, chapter 5. August 2007. http://eippcb.jrc.es.

[R] ECETOC (2006). "Synthetic Amorphous Silica (CAS No. 7631-86-9)". JACC No. 51. ISSN-0773-6339-51

[R] Farré M. (2009). Farré, M., Gajda-Schrants, K., Kantiani, L. and Barceló, D. "Ecotoxicity and analysis of nanomaterials in the aquatic environment". Anal. Bioanal. Chem., vol. 393, (2009), pp. 81-95.

[] Fent (2010). FEnt K., Weisbrod C.J., Wirth-Heller A. and Pieles U. "Assessment of uptake and toxicity of fluorescent silica nanoparticles in zebrafish (*Danio rerio*) early life stages." Aquatic Toxicology 100 (2010) pp. 218-228

[] Fujiwara K. (2008). Fujiwara, K., Suematsu, H., Kiyomiya, E., Aoki, M., Sata M.and Moritoki N. "Size dependent toxicity of silica nano-particles to *Chlorella kessleri*". J. Environ. Sci. and Health, Part A, vol. 43, iss. 10, (2008), pp. 1167-1173.

[] Garcia-Saucedo C. (2011). Garcia-Saucedo, C., Field, J.A., Otero-Gonzalez, L. and Sierra-Alvarez, R. (2011) Low Toxicity of HfO_2, SiO_2, $Al2O_3$ and CeO_2 nanoparticles to the yeast, *saccharomyces cerevisiae*. J. Haz. Mat. **192:** 1572-1579

[R] Handy R.D. (2008). Handy R.D., Owen, R. and Valsami-Jones, E. "The ecotoxicology of nanoparticles and nanomaterials: current status, knowledge gaps, challenges and future needs". Ecotoxicology, vol. 17, (2008), pp. 315-325.

[] Ji J. (2011). Ji j., Long Z. and Lin D. "Toxicity of oxide nanoparticles to the green algae *Chlorella* sp." Chemical Engeneering Journal 170 (2011) 525-530

[]W. (2009 Jiang). Jiang, W., Mashayekhi, H. and Xing, B. "Bacterial toxicity comparison between nano- and micro-sized oxide particles". Environmnetal Pollution, vol. 157, (2009), pp. 1619-1625.

[] Kalteh (2014). Kalteh M., Alipour Z.T., Ashraf S., Aliabadi M.M. and Nosratabadi A.F. "Effect of silica Nanoparticles on Basil (Ocimum basilicum) Under Saline Stress". Journal of Chemical Health Risks (2014) 4(3), 49-55

[R] Klaine S.J. (2008). Klaine, S.J., Alvarez, P.J.J., Batley, G.E., Fernandes, T.F., Handy, R. D., Lyon, D.Y., Mahendra, S., McLaughlin M.J. and Lead J.R. "Nanomaterials in the Environment: Behaviour, fate bioavailability and effects". Environ. Tox. Chem., vol. 27, iss. 9, (2008), pp. 1825-1851.

[] Lee S.-W. (2009). Lee, S.-W., Kim, S.-M. and Choi, J. "Genotoxicity and ecotoxicity assays using the freshwater crustacean *Daphnia Magna* and the larva of the aquatic midge *Chironomus riparius* to screen the ecological risks of nanoparticle exposure". Environ. Tox. Pharm, vol. 28, (2009), pp. 86-91.

[R] Liang (2007). Liang, Y., Sun, W., Zhu, Y.-G. and Christie, P. (2007) Mechanisms of silicon-mediated alleviation of abiotic stresses in higher plants: A review. Env. Poll. **147:** 422-428.

[] Lovestam G. (2010) Lovestam, G., Rauscher, H., Roebben, G. Sokull-Klüttgen, B. Gibson, N., Putuad, J.-P. and Stamm,H. "Considerations on a Definition of Nanomaterial for Regulatory Purposes". European Commission, Joint Research Centre, EUR-report 24403 (2010)

[] Mankiewicz-Boczek (2009). Mankiewicz-Boczek j., Osiecki R. and Rydzynski K. "Effect of Ceria and Silica Nanoparticles on Pelagic (Thamnocephalus platyurus) and Benthic (Heterocypris incongruens) Crustaceans " Poster presented at the 14th International Symposium on Toxicity Assessment, Metz, France, August 30 – September 4, 2009

[] Metzler (2012). Metzler D.M., Erdem A., Tseng Y.H. and Huang C.P. "Response of Algal Cells to Engineered Nanoparticles Measured as Algal Cell Population, Chlorophyll a, and Lipid Peroxidation: Effect of Particle Size and Type". Journal of Nanotechnology, Vol. 2012.

[R] Moore (2006). Moore, M.N. "Do nanoparticles present ecotoxicological risks for the health of the aquatic environment?". Env. Int., vol. 32, (2006), pp. 967-976.

[R] Nowack B. (2007). Nowack B. and Bucheli T.D. "Occurrence, behaviour and effects of nanoparticles in the environment". Environmental Pollution.150, (2007) pp. 5-22.

[R] OECD (2004a). OECD SIDS report "Synthetic Amorphous Silica and Silicates". UNEP publication. 2004. Available from http://www.chem.unep.ch/irptc/sids/oecdsids/sidspub.html at http://www.chem.unep.ch/irptc/sids/OECDSIDS/silicates.pdf .

[R] OECD (2004b). OECD SIDS report "Soluble Silicates". UNEP publication. 2004. Available from http://www.chem.unep.ch/irptc/sids/oecdsids/sidspub.html at http://www.chem.unep.ch/irptc/sids/OECDSIDS/silicates.pdf .

[] OECD (2009). Preliminary Review of OECD Test Guidelines for their Applicability to Manufactured Nanomaterials (2009). ENV/JM/MONO(2009)21 .OECD (2010). "Guidance Manual for the Testing of Manufactured Nanomaterials: OECD's Sponsorship Programme". ENV/JM/MONO(2009)20. OECD, Paris.

[] OECD (2012). ENV/JM/MONO(2012)40. Guidance on sample preparation and dosimetry for the safety testing of manufactured nanomaterials, OECD, Paris.

[] OECD [2014]. Report of the OECD Expert Meeting on the Physical Chemical Properties of Manufactured Nanomaterials and Test Guidelines. ENV/JM/MONO(2014)15. Available at http://www.oecd.org/officialdocuments/publicdisplaydocumentpdf/?cote=ENV/JM/MONO(2014)15&docLanguage=En

[] Oya San N. (2014). Oya San N., Kursungoz C., Tumtas Y. Yasa O, Ortac B. and Tekinay T. "Novel one-step synthesis of silica nanoparticles from sugarbeet bagasse by laser ablation and their effects on the growth of freshwater algae culture" Particuology. (2014) in press.

[] Pluskota (2009). Pluskota, A., Horzowski, E., Bossinger, O. and von Mikecz, A. (2009) In *caenorhabditis elegans* nanoparticle-bio-interactions become transparent: Silica nano-particles induce reproductive senescence. PLoS ONE **4(8):** e6622.

[] Rasmussen K.(2013). Rasmussen K., Mech A., Mast J., De Temmerman P.-J, Waegeneers N., Van Steen F., Pizzolon J.C., De Temmerman L., Van Doren E., Jensen K. A., Birkedal R., Levin M., Nielsen S.H., Koponen I.K., Clausen P.A., Kembouche Y., Thieriet N., Spalla O., Giuot C., Rousset D., Witschger O., Bau S., Bianchi B., Shivachev B., Gilliland D., Pianella F., Ceccone G., Cotogno G., Rauscher H., Gibson N. and Stamm H. "Synthetic Amorphous Silicon Dioxide (NM-200, NM-201, NM-202, NM-203, NM-204). Characterisation and Physico-Chemical Properties" European Commission, Joint Research Centre, EUR 26046. (2013)

[] Ramesh (2013). Ramesh, R., Kavitha, P., Kanipandian, N., Arun, S., Thirumurugan, R. and Subra, P. (2013) Alteration of antioxidant enzymes and impairment of DNA in the SiO2 nanoparticles exposed zebra fish (Danio rerio). Environ. Monit. Assess. **185:** 5873-5881.

[] Reijnders L. (2009). L. Reijnders "The release of TiO_2 and SiO_2 nanoparticles from nanocomposites". Polymer Degradation and Stability, 94 (2009) pp. 873-876.

[R] SASSI (2008). "Nanoscale Materials Stewardship programme (NMSP) Voluntary Submittal Package for Synthetic Amorphous Silica (CAS No. 7631-86-9)" prepared by The Synthetic Amorphous Silaca and Silicates Industry Association, SASSI. http://www.epa.gov/oppt/nano/sassia.pdf

[] Sharif (2012). Sharif, F., Porta, F., Meijer, A.H., Kros, A. and Richardson, M.K. (2012) Mesoporous sílica nanoparticles as a compound delivery system in zebrafish embryos. Int. J. Nanomed. **2012:7**, 1875-1890.

[] Siddiqui (2014). Siddiqui M.H. and Al-Whaibi M.H. "Role of nano-SiO_2 in germination of tomato (*Lycopersicum esculentum* seeds Mill.)" Saudi Journal of Biological Sciences (2014) 21, pp. 13-17

[] Sneh (1995). Sneh O. and George S."Thermal Stability of Hydroxyl Groups on a Well-Defined Silica Surface", J Phys Chem vol 99, p. 4639

[] Stone V. (2010). Stone, V., Nowack, B., Baun, A., van den Brink, N., Von der Kammer, F., Dusinska, M., Handy, R., Hankin, S., Hassellöv, M., Joner E.,and Fernandes T.F. "Nanomaterials for environmental studies: Classification, reference materials issues and strategies for physico-chemical characterisation". Sci.Total Environ (2010) Mar 1;408(7):1745-54.

[] Yang K. (2009). Yang, K., Lin, D. and Xing, B. "Interactions of Humic Acid with Nanosized Inorganic Oxides". Langmuir, 25 (2009), pp. 3571-3576.

[] van Hoecke K. (2008). van Hoecke, K., de Schamphelaere, K.A.C., van der Meeren, P., Lucas, S. and Janssen, C.R. "Ecotoxicity of silica nanoparticles to the green alga *pseudokirchneriella subcapitata*: importance of surface area". Environ. Tox. Chem. vol. 27, iss. 9, (2008), pp. 1948-1957.

[] van Hoecke K. (2011). van Hoecke, K., de Schamphelaere, K.A.C., Ramirez-Garcia, S., Smagghe, G. and Janssen, C.R. "Influence of alumina coating on characteristics and effects of SiO_2 nanoparticles in algal growth inhibition assays at various pH and organic matter contents. Environ. Int., 2011, **3:** 1118-1125.

[] Wei (2010). Wei, C., Zhang, Y., Guo, J., Han, B., Yang, X. and Yuan, J. (2010) Effects of silica nanoparticles on growth and photo synthetic pigment contents of *Scenedesmus obliquus*. J. Env. Sci. **22(1)**: 155-160.

Silica and Mammalian Toxicology

In vivo

[] Arts J.H. (2007) Arts, J.H., Muijser, H., Duistermaat, E., Junker, K., and Kuper, C.F. (2007) Five-day inhalation toxicity study of three types of synthetic amorphous silicas in Wistar rats and post-exposure evaluations for up to 3 months. *Food Chem Toxicol* 2007 Oct; 45(10):1856-67.

[] Chen Y. (2004). Chen,Y., Chen,J., Dong,J. and Jin,Y. (2004) Comparing study of the effect of nanosized silicon dioxide and microsized silicon dioxide on fibrogenesis in rats. *Toxicol Ind Health* **20**: 21-27.

[] Cho W.S. (2007). Cho, W.S., Choi, M., Han, B.S., Cho, M., Oh, J., Park, K. Kim, S.J., Kim, S.H. and Jeong, J. (2007) Inflammatory mediators induced by intratracheal instillation of ultrafine amorphous silica particles. *Toxicol. Lett*. Dec 10; **175**(1-3):24-33.

[] Cho M. (2009). Cho, M., Cho, W.S., Choi, M., Kim, S.J., Han, B.S., Kim, S.H., Kim, H.O., Sheen, Y.Y., and Jeong, J. (2009) The impact of size on tissue distribution and elimination by single intravenous injection of silica nanoparticles. Toxicol Lett. **189**: 177-183.

[] Downs T.R. (2012). Downs, T. R., Crosby, M. E., Hu, T., Kumar, S., Sullivan, A., Sarlo, K., Reeder, B., Lynch, M., Wagner, M., Mills, T. and Pfuhler, S. (2012). Silica nanoparticles administered at the maximum tolerated dose induce genotoxic effects through an inflammatory reaction while gold nanoparticles do not. *Mutat Res* **745**: 38-50

[] Ernst H. (2002). Ernst, H., Rittinghausen, S., Bartsch, W., Creutzenberg, O., Dasenbrock, C., Gorlitz,B.D., Hecht, M., Kairies, U., Muhle, H., Müller, M., Heinrich, U. and Pott, F. (2002) Pulmonary inflammation in rats after intratracheal instillation of quartz, amorphous SiO2, carbon black, and coal dust and the influence of poly-2-vinylpyridine-N-oxide (PVNO). *Exp Toxicol Pathol* **54**.

[] Hamilton R.F. (2008). Hamilton, R.F., Jr., Thakur, S.A. and Holian, A. (2008) Silica binding and toxicity in alveolar macrophages. *Free Radic Biol Med* **44**: 1246-1258.

[] Iyer R. (1996). Iyer, R., Hamilton, R.F., Li, L., and Holian, A. (1996) Silica-induced apoptosis mediated via scavenger receptor in human alveolar macrophages. *Toxicol Appl Pharmacol* **141**: 84-92.

[] Kaewamatawong T. (2005). Kaewamatawong,T., Kawamura,N., Okajima,M., Sawada, M., Morita,T. and Shimada,A. (2005) Acute pulmonary toxicity caused by exposure to colloidal silica: particle size dependent pathological changes in mice. *Toxicol Pathol* **33 (7)**:743-9

[] Merget R. (2002). Merget, R., Bauer, T., Kupper, H.U., Philippou, S., Bauer, H.D., Breitstadt, R., and Bruening, T. (2002) Health hazards due to the inhalation of amorphous silica. *Arch Toxicol* **75**: 625-634.

[] Napierska D. (2009). Napierska, D., Thomassen, L.C., Rabolli, V., Lison, D., Gonzalez, L., Kirsch-Volders, M., Martens, J.A. and Hoet, P.H. (2009) Size-dependent cytotoxicity of monodisperse silica nanoparticles in human endothelial cells. *Small* **5**. Apr;5(7):846-53.

[] Nemmar A. (2006). Nemmar, A., Hoet, P.H., and Nemery, B. (2006) Translocation of ultrafine particles. *Environ Health Perspect* **114**: A211-A212.

[] Park E.J. (2009). Park, E.J., and Park, K. (2009) Oxidative stress and pro-inflammatory responses induced by silica nanoparticles in vivo and in vitro. *Toxicol Lett* **184**(1): 18-25.

[] Park E.J. (2011). Park, E.J., Roh, J.K., Kim, Y., and Choi, K. (2011) A single instillation of amorphous silica nanoparticles into mouse lungs induced subchronic inflammatory response. Environ Res. J. Health Sci. 57(1) 60-71.

[] Reuzel P.G. (1991). Reuzel, P.G., Bruijntjes, J.P., Feron, V.J., and Woutersen, R.A. (1991) Subchronic inhalation toxicity of amorphous silicas and quartz dust in rats. *Food Chem Toxicol* **29**: 341-354.

[] So S.J. (2008). So, S.J., Jang, I.S. and Han, C.S. (2008) Effect of micro/nano silica particle feeding for mice. *J Nanosci Nanotechnol.* **8(10)**: 5367-5371.

[] TakizawaY. (1988). Takizawa, Y., Hirasawa, F., Noritomi, E., Aida, M., Tsunoda, H. and Uesugi, S. (1988) Oral ingestion to mice and rats and its chronic toxicity and carcinogenicity. Acta Medica et Biologica, 36, 27-56

[] Warheit D. (2006). Warheit, D.B., Webb, T.R., and Reed, K.L. (2006) Pulmonary toxicity screening studies in male rats with TiO2 particulates substantially encapsulated with pyrogenically deposited, amorphous silica. *Part Fibre Toxicol* **3**.

[] Warheit D. (1995). Warheit, D.B., McHugh, T.A., and Hartsky, M.A. (1995) Differential pulmonary responses in rats inhaling crystalline, colloidal or amorphous silica dusts. *Scand J Work Environ Health* **21 Suppl 2**: 19-21.

In vitro

[] Barik T.K. (2008). Barik, T. K., Sahu, B. and Swain V. "Nanosilica-from medicine to pest control." Parasitol.Res. 103.2 (2008): 253-58.

[] Barnes C.A. (2008). Barnes, C.A., Elsaesser, A., Arkusz, J., Smok, A., Palus, J., Lesniak, A. *et al.* (2008) Reproducible comet assay of amorphous silica nanoparticles detects no genotoxicity. *Nano Lett* **8**: 3069-3074.

[] Brown S.C. (2007). Brown, S.C., Kamal, M., Nasreen, N., Baumuratov, A., Sharma, P., Antony, V.b. and Moudgil, B.M. (2007) Influence of shape, adhesion and simulated lung mechanics on amorphous silica nanoparticle toxicity. *Advanced Powder Technol* **18**: 69-79.

[] Chang J.S. (2007). Chang, J.S., Chang,K.L., Hwang,D.F., and Kong,Z.L. (2007) In vitro cytotoxicitiy of silica nanoparticles at high concentrations strongly depends on the metabolic activity type of the cell line. *Environ Sci Technol* **41**.

[] Choi S.J. (2009). Choi, S.J., Oh, J.M. and Choy, J.H. (2009) Toxicological effects of inorganic nanoparticles on human lung cancer A549 cells. *J Inorg Biochem* **103**: 463-471.

[] Eom H.J. (2009). Eom,H.J., and Choi,J. (2009) Oxidative stress of silica nanoparticles in human bronchial epithelial cell, Beas-2B. *Toxicol In Vitro* **23**: 1326-1332.

[] Gonzalez L. (2010). Gonzalez, L., Thomassen, L.C., Plas, G., Rabolli, V., Napierska, D. and Decordier, I. et al. Exploring the aneugenic and clastogenic potential in the nanosize range: A549 human lung carcinoma cells and amorphous monodisperse silica nanoparticles as models. Nanotoxicology 2010 Dec;4:382-95.

[] Jin Y. (2007). Jin,Y., Kannan,S., Wu,M., and Zhao,J.X. (2007) Toxicity of luminescent silica nanoparticles to living cells. *Chem Res Toxicol* **20**.

[] Lin W. (2006). Lin,W., Huang,Y.W., Zhou,X.D., and Ma,Y. (2006) In vitro toxicity of silica nanoparticles in human lung cancer cells. *Toxicol Appl Pharmacol* **217**.

[] Lison D. (2008). Lison,D., Thomassen,L.C., Rabolli,V., Gonzalez,L., Napierska,D., Seo,J.W. *et al.* (2008) Nominal and effective dosimetry of silica nanoparticles in cytotoxicity assays. *Toxicol Sci* **104**.

[] Lu F. (2009). Lu,F., Wu,S.H., Hung,Y., and Mou,C.Y. (2009) Size effect on cell uptake in well-suspended, uniform mesoporous silica nanoparticles. *Small* **5**: 1408-1413.

[] Napierska D. (2009). Napierska,D., Thomassen,L.C., Rabolli,V., Lison,D., Gonzalez,L., Kirsch-Volders,M. *et al.* (2009) Size-dependent cytotoxicity of monodisperse silica nanoparticles in human endothelial cells. *Small* **5**.

[] Park E.J.(2009). Park,E.J., and Park,K. (2009) Oxidative stress and pro-inflammatory responses induced by silica nanoparticles in vivo and in vitro. *Toxicol Lett* **184**.

[] Sayes C.M. (2007). Sayes,C.M., Reed,K.L., and Warheit,D.B. (2007) Assessing toxicity of fine and nanoparticles: comparing in vitro measurements to in vivo pulmonary toxicity profiles. *Toxicol Sci* **97**.

[] Slowing (2009). Slowing, II, Wu,C.W., Vivero-Escoto,J.L. and Lin,V.S. (2009) Mesoporous silica nanoparticles for reducing hemolytic activity towards mammalian red blood cells. *Small* **5**.

[] Wahl B. (2008). Wahl,B., Daum,N., Ohrem,H.L., and Lehr,C.M. (2008) Novel luminescence assay offers new possibilities for the risk assessment of silica nanoparticles. *Nanotoxicology* **2**: 243-251.

[] Yang X. (2010). Yang,X., Liu,J., He,H., Zhou,L., Gong,C., Wang,X. *et al.* (2010) SiO2 nanoparticles induce cytotoxicity and protein expression alteration in HaCaT cells. *Part Fibre Toxicol* **7**: 1.

[] Ye Y. (2010). Ye,Y., Liu,J., Xu,J., Sun,L., Chen,M., and Lan,M. (2010) Nano-SiO2 induces apoptosis via activation of p53 and Bax mediated by oxidative stress in human hepatic cell line. *Toxicol In Vitro* **24**: 751-758.

[R] O'Farrell N. (2006). N. O'Farrell, A. Houlton and B.R. Horrocks. "Silicon nanoparticles: applications in cell biology and medicine". Int. J. Nanomedicine, I(4), (2006) pp. 451-472.

[] Park Y.H. (2010). Park Y.H., Kim, J.N., Jeong, S.H., Choi, J.E., Lee, S.H., Choi, B.H., Lee, J.P., Sohn, K.H., Park, K.L., Kim, M.K., and Son, S.W. (2010) Assessment of dermal toxicity of nanosilica using cultured keratinocytes, a human skin equivalent model and an in vivo model. Toxicology. 267: 178-181.

[] Rabolli (2010). Rabolli V, Thomassen LC, Princen C, Napierska D, Gonzalez L, Kirsch-Volders M, et al. Influence of size, surface area and microporosity on the in vitro cytotoxic activity of amorphous silica nanoparticles in different cell types. Nanotoxicology 2010 Sep;4(3):307-18.

[] Thomassen L.C.(2010). Thomassen, L.C., Aerts, A., Rabolli, V., Lison, D., Gonzalez, L., Kirsch-Volders M, et al. Synthesis and characterization of stable monodisperse silica nanoparticle sols for in vitro cytotoxicity testing. Langmuir 2010 Jan 5;26(1):328-35.

I. ANNEX I: MATERIAL SELECTION

Silicon dioxide (SiO_2) exists in a number of different structural forms, and for the materials selection some background information was needed, and it is outlined below.

Silicon dioxide forms

Silicon dioxide has the general CAS no. 7631-86-9, covering all forms i.e. both crystalline and non-crystalline (amorphous) forms. Amorphous silica forms are subdivided in naturally occurring amorphous silica (diatomite) and synthetic forms. Synthetic amorphous silica (SAS) as defined here is intentionally manufactured and does therefore not contain measurable levels of crystalline silica which causes adverse health effects such as silicosis (Arts et al. ; Merget et al. 625-34).

Synthetic amorphous silica can be divided in two groups according to whether the manufacturing process is by the wet route (precipitated silica, silica gel, colloidal silica, CAS No 112926-00-8) or the thermal route (pyrogenic silica, CAS No 112945-52-5). Colloidal silica (silica sols) is stable dispersions of SASs in a liquid, usually water.

Furthermore, SASs, which are generally hydrophilic, may become hydrophobic after surface treatment. SASs exist as highly pure, white, fluffy powders or milky-white dispersions of these powders in liquids (usually water). The different SASs have different CAS numbers according to the route of production, see figure IV.1.

From figure IV.1, it is evident that "synthetic amorphous silica" a general description of the output of chemical manufacturing processes. A specific final product is described e.g. by giving the manufacturing process, the processing plant, trade name and the physical-chemical characteristics. In the following the term "source" will used as denominator for such a specific final product.

Figure IV.1. Overview of forms of Silicon Dioxide [CAS No. in brackets]

<table>
<tr><th colspan="3">Silicon Dioxide [CAS No. 7631-86-9]</th></tr>
<tr>
<td>Synthetic Amorphous Silica [7631-86-9]
Wet Route production
* Silica gel [112926-00-8]
* Precipitated Silica [112926-00-8]
Thermal Route Production
* Pyrogenic Silica [112945-52-5]
Surface modified silica
For example:
* [67762-90-7],
* 68611-44-9],
* [68909-20-6]</td>
<td>Amorphous Silica [7631-86-9]
Natural:
* Kieselguhr [61790-53-2]
* Calcinated [91053-39-3]
* Flux-calcinated [68855-54-9]
By-products
* Fused silica [60676-86-0]
* Silica fume [69012-64-2]</td>
<td>Crystalline Silica [7631-86-9]
* Crystobalite [14464-46-1]
* Quartz [14808-60-7]
* Tridymite [15468-32-3]</td>
</tr>
</table>

In the OECD Sponsorship Program, the main criteria for selecting a principal material are widespread application(s) combined with a significant market for the material, and the nano status is implicit as the material is proposed under the sponsorship programme. When discussing with BIAC which of the SASs to choose as a principal material, BIAC highlighted that many of the qualities of SAS on the market would be micron scale rather than nano scale due.

In order to select the principal SAS, a further understanding of the structure of SASs was needed and several meetings with ASASPS took place during 2009. The first one was held 12 January 2009, where BIAC stated that synthetic amorphous silica is, according to ISO definitions, a nanostructured material consisting of primary nanoparticles which quickly aggregate and agglomerate. In addition, the meeting concluded that little or no material characterization with regard to physical-chemical properties as required under the OECD Sponsorship program was available for the test materials used in the toxicological and ecotoxicological studies[5] presented on this occasion. Since SAS consists of aggregates with a mean size above the nanoscale, which build up agglomerates with a size range above 100µm, it was not straight forward to decide which SAS material(s) to select as a principal material for the Sponsorship Program and quite some discussion took place, arriving at the following conclusions:

Based on current information available the aggregates and agglomerates of SASs used in the current main applications do not belong to the nano-scale.

In addition, while the SAS aggregates and agglomerates are known to be nanostructured, the number of discrete nanoparticles and/or nano-sized aggregates which they may contain is not clear as characterization data are lacking.

The particle size of SAS particles corresponds to the aggregates, which have a size distribution, so that a tail of particles with smaller sizes may be present.

Analysis of some background information

Three main reference reports on silicon dioxide have been identified: the aforementioned reports ECETOC JACC report No. 51 and the OECD HPV report and the SASSI report.

Analysing the available information relating to the physical-chemical data presented in these reports, and especially the characterization of size of particles used in the studies, clearly underline that a thorough material characterization is needed for the OECD sponsorship program, as neither report contain any detailed characterization data with regard to physical-chemical properties as required under the OECD Sponsorship program. The registration dossier under REACH provides "classical" physic-chemical characterisation and only little information relevant for the end-points under the OECD Sponsorship Program.

The OECD High Production Volume (HPV) Chemicals report on synthetic amorphous silica and silicates gives a good general description of SAS under the HPV program. An underlying assumption in this report, which was agreed to by OECD under the HPV program, is that the different SASs are sufficiently similar that their data obtained by using OECD test guidelines for chemicals can be combined into one HPV dataset. As a consequence of this combination of data, the base data set for one source of SAS which is required under the OECD WPMN program cannot be extracted from the summary information presented. ASASP has offered to support the sponsors for extracting from the original study reports a base data set for one source of SAS as far as data are available. The report contains limited detailed characterization data with regard to the physical-chemical properties as required under the OECD Sponsorship program. In order to possibly use the data for the OECD sponsorship program for nanomaterials it would be necessary to extract and evaluate the substance characterization information, if available, from each original study.

[5] The outcome of those studies are part of the information found the document published by ECETOC, Synthetic amorphous silica, JACC n° 51, ISSN-0773-6339-51, 2006.

The JACC report, p.12, cites information that the primary particle size is in the range of 0.001 to 0.1 micron, i.e. the primary particles are nano-sized, adding the footnote that "Primary particles do not normally exist as individual units". The report analyses in more detail the size of particles concluding that (p. 38) "Under conditions of normal technical handling and use, agglomerates[6] are the relevant particles, both for pyrogenic and precipitated SAS." Appendix B of the JACC report lists the SAS types mentioned in the report and the list contains 49 hydrophilic SAS, which are the ones of interest for the OECD sponsorship program. The report does not give a detailed material characterization with regard to the physical-chemical properties as required under the OECD Sponsorship program. The JACC report indicates [p. 25] that the different sources of SAS have different particle structures depending on the route of manufacture. In order to possibly use the data for the OECD Sponsorship Program it would be necessary to extract and evaluate the substance characterization information, if available, from each original study.

The SASSI report is essentially based on data presented in the two reports mentioned above and it demonstrates that SAS is a nanostructured material, but does not provide in-depth characterization data for individual sources of SAS with regard to the physical-chemical properties as required under the OECD Sponsorship program. In addition, the SASSI report indicates [page 16] that depending on the manufacturing process, the different sources of SAS differ across several physical-chemical properties, including size and surface area.

It is important, in this context, to note that the OECD WPMN and the OECD HPV programme are two programmes addressing different issues. The OECD HPV programme addresses industrial chemicals reported to be produced or imported at levels greater than 1,000 tonnes through hazard assessment of those chemicals based on the Screening Information Data Set (SIDS, guideline and overview of tests available at http://www.oecd.org/dataoecd/13/18/36045056.pdf) obtained by applying current OECD test guidelines. The OECD WPMN agreed an initial list of fourteen representative manufactured nanomaterials and a list of endpoints, which would be addressed for the hazard assessment of those materials. The WPMN then launched the OECD's Sponsorship Programme on the Testing on Manufactured Nanomaterials, to generate this information for the selected manufactured nanomaterials through actual testing, preferably using the OECD test guidelines. Based on the results it is hoped to be possible to evaluate (1) best ways to characterise the physical-chemical properties of nanomaterials, (2) if the OECD test guidelines are applicable to nanomaterials or if modifications or new methods are needed, and (3) how far properties of a nanomaterial differ from the bulk equivalent, if existing, with respect to human health and environmental safety. Thus the two programmes have different scopes, and results from one programme are not necessarily transferable to the other.

Thus, under WPMN's sponsorship programme, the principal SAS needs its own specific data set where the reported test results relate to tests performed using specifically the principal SAS. Alternate SASs will also be tested, at least with regard to the physical-chemical data.

In conclusion, the reports mentioned above present information on different nanostructured sources of SAS which are combined into one dataset. This is not the objective of the sponsorship programme, where a complete sponsorship programme dataset is required for one principal material and also characterization of the SAS with regard to the physical-chemical properties as required under the OECD Sponsorship program. For the (eco-) toxicological testing the substance used in the tests performed is either not mentioned in the reports or the source is given, but the physical-chemical

[6] In the JACC report, p. 24, the convention is described: "Agglomerates are assemblies of aggregates"

characterisation data are not. The reports are thus good background information giving a general overview of SASs.

Towards selecting principal material

After several meetings, ASASP, a member of CEFIC which belongs to BIAC, suggested a number of materials with different uses and process of production; the colloidal silicon dioxides were then excluded as the liquid phase could contain anti-microbial agents, necessitating a number of additional studies to if this would influence the outcome of the (eco)toxicity testing. A number of candidate materials were identified, based on volume and use, see table IV.1:

Table IV.1. Possible principal material for synthetic amorphous silica.

JRC Reference	Sample Refer.	Use	Production process
NM-200	PR-A-02	Food	precipitated
NM-201	PR-B-01	Rubber	precipitated
NM-202	PY-AB-03	Rubber and Food	pyrogenic
NM-203	PY-A-04	Food	pyrogenic
NM-204	PR-A-05	Food	precipitated

The background reports mentioned before outline a number of differences in the properties of the silicon dioxide obtained through the two production methods: The JACC report describes (p.24-25) that the different routes of manufacture for SAS lead to different particle structures: the precipitation route leads to compact aggregates whereas the pyrogenic route leads to open branch chain aggregates. Another interesting difference is the number of silanol groups (Si-OH) per unit surface area (per nm^2) which varies from 5.0 to 5.7 for precipitated silica, to 1.25 to 2.5 for pyrogenic silica (p.15). The silanol group is hydrophilic and the solubility of SAS depends on the number of silanol groups per unit surface area, i.e. the solubility of silicon dioxide depends on route of production.

II. ANNEX II: CONTACT DETAILS FOR INVOLVED INSTITUTIONS

A. European Commission (EC)

Joint Research Centre, Institute for Health and Consumer Protection (JRC, IHCP)
Kirsten Rasmussen
TP 202, Via E Fermi 2749
21027 Ispra (VA), Italy
Tel.: +(39) 0332 78 5344
E-mail: Kirsten.Rasmussen@ec.europa.eu

B. France

Ministère de la Santé, de la Jeunesse et des Sports
Direction Générale de la Santé
Myriam Saihi
14 avenue Duquesne
75350 Paris 07 SP
Tel: +33 1 4056 7929
Fax: +33 1 4056 5056

ANSES (French Agency for Food, Environmental and Occupational Health & Safety)
Nathalie Thieriet
253, Av. Du General Leclerc
F-94701 Maisons-Alfort Cedex
Tel: +33 1 5629 5199
Fax: +33 1 4396 3767
E-mail: nathalie.thieriet@afsset.fr

C. Belgium

Scientific Institute of Public Health
Paul Troisfontaines
Juliette Wytsmanstraat 14
B-1050 Brussels
Tel: +(32) 2 642 53 86
Fax: +(32) 2 642 52 24
Email: paul.troisfontaines@iph.fgov.be

SPF Sante publique, Sécurité de la chaine alimentaire et environnement
Juan David Piñeros Garcet
Direction générale Environnement
Service Maîtrise des risques
Place Victor Horta 40, bte 10
B-1060 Bruxelles.
Tel: +32 (0)2 524 96 72
Fax: + 32 (0)2 524 96 03
E-mail: Juan.pineros@health.fgov.be

D. Korea

National Institute of Environmental Research (NIER)

Ministry of Environment

Kyunghee Choi
Environmental Research Complex
Kyungseo-dong,
Seo-gu,
404-708 Incheon
Korea
Tel.: +(82) 32 560 7206
Fax: +(82) 32 568 2041
E-mail: nierchoi@me.go.kr

Sang Hee Lee
Environmental Exposure Assessment Division
National Institute of Environmental Research
Gyeongseo-dong, Seo-gu
404-708 Incheon,
Korea
Tel.: +(82) 32 560 7216
Fax: +(82) 32 568 2041
E-mail: envirlee@korea.kr

E. BIAC

On behalf of CEFIC ASASP sector group

Monika Maier, PhD
Evonik Degussa GmbH
Rodenbacher Chaussee 4
63457 Hanau-Wolfgang
Germany
Tel: 0049-6181-59-4964
Fax:0049-6181-59-4205
E-mail: Monika.Maier@evonik.com

Bernard Hendrickx, PhD
Rhodia Services
20, rue Marcel Sembat
BP 70026
69191 Saint Fons Cedex
Tel.:0033 4 72 80 21 58
Fax:0033 4 72 80 21 41
E-Mail:
bernhard.hendrickx@eu.rodia.com

Philippe Cochet
Rhodia Operations
190 Avenue Thiers
F-69006 Lyon
Tel: 0033 4 37 24 88 88
Fax: 0033 4 37 24 88 89
E-Mail: philippe.cochet@eu.rodia.com

Mario Heienmann, PhD
Wacker Chemie AG
Johannes-Hess-Straße24
D-84489 Burghausen
Tel: 00498677 83-4022
Fax: 00498677 83-6814
E-Mail: mario.heinemann@wacker.com

F. Denmark

National Research Centre for the Working Environment (NRCWE)

Keld Alstrup Jensen
Nanotoxicology and Occupational Hygiene Group
Lersø Parkallé 105
DK-2100 Copenhagen, Denmark
Tel. direct: +45 3916 5302
E-mail kaj@nrcwe.dk

III. ANNEX III: ENDPOINTS IN THE WPMN TESTING PROGRAMME

Nanomaterial Information / Identification		**Environmental fate**	
1	Nano material name	27	Dispersion stability in water
2	CAS number	28	Biotic degradability
3	Structural formula / molecular structure	29	- Ready biodegradability
4	Composition of NM being tested (incl. degree of purity, known impurities or additives)	30	- Simulation testing on ultimate degradation in surface water
5	Basic Morphology	31	- Soil simulation testing
6	Description of surface chemistry (e.g. coating or modification)	32	- Sediment simulation testing
7	Major commercial uses	33	- Sewage treatment simulation testing
8	Known catalytic activity	34	Identification of degradation product(s)
9	Method of production (e.g. precipitation, gas phase)	35	Further testing of degradation product(s) as required
Physical-chemical Properties and Material Characterization		36	Abiotic degradability and fate
10	Agglomeration / aggregation	37	- Hydrolysis, for surface modified nanomaterials
11	Water solubility	38	Adsorption- desorption
12	Crystalline phase	39	Adsorption to soil or sediment
13	Dustiness	40	Bioaccumulation potential
14	Crystallite size	41	Bioaccumulation in sediment
15	Representative TEM picture(s)	**Environmental toxicology**	
16	Particle size distribution	42	Effects on pelagic species (short/ long term)
17	Specific surface area	43	Effects on sediment species (short/ long term)
18	Zeta potential (surface charge)	44	Effects on soil species (short/ long term)
19	Surface chemistry (where appropriate)	45	Effect on terrestrial species
20	Photo-catalytic activity	46	Effect on micro-organisms
21	Pour density Must be completed	47	Other relevant information
22	Porosity	**Mammalian toxicology**	
23	Octanol-water partition coefficient, where relevant	48	Pharmacokinetics (ADME)
24	Redox potential	49	Acute Toxicity
25	Radical formation	50	Repeated dose toxicity
26	Other relevant information (where available)		IF AVAILABLE
		51	Chronic toxicity
Material safety		52	Reproductive toxicity
57	Flammability	53	Developmental toxicity
58	Explosivity	54	Genetic toxicity
59	Incompatability	55	Experience with human exposure
		56	Other relevant test data

IV. ANNEX IV: PARTNERS OF THE JOINT ACTION NANOGENOTOX

List of collaborating partners in NANOGENOTOX:

Institution	**Name**	**Address (city, country)**
Ministère des affaires sociales et de la santé - Ministry of Social Affairs and Health	Huguette Dechariaux	Paris, France
Joint Research Centre (JRC)	Kirsten Rasmussen	Ispra, Italy
Sosiaali- ja terveysministeriö -Finland Ministry of Social Affairs and Health	Anneli Törrönen	Helsinki, Finland
Federal public service for health, food chain safety and the environment	Juan D. Piñeros Garcet	Brussels, Belgium
Ministerie van Infrastructuur en Milieu - Ministry of Infrastructure and the Environment	Willem Jan Kemmeren	Den Haag, the Netherlands
Health Protection Agency	Robert Maynard	London, United Kingdom
Ministerio de Sanidad y Politica Social	Fernando Carreras Vaquer	Madrid, Spain
Ministero della salute	Carlo Donati	Roma, Italy
Bundesministerium für Umwelt, Naturschutz und Reaktorsicherheit – Federal Ministry for the Environment Natur Conservation and Nuclear Safety	Anke Jesse	Berlin, Germany
University College Dublin	Iseult Lynch	Dublin, Ireland
Agence Nationale de Sécurité du Médicament et des Produits de Santé (ANSM) - French Health Products Safety Agency	Dominique Masset	Saint Denis, France
Laboratoire national de métrologie et d'essais (LNE)	Charles Motzkus	Paris, France
Institut national de l'environnement industriel et des risques (INERIS)	Bénédicte Trouiller	Verneuil-en-Halatte, France
Rennes 1 University	Agnès Burel	Renne, France
Duke University	Lee Ferguson	Durham, USA

V. ANNEX V: OVERVIEW OF CHARACTERISATION RESULTS FOR NM-201, NM-202, NM-203 AND NM-204

NM-201, summary of physical-chemical characterisation results

Method	Institution	Results for NM-201
Homogeneity		
DLS		Study not performed
Agglomeration / aggregation		
SAXS	CEA	Structure and size parameters extracted from SAXS data. Gyration radius of primary particles and aggregates $2xRg_1$: 20 nm and $2xRg_2$: 180 nm, fractal dimension D_f: 2.45 and number $N_{part/agg}$ of particles per aggregate: 457
DLS	CEA	• Ultra-pure water dispersion (intra vial study) Z-average (nm): 208.1±34.5, PdI: 0.352±0.028 • Ultra-pure water dispersion (inter vial study) Z-average (nm): 197.0±15.7, PdI: 0.337±0.020
	JRC	• miliQ water dispersion. Z-average (nm): peak 1: 161, peak 2: 968, PdI: 0.420
TEM	CODA-CERVA, IMC-BAS	High porosity nanostructured material which may be considered aggregates of primary particles. Mean diamater (nm): 43±4. Feret min: 25.4 nm (median of 5331) Feret max: 34.5 nm (median of 5331) Morphology of aggregates/agglomerates: Medium sphericity, rounded to well--rounded. % of aggegates <100 nm: 91±2
AFM	CEA	Third dimension of the agglomerates/aggregates: median (of 1275): 33.5 nm
Water Solubility		
24-hour acellular *in vitro* incubation test	NRCWE	The 24-hour dissolution ratio of NM-201 was measured in three different media: 0.05% BSA in water, Gambles solution and Caco 2 media. Both NM-201 and the Al impurities are partially soluble in Gambles Solution and Caco2 media but amounts vary considerably with the medium. In 0.05% BSA in water only the Al impurities were partially soluble, Si was below the detection limit. The relative amounts of dissolved Al impurities and dissolved Si differed depending on medium, which suggests different solubility behaviour of the Al impurity and NM-201 depending on the medium.

Method	Institution	Results for NM-201
Crystalline phase		
XRD	JRC	Synthetic amorphous silica. Traces of crystalline material seen around 2-Theta equal to 32° and 34°, which is consistent with the suggested presence of Na_2SO_4
	NRCWE	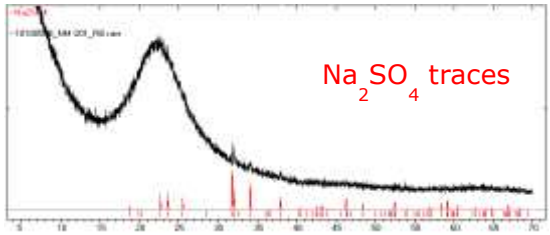 Synthetic Amorphous silicon dioxide; impurities of Na_2SO_4.
	IMC-BAS	Synthetic amorphous silicon dioxide.
Dustiness		
Small Rotating Drum	NRCWE	Inhalable dustiness index (n=3) 6034±199 Respirable dustiness index (n=3) 218±24
Vortex Shaker Method	INRS	Respirable dustiness index (n=1) 65000
Crystallite size		
SAXS	CEA	Amorphous material. Equivalent diameter for spheres: 22 nm, gyration radius $2xRg_1$ = 20 nm
XRD	JRC	Synthetic amorphous silica. Traces of crystalline material seen around 2-Theta equal to 32° and 34°, which is consistent with the suggested presence of Na_2SO_4
	NRCWE	Synthetic amorphous silicon dioxide. Crystalline impurities of Na_2SO_4.
Representative TEM picture(s)		
TEM	CODA-CERVA, IMC-BAS	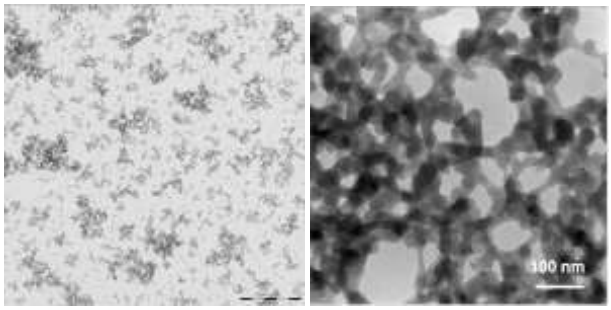 Aggregates with complex, open network structure.

Method	Institution	Results for NM-201
Particle size distribution		
SAXS	CEA	Equivalent diameter for spheres: 22 nm, gyration radius $2xRg_1$ = 20 nm
TEM	CODA-CERVA	Primary particle size: 17±8 nm
	IMC-BAS	Primary particle size: 18
	INRS	Primary particle size: 19±4 nm
TEM	CODA-CERVA, IMC-BAS	Number (expressed in %) of SAS NM particles smaller than 100nm, 50nm and 10nm <100 nm - 81.5%, <50 nm – 55.3% <10 nm – 1.1%
DLS	CEA	The material is polydisperse. The intensity size distribution, which consists of two main peaks is very broad and revels the presence of large aggregates of few microns. • Ultra-pure water dispersion (intra vial study) Z-average (nm): 208.1±34.5, PdI: 0.352±0.028, FWHM peak width(nm): 140.4±105.7 • Ultra-pure water dispersion (inter vial study) Z-average (nm): 197.0±15.7, PdI: 0.337±0.020 FWHM peak width(nm): 105.6±49.3
	JRC	The material is polydisperse. The intensity size distribution, which consists of two main peaks is very broad and revels the presence of large aggregates of few microns. • miliQ water dispersion. Z-average (nm): peak 1: 161, peak 2: 968, PdI: 0.420
CLS	JRC	Peak (nm): 88, half width: 136, CLS Pdl: 2.65
Specific Surface Area		
BET	IMC-BAS	140.46 (m^2/g)
SAXS	CEA	123.3±8.3 (m^2/g)
Zeta Potential (surface charge)		
Zetametry	CEA	NM-201 forms a stable suspension, with negatively to neutral charged particles. The zeta potential varied greatly as function of pH and reached -40 mV around pH 7. IEP <2
	JRC	Zeta potential at pH 6.9, milliQ water: -51.7 (mV).
Surface Chemistry		
XPS	JRC	The following elements were identified in the surface of NM-201: O (70.3 at%), Si (23.6 at%), C (4.5 at%), Na (1.5 at%), Ce (0.25 at%) and S (0.01 at%).The presence of C is considered to be due to surface contamination.
TGA	NRCWE	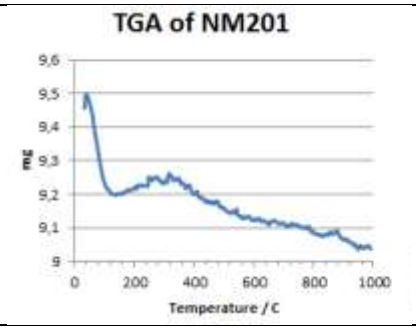 A significant mass loss is observed below 100°C (water). Gradual 3 wt% mass loss was observed above 110°C and may indicate some associated organic compounds.

Method	Institution	Results for NM-201
Photo-catalytic activity		
End-point not relevant for SAS		
Pour-density		
Weighing	INRS	0.28 g/cm^3 (8 wt.% water content)
Porosity		
BET	IMC-BAS	Micropore volume (mL/g): 0.00916
Octanol-water partition coefficient,		
End-point not relevant		
Redox potential		
OxoDish fluorescent sensor plate for O_2 detection	NRCWE	The evolution of O_2 level during 24-hour incubation was measured in three different media. Different dO_2 values were observed for all applied media. In the Gambles solution and Caco 2 media the concentration of dO_2 was the highest (increased ca. 40 µmol/l) for 0.16mg/ml concentration of NM-201. In the 0.05% BSA in water the dO_2 level increases along with the concentration of NM-201 The results suggest that NM-201 has oxidative behaviour in these incubation media.
Radical formation		
HPLC + UV	NRCWE	Using the benzoic acid probe to form 4 hydroxy benzoic acid in a phosphate buffered hydrous solution, gave no detectable concentration OH radicals.
Composition		
ICP-OES	CODA-CERVA	>0.01%: Al(>0.1%), Ca, Na(>0.1%), S; 00.5-0.01%: Zr; 0.001-0.005%: Fe, K, Mg
EDS	IMC-BAS	Na-4400ppm, Al- 7400ppm, S- 4600ppm, Si -45.27 (wt %), O (wt%) calculated- 53.08

NM-202, summary of physical-chemical characterisation results

Method	Institution	Results for NM-202
Homogeneity		
DLS		Study not performed.
Agglomeration / aggregation		
SAXS	CEA	Structure and size parameters extracted from SAXS data. Gyration radius of primary particles and aggregates Rg_1: 16 nm and Rg_2: 100 nm, fractal dimension D_f: 2.5 and number $N_{part/agg}$ of particles per aggregate: 200
DLS	CEA	• Ultra-pure water dispersion (intra vial study) Z-average (nm): 175.9±4.5, PdI: 0.355±0.001
	JRC	• miliQ water dispersion. Z-average (nm): peak 1: 156, peak 2: 200, PdI: 0.160
TEM	CODA-CERVA, IMC-BAS	High porosity nanostructured material which may be considered aggregates of primary silicon dioxide particles. Mean diamater (nm): 53±9. Feret min: 37.2 nm (median of 4248)

Method	Institution	Results for NM-202
		Feret max: 58.4 nm (median of 4248) Morphology of aggregates/agglomerates: Low sphericity—very angular to sub-angular. % of aggregates <100 nm: 87±2
AFM	CEA	Third dimension of the agglomerates/aggregates: median (of 1103): 38.2 nm
Water Solubility		
24-hour acellular *in vitro* incubation test	NRCWE	The 24-hour dissolution ratio of NM-202 was measured in three different media: 0.05% BSA in water, Gambles solution and Caco 2 media. Both NM-202 and the Al impurities are partially soluble in all media but amounts vary considerably with medium as does the relative amounts of dissolved Al impurities compared with dissolved Si suggesting different solubility behaviour of the Al impurity and NM-202 depending on the medium.
Crystalline phase		
XRD	JRC	Synthetic amorphous silicon dioxide.
	NRCWE	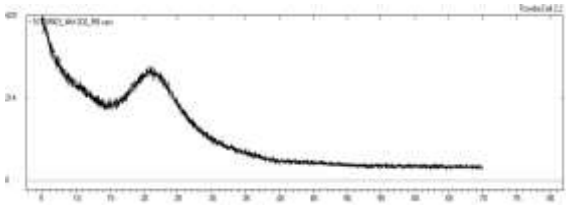 Synthetic amorphous silicon dioxide; impurities of Böhmite (γ-AlO(OH)).
	IMC-BAS	Synthetic amorphous silicon dioxide.
Dustiness		
Small Rotating Drum	NRCWE	Inhalable dustiness index (n=3) 4988±1866 Respirable dustiness index (n=3) 91±11
Vortex Shaker Method	INRS	Respirable dustiness index (n=1) 510000
Crystallite size		
SAXS	CEA	Amorphous material. Equivalent diameter for spheres: 22 nm, gyration radius $2xRg_1$ = 15 nm
XRD	JRC	Synthetic amorphous silicon dioxide.
	NRCWE	Synthetic amorphous silicon dioxide. Crystalline impurities of Böhmite (γ-AlO(OH)).

Method	Institution	Results for NM-202
Representative TEM picture(s)		
TEM	CODA-CERVA, IMC-BAS	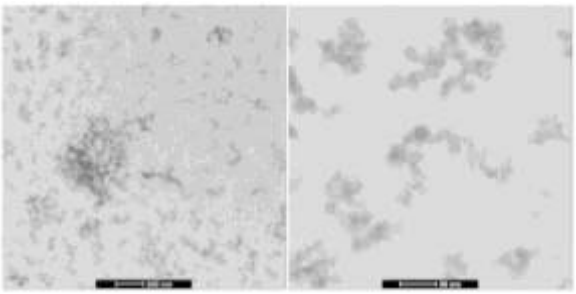 Aggregates with complex, open network structure.
Particle size distribution		
SAXS	CEA	Equivalent diameter for spheres: 22 nm, gyration radius $2xRg_1$ = 15 nm
TEM	CODA-CERVA	Primary particle size: 15±7 nm
	IMC-BAS	Primary particle size: 20 nm
	INRS	Primary particle size: 18±3 nm
TEM	CODA-CERVA, IMC-BAS	Number (expressed in %) of SAS NM particles smaller than 100nm, 50nm and 10nm <100 nm - 80.4%, <50 nm – 55% <10 nm – 0.9%
DLS	CEA	The material is polydisperse. The intensity size distribution, which consists of two main peaks is very broad and revels the presence of large aggregates of few microns. • Ultra-pure water dispersion (intra vial study) Z-average (nm): 175.9±4.5, PdI: 0.355±0.001, FWHM peak width (nm): 56.2±2.9
	JRC	The material is polydisperse. The intensity size distribution, which consists of two main peaks is very broad and revels the presence of large aggregates of few microns. • miliQ water dispersion. Z-average (nm): peak 1: 156, peak 2: 200, PdI: 0.160
CLS	JRC	Peak (nm): 73, half width: 45, CLS Pdl: 1.43
Specific Surface Area		
BET	IMC-BAS	204.11 (m^2/g)
SAXS	CEA	184±17.8 (m^2/g)
BET	JRC	Sample stored at 40°C: single point: 186.5392 (m^2/g); multi point: 191.9871 (m^2/g). Sample stored at -80°C: single point: 187.4781 (m^2/g); multi point: 192.9282 (m^2/g).
Zeta Potential (surface charge)		
Zetametry	CEA	NM-202 forms a stable suspension, with negatively to neutral charged particles. The zeta potential, however, varied greatly as function of pH and reached -40 mV around pH 7. IEP 2-4.
	JRC	Zeta potential at pH 6.5, milliQ water: -43.7 (mV).

Method	Institution	Results for NM-202
Surface Chemistry		
XPS	JRC	The following elements were identified in the surface of NM-202: O (72.1 at%), Si (25.0 at%) and C (2.9 at%). The presence of C is considered to be due to surface contamination.
TGA	NRCWE	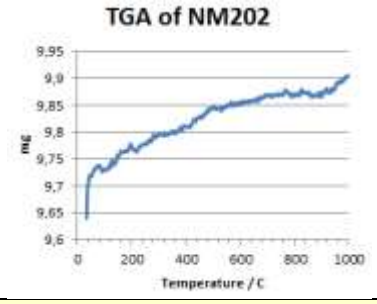 No mass loss observed. Observed mass-increase in graph is due to boyancy.
Photo-catalytic activity		
End-point not relevant for SAS		
Pour-density		
Weighing	INRS	0.13 g/cm^3 (1 wt.% water content)
Porosity		
BET	IMC-BAS	Micropore volume (mL/g): 0.0.00084
Octanol-water partition coefficient,		
End-point not relevant		
Redox potential		
OxoDish fluorescent sensor plate for O_2 detection	NRCWE	The evolution of O_2 level during 24-hour incubation was measured in three different media. Different dO_2 values were observed for all applied media. In the Caco 2 media the concentration of dO_2 was the highest for 0.16mg/ml concentration of NM-202. In the Gambles solution and in 0.05% BSA in water the dO_2 level increased along with the concentration of NM-202. Maximum increase of ca. 30 µmol/l was observed in 0.05% BSA water. The results suggest that NM-202 has oxidative behaviour in these incubation media.
Radical formation		
HPLC + UV	NRCWE	Using the benzoic acid probe to form 4 hydroxy benzoic acid in a phosphate buffered hydrous solution, gave no detectable concentration OH radicals.
Composition		
ICP-OES	CODA-CERVA	No impurities detected
EDS	IMC-BAS	Al- 4500 ppm, Ca- 1800 ppm, Si -46.23 (wt %), O (wt%) calculated- 53.14

NM-203, summary of physical-chemical characterisation results

Method	Institution	Results for NM-203
Homogeneity		
DLS	CEA, INRS, NRCWE	Repeated DLS studies were performed between vials and within vials. The observed variability between the vials is very low (2-3%) but intra-vial is high, ca. 20%.
Agglomeration / aggregation		
SAXS	CEA	Structure and size parameters extracted from SAXS data: Gyration radius of primary particles and aggregates Rg_1: and Rg_2: fractal dimension D_f and number $N_{part/agg}$ of particles per aggregate could not be calculated as parameters could not be fitted.
DLS	CEA	• Ultra-pure water dispersion (intra vial study) Z-average (nm): 172.9±9.2. PdI:0.427±0.025 • Ultra-pure water dispersion (inter vial study) Z-average (nm): 176.9, PdI: 0.425
	NRCWE	• Ultra-pure water dispersion (intra vial study) Z-average (nm): 147.5±4.5. PdI: 0.244±0.017 • Ultra-pure water dispersion (inter vial study) Z-average (nm): 146.8±0.06, PdI: 0.229±0.015
	INRS	• Ultra-pure water dispersion (intra vial study) Z-average (nm): 245.7±37.2. PdI: 0.299±0.024
	JRC	• miliQ water dispersion. Z-average (nm): peak 1: 133, peak 2: 221, PdI: 0.490 • culture media dispersion Z-average (nm): peak : 94.5, PdI: 0.123 • PBS dispersion Z-average (nm): peak: 170.3, PdI: 0.202
TEM	CODA-CERVA, IMC-BAS	High porosity nanostructured material which may be considered aggregetes of primary silicon dioxide particles. Mean diamater (nm): 48±4 Feret min: 33.5 nm (median of 4889) Feret max: 53.2 nm (median of 4889). % of aggregates <100nm: 88±2. Morphology of aggregates/agglomerates: Low sphericity, angular.
TEM-tomography	CODA-CERVA	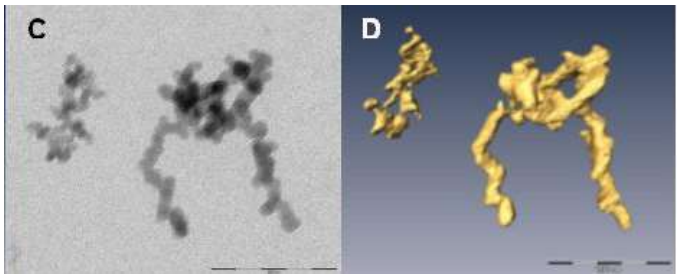 Aggregates of very complex morphology composed of a variable number of interconnected primary subunits.
AFM	CEA	Third dimension of the agglomerates/aggregates: median (of 593): 24.2 nm.
Water Solubility		
24-hour acellular *in vitro* incubation test	NRCWE	The 24-hour dissolution ratio of NM-203 was measured in three different media: 0.05% BSA in water, Gambles solution and Caco 2 media. Both NM-203 and the Al impurities are partially soluble in all media but amounts vary considerably with medium, as does the relative amounts of dissolved Al impurities compared with dissolved Si, suggesting that the solubility behaviour of the Al impurity and NM-203 depend on the medium.

Method	Institution	Results for NM-203
Crystalline phase		
XRD	JRC	Synthetic amorphous silicon dioxide
	NRCWE	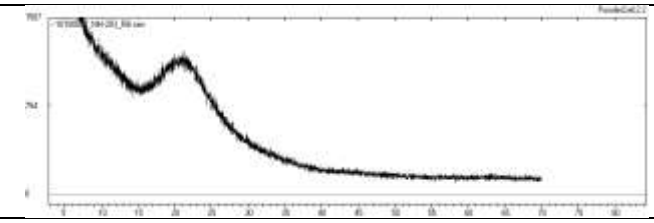 Synthetic amorphous silicon dioxide.
	IMC-BAS	Synthetic amorphous silicon dioxide.
Dustiness		
Small Rotating Drum	NRCWE	Inhalable dustiness index (n=3) 5800±1488 Respirable dustiness index (n=3) 354±6
Vortex Shaker Method	INRS	Respirable dustiness index (n=1) 510000
Crystallite size		
SAXS	CEA	Parameters could not be fitted
XRD	JRC	Synthetic amorphous silicon dioxide
	NRCWE	Synthetic amorphous silicon dioxide.
	IMC-BAS	Synthetic amorphous silicon dioxide
Representative TEM picture(s)		
TEM	CODA-CERVA, IMC-BAS	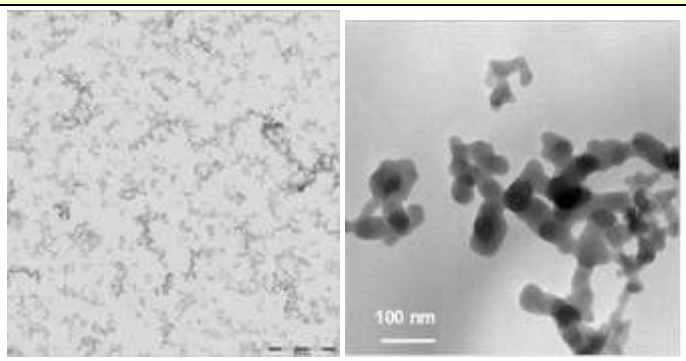 Aggregates with complex open structure.

Method	Institution	Results for NM-203
Particle size distribution		
SAXS	CEA	Parameters could not be fitted.
TEM	CODA-CERVA	Primary particle size: 13±6 nm
	IMC-BAS	Primary particle size: 45
	INRS	Primary particle size: 16±3 nm
TEM	CODA-CERVA, IMC-BAS	Number (expressed in %) of SAS NM particles smaller than 100nm, 50nm and 10nm <100 nm – 77.5%, <50 nm – 48.4% <10 nm – 0.3%
DLS	CEA	The material is polydisperse. The intensity size distribution, which consists of two main peaks is very broad and revels the presence of large aggregates of few microns. • Ultra-pure water dispersion (intra vial study) Z-average (nm): 172.9±9.2. PdI: 0.427±0.025, FWHM peak width: 82.5±11.3 • Ultra-pure water dispersion (inter vial study) Z-average (nm): 176.9, PdI: 0.425, FWHM peak width: 73.15
	JRC	The material is polydisperse. The intensity size distribution, which consists of two main peaks is very broad and revels the presence of large aggregates of few microns. • miliQ water dispersion. Z-average (nm): peak 1: 133, peak 2: 221, PdI: 0.490 • culture media dispersion Z-average (nm): peak : 94.5, PdI: 0.123 • PBS dispersion Z-average (nm): peak: 170.3, PdI: 0.202
	NRCWE	• Ultra-pure water dispersion (intra vial study) Z-average (nm): 147.5±4.5. PdI: 0.244±0.017, FWHM: 84.4±10.4 • Ultra-pure water dispersion (inter vial study) Z-average (nm): 146.8, PdI: 0.06, FWHM: 83.8±0.6
	INRS	The material is polydisperse. • Ultra-pure water dispersion (intra vial study) Z-average (nm): 245.7±37.2. PdI: 0.299±0.024
CLS	JRC	Peak (nm): 64, half width: 50, CLS Pdl: 1.35
Specific Surface Area		
BET	IMC-BAS	203.92 (m^2/g)
SAXS	CEA	167.2±13.4 (m^2/g)
TEM-tomography	CODA-CERVA	219±23 (m^2/cm^3) (Volume specific surface area)
BET	JRC	Sample stored at 40°C: single point: 192.4628 (m^2/g); multi point: 198.0809 (m^2/g). Sample stored at -80°C: single point: 189.8376 (m^2/g); multi point: 195.4241 (m^2/g).

Method	Institution	Results for NM-203
Zeta Potential (surface charge)		
Zetametry	CEA	NM-203 forms a stable suspension, with negatively to neutral charged particles. The zeta potential, however, varied greatly as function of pH and reached -35 mV around pH 7. IEP 2-4
	JRC	Zeta potential at pH 6.6, milliQ water: -46.1 (mV). Zeta potential at pH 7.1, PBS: -18 (mV)
Surface Chemistry		
XPS	JRC	The following elements were identified in the surface of NM-203: O (71.7 at%), Si (26.0 at%) and C (2.31 at%). The presence of C is considered to be due to surface contamination.
TGA	NRCWE	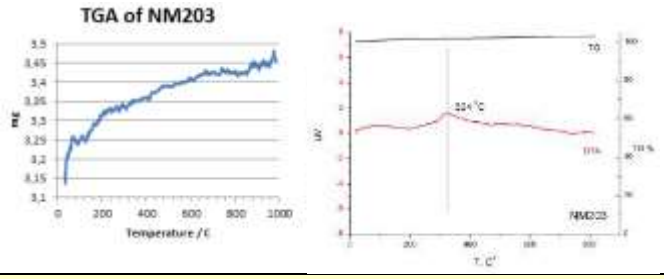 No mass loss detec-ted. Phase transtion detected at 324 ºC (DTA). Observed mass-increase in TGA graph is due to boyancy.
Photo-catalytic activity		
End-point not relevant for SAS		
Pour-density		
Weighing	INRS	0.03 g/cm^3 (1 wt.% water content)
Porosity		
BET	IMC-BAS	Micropore volume (mL/g): 0.0
Octanol-water partition coefficient,		
End-point not relevant		
Redox potential		
OxoDish fluorescent sensor plate for O_2 detection	NRCWE	The evolution of O_2 level during 24-hour incubation was measured in three different media. Different dO_2 values were observed for all applied media however in all three media the level of dO_2 increases with increased concentration of NM-203. The most profound increases with up to ca. 30 µmol O_2/l were observed in the 0.05% BSA water and Caco2 medium. The results suggest oxidative reactivity of NM-203.
Radical formation		
HPLC + UV	NRCWE	Using the benzoic acid probe to form 4 hydroxy benzoic acid in a phosphate buffered hydrous solution, gave no detectable concentration OH radicals.
Composition		
ICP-OES	CODA-CERVA	00.5-0.01%: Na in one of the vials tested
EDS	IMC-BAS	Al: 4300 ppm, S: 400 ppm, Si: 46.32 (wt %), O (wt%) calculated: 53.21

NM-204, summary of physical-chemical characterisation results

Method	Institution	Results for NM-204
Homogeneity		
DLS		Study not performed
Agglomeration / aggregation		
SAXS	CEA	Data regarding structure and size parameters not extracted from SAXS data.
DLS		Study not performed
TEM	CODA-CERVA, IMC-BAS	The amount of particles smaller than 100 nm is 71.2%. Quantitative study for aggregates/agglomerates not performed.
AFM		Study not performed
Water Solubility		
24-hour acellular *in vitro* incubation test	NRCWE	The 24-hour dissolution ratio of NM-204 was measured in three different media: 0.05% BSA in water, Gambles solution and Caco 2 media. Both NM-204 and the Al impurities are partially soluble in 0.05% BSA in water and Caco2 media but amounts vary considerably with medium. In Gambles solution only NM-204 is partially soluble. The relative amounts of dissolved Al impurities compared with dissolved Si differ depending on medium, which suggests different solubility behaviour of the Al impurity and NM-204 depending on the medium.
Crystalline phase		
XRD	JRC	Synthetic amorphous silicon dioxide
	NRCWE	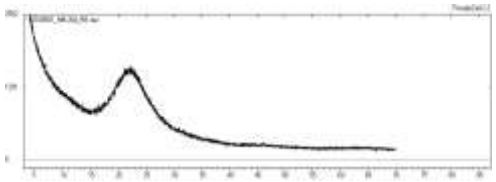 Synthetic amorphous silicon dioxide
	IMC-BAS	Synthetic amorphous silicon dioxide
Dustiness		
Small Rotating Drum	NRCWE	Inhalable dustiness index (n=3) 24969±601 Respirable dustiness index (n=3) 1058
Vortex Shaker Method	INRS	Respirable dustiness index (n=1) 140000
Crystallite size		
SAXS	CEA	Amorphous material
XRD	JRC	Synthetic amorphous silicon dioxide
	NRCWE	Synthetic amorphous silicon dioxide
	IMC-BAS	Synthetic amorphous silicon dioxide

Method	Institution	Results for NM-204
Representative TEM picture(s)		
TEM	CODA-CERVA, IMC-BAS	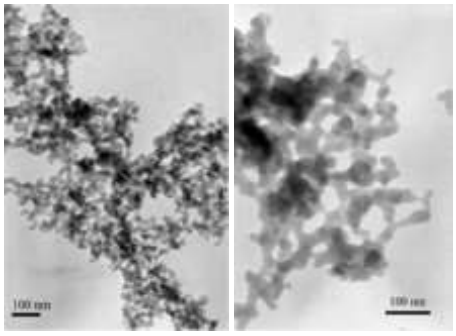 Aggregates with complex, open structure.
Particle size distribution		
SAXS	CEA	Equivalent diameter for spheres: 21nm (Primary particle size)
TEM	CODA-CERVA	Primary particle size: 10-15 nm (manual measurements)
	IMC-BAS	Primary particle size: 19
TEM	CODA-CERVA, IMC-BAS	Number (expressed in %) of SAS NM particles smaller than 100nm, 50nm and 10nm <100 nm - 71.2%, <50 nm - 36.4% <10 nm - 0.3%
DLS		Study not performed
CLS	JRC	Peak (nm): 98, half width: 203, CLS Pdl: 2.99
Specific Surface Area		
BET	IMC-BAS	136.6 (m^2/g)
SAXS	CEA	131±22.9 (m^2/g)
BET	JRC	Sample stored at 40°C: single point: 131.7462 (m^2/g); multi point: 134.3128 (m^2/g). Sample stored at -80°C: single point: 132.057 (m^2/g); multi point: 134.6187 (m^2/g).
Zeta Potential (surface charge)		
Zetametry		Study not performed
Surface Chemistry		
XPS	JRC	The following elements were identified in the surface of NM-204: O (71.9 at%), Si (23.2 at%), Na (0.5 at%) and C (4.3 at%). The presence of C is considered to be due to surface contamination.
TGA	NRCWE	Significant mass loss below 100°C (water). A 0.5 wt% gradual mass-loss above 110°C may indicate organic coating 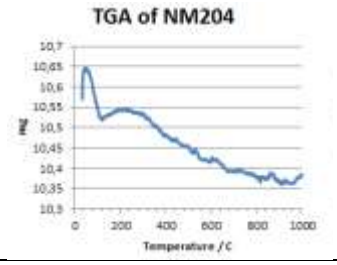
GC-MS	NRCWE	GC-MS analysis results (retention time in min.): Tetramtehyl silicate: 4.9; Hexa-decanoic acid methyl ester: 33.4; Hexadecanoic acid: 33.9; Octadecanoic acid: 35.8
Photo-catalytic activity		
End-point not relevant for SAS		

Method	Institution	Results for NM-204
Pour-density		
Weighing	INRS	0.16 g/cm^3 (6 wt.% water content)
Porosity		
BET	IMC-BAS	Micropore volume (mL/g): 0.00666
Octanol-water partition coefficient,		
End-point not relevant		
Redox potential		
OxoDish fluorescent sensor plate for O_2 detection	NRCWE	The evolution of O_2 level during 24-hour incubation was measured in three different media. Different dO_2 values were observed for all applied media however in 0.05% BSA in water and Gambles solution, for all three different concentration of NM-204, the same behaviour of dO_2 was observed. In case of Caco2 media a clear increment in dO_2 level was only observed at lowest dose suggesting O_2.The maximum O_2 changes observed for NM-204 is on the order of 30 µmol/ml. The results suggest that NM-204 generally has negligible redox activty.

VI. ANNEX VI: PROTOCOLS FOR CHARACTERISATION OF NANOMATERIAL SYNTHESISED IN KOREA

Information on Particle size distribution – dry and in relevant media

Methods

Media: Distilled water

Method/guideline followed: TEM and DLS size measurement procedures are as follows:

a) Protocol for TEM measurements

ⅰ) Sample preparation

- Holey carbon-coated copper TEM grids were chosen for the preparation of TEM nanoparticle specimens.
- One or two droplets of SiO_2 nanoparticle suspension were dropped onto the shiny side of the grids.
- The grids were dried in a desiccator.

ⅱ) Observation and analysis by TEM

- A 300 kV accelerating voltage was used (FEI Tecnai G2 F30 field emission gun (FEG) TEM).
- The microscope magnification was calibrated by imaging silicon {111} lattice fringes at the eucentric specimen position and assuming a 0.31355 nm spacing.
- Coarse focusing was accomplished by raising and lowering the specimen along the *z*-axis (optic axis) and fine focusing was accomplished by adjusting the objective lens current.
- As the actual magnification is sensitive to the objective lens current, the current was precisely controlled during experiments.
- Bright field images were collected using a CCD camera (UIltraScan^{TM}) and DigitalMicrograph software (Gatan, Inc.).
- The SiO_2 nanoparticle sizes were measured manually from the TEM images using DigitalMicrograph software (Gatan, Inc.).

b) Protocol for DLS measurement of a SiO_2 suspension using ELS-Z

- Measure the UV/Vis absorption spectrum of a 150 μL aliquot of the suspension between 200 and 800 nm against solvents (DW) as a baseline using a spectrophotometer (UV-1700, Shimadzu).
- Measure the DLS size on a 1 mL aliquot of the suspension using a particle analyzer (ELS-Z, Otzuka Electronics Co. LTD). Perform 15 runs/measurement × 5 measurements and average of 5 data points.
- Dilute the suspension in DW to 1/10 of the original concentration.
- Measure the DLS size of a 1 mL aliquot of the suspension.
- Repeat the dilution and DLS size measurement until the DLS size is constant within 20 %.
- Obtain the DLS size of SiO_2 nanoparticles from the most dilute suspension in the valid concentration range[1].
- *The instrument performance was qualified using a nanoparticle size reference (Gold Nanoparticle, RM 1980 – NIST).*

[1]*Valid concentration range means that the DLS size is constant within 20 %.*

c) The protocol for the DLS measurement of a SiO_2 suspension using a Brookhaven particle size analyzer is described in Ref. [1].

Year (study performed): 2010 - 2011

GLP: No

Analytical monitoring: TEM (FEI Tecnai G2 F30) and two Particle size analyzers (Brookhaven Instrument Co., ELS-Z, Otzuka Electronics Co. LTD. Japan)

Exposure period (duration): 1 year

Doses/concentration levels: 20 mg/mL for 30 nm SiO_2 nanoparticle suspension and
44 mg/mL for 40 nm SiO_2 nanoparticle suspension

Test conditions

Dilution water source: Distilled water

Stock and test solutions and their preparation: A stock suspension (> 150 mL) was prepared by mixing three batches (>50 mL) of synthesised SiO_2 nanoparticle suspensions. The suspension was stirred for 24 h using a magnetic bar. Three 1 mL aliquots of the suspension were sampled to obtain nanoparticle concentrations by drying-and-weighing. Next, 5 mL aliquots of the suspension were transferred to Teflon-capped vials and labelled with the time of characterization (0, 7, 14, 30, 60, 90, 180, 270 and 360 days after sampling). Each bottle was analyzed at the predetermined storage times.

Stability of the test chemical solutions: Suspensions were stable up to 12 months

Exposure vessel type: not described

Test temperature range: 26 - 28 °C (ambient temperature).

ZETA POTENTIAL/SURFACE CHARGE

Methods

Media: Distilled water

Method/guideline followed: The procedure for zeta potential measurement was as follows (*3 batches of SiO_2 nanoparticle suspensions were measured independently*):

- Measure the UV/Vis absorption spectrum of a 150 μL aliquot of the suspension between 200 and 800 nm against solvents (DW or pH-buffered solution) as a baseline using a spectrophotometer (UV-1700, Shimadzu).
- Measure the DLS size of a 1 mL aliquot of the suspension using a particle analyzer (ELS-Z, Otzuka Electronics Co. LTD.). Perform 15 runs/measurement × 5 measurements and average 5 independent data points.
- *The instrument performance was qualified using a nanoparticle size reference (Gold Nanoparticle, RM 1980 – NIST).*
- Measure the zeta potential of a 1 mL aliquot of the suspension using an electrophoretic mobility analyzer (Zetasizer Nano Z, Malvern). Perform 20 runs/measurement × 5 measurements and average 5 independent data points.
- *The instrument performance was qualified using a vendor-supplied -50 mV transfer standard referred to SRM 1980.*

The measurement procedure for suspension pH was as follows:

- Divide a 6 mL aliquot of the suspension into 4 aliquots of 1.5 mL each and transfer them into 2 mL microcentrifuge tubes. Centrifuge the solutions at 10,000 rpm for 20 min (HM-150IV, Hanil Science Ind.).

- Add 1.3 mL aliquots of the supernatant from the 4 microcentrifuge tubes to a 50 mL conical tube (Cat. No. 50050, SPL Lifesciences).
- Measure the pH of the DW and the supernatant using a pH meter (Orion 3 star pH Benchtop, Thermo Electron Co.) according to the following procedure. After each measurement, wash the pH electrode with DW.
  • Measure the solution pH (DW or supernatant) in a 50 mL conical tube (3 times).
  • Measure the pH of a pH 4.01 standard buffer solution (Orion 910104) (3 times).
  • Measure the solution pH (DW or supernatant) in a 50 mL conical tube (3 times).
  • Measure the pH of a pH 10.01 standard buffer solution (Orion 910110) (3 times).
  • Measure the solution pH (DW or supernatant) in a 50 mL conical tube (3 times).
- *The instrument performance was qualified using standard pH buffers of pH 4.01 (Orion 910104), pH 10.01(Orion 910110) and pH 7.00 (Orion 910107).*

Year (study performed): 2010-2011

GLP: No

Analytical monitoring: Zetasizer (Nano Z, Malvern, UK)

Exposure period (duration): 1 year

Doses/concentration levels: 20 mg/mL for 30 nm SiO_2 nanoparticle suspension and
44 mg/mL for 40 nm SiO_2 nanoparticle suspension

Test conditions

Dilution water source: Distilled water

Stock and test solutions and how they are prepared: A stock suspension (> 150 mL) was prepared by mixing three batches (>50 mL) of synthesised SiO_2 nanoparticle suspensions. The suspension was stirred for 24 h using a magnetic bar. Three 1 mL aliquots of the suspension were sampled to obtain nanoparticle concentrations by drying-and-weighing. Next, 5 mL aliquots of the suspension were transferred to Teflon-capped vials and labelled with the time of characterization (0, 7, 14, 30, 60, 90, 180, 270 and 360 days after sampling). Each bottle was analyzed at the predetermined storage times.

Stability of the test chemical solutions: Zeta potential was stable up to 3 months

Exposure vessel type: not described

Test temperature range: not described

VII. ANNEX VII: NANOGENOTOX STANDARD OPERATING PROCEDURE: DYNAMIC LIGHT SCATTERING MEASUREMENTS AND DATA TREATMENT

General description of scientific background

Dynamic Light Scattering (DLS), also called Photon Correlation Spectroscopy (PCS) or Quasi-Elastic Light Scattering (QELS), is a technique of characterization of colloidal systems based on the scattering of visible light resulting from the difference in refractive index between the dispersed colloids and the dispersion medium. The method may be applied for sizing particles suspended in a liquid in the range from about 0.6 nm to about 6 μm depending on the optical properties of the material and medium.

The principle in DLS is measurement of fluctuations in laser light scattered by vibrating particles suspended in a liquid as function of time. The vibration is due to Brownian motion caused by collision with solvent molecules of the liquid. The Brownian motion varies as a function of particle size and causes variation in the intensity of scattered light as function of time. A correlator compares the signal measured at a time t_0 with different very short time delays *dt* (autocorrelation). As the particles move, the correlation between t_0 and subsequent *dt* signals decreases with time, from a perfect correlation (1) at t_0, to a complete decorrelation (0) at infinite time (order of milliseconds). In the case of big particles, the signal changes slowly and the correlation persists for a long time, whereas small particles have high Brownian movement causing rapid decorrelation.

A DLS instrument measures the velocity of Brownian motion, defined by the translational diffusion coefficient *D* of the particles. The particle size, or more precisely its hydrodynamic diameter d_h, is then estimated using the Stokes-Einstein equation assuming spherical shape:

$$d_h = \frac{kT}{3\pi\eta D}$$

k: Boltzmann's constant
D: translational diffusion coefficient
T: absolute temperature
η: viscosity

It should be noted that even if a particle is really spherical, the spherical DLS size is fundamentally different from the physical spherical size. The hydrodynamic size includes the double-layer of highly polarized water molecules around the physical particle. When the particle morphology is highly non-

spherical, the hydrodynamic size should be understood as the equivalent hydrodynamic spherical size. Establishment of mean hydrodynamic size and size distributions (intensity, number, volume) is reached by DTS software algorithms, by fitting the correlation function in the data treatment.

Chemicals and equipment

- Test material or chemical
- Dispersion medium
- Ultrasonic probe equipped with a standard 13 mm disruptor horn
- Dynamic Light Scattering apparatus
- Viscosimeter (e.g, Malvern Inc., SV-10 Vibro Viscometer) *Optional for measurement of true viscosities*
- Pipette and pipette tips
- Syringes and syringe filters or filter paper

Specificities for Zetasizer NanoZS from Malvern Instruments

DLS measurements rely on non-invasive back scatter (NIBS®) technology developed by Malvern Instruments, in which the signal is detected at 173°. The signal is treated by a digital correlator, and transmitted to the computer. DTS software enables the fitting of correlation data either by a monomodal mode, called the cumulant analysis (as defined by ISO 13321 Part 8) to obtain a mean size (Z-average diameter) and a polydispersity index (PdI), or by a multiple exponential known as the **CONTIN method** to obtain a distribution of particle sizes.

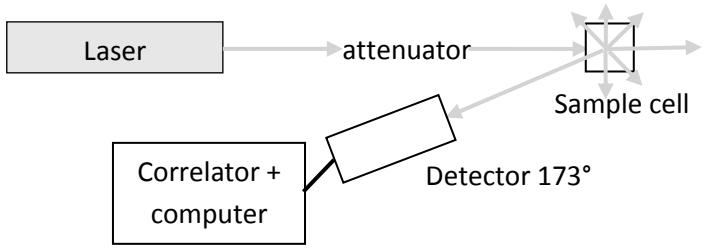

Figure A1. Simplified sketch of the optical configuration for DLS measurement on Zetasizer Nano ZS

Specificities for Vasco Cordouan

The VASCO™ has an original design of the sample cell (thin layer technology) and optics arrangement. The configuration allows also the photo-detector to collect the back-scattered light signal at an angle of 135° (Figure C.2 below). In addition, the cell is hermetically closed by a mechanical system that includes a mobile glass rod with a photon trap. This rod can both absorb the excess of

transmitted light and control the sample thickness, down to few tens of microns. Decreasing the thickness of the sample (and then volume of analysis) reduces significantly the probability for a photon to be scattered several times. Thus, the multiple-scattering artifact is well reduced using this unique design. Also the thin layer technology prevents the sample from local heating.

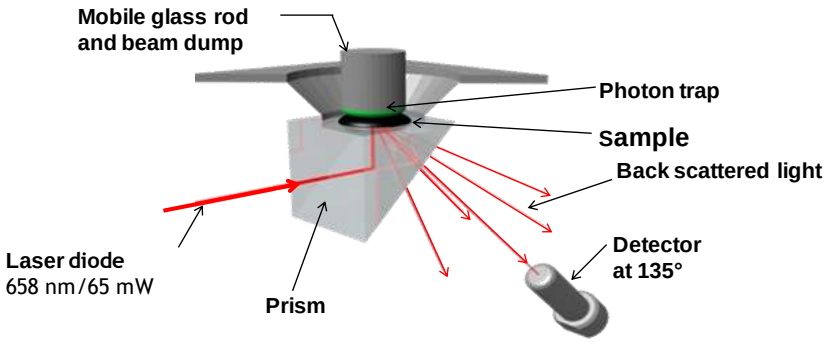

Figure A2. Configuration for DLS measurement on VASCO™

The NanoQ™ software proposes two acquisition modes:

- **Continuous mode where the data acquisition is stopped by the user.**
- Statistical mode where successive data acquisitions are performed automatically following a pattern set by the user (e. g. 15 successive acquisitions of 60s each).

The NanoQ™ software supports two different algorithms for data analysis:

- **Cumulant method** (according to ISO 13321) for mono-disperse samples. The monomodal analysis of the autocorrelation function provides only a mean size value (light scattering intensity-averaged diameter also named as Z-averaged diameter) and a measure of the broadness of the distribution through the polydispersity index.
- **Padé-Laplace** method for polydisperse samples, which does not make any hypothesis for the number of components for multi-exponential analysis. The method gives as a result a discrete density of intensities (histogram), each of them corresponding to a given hydrodynamic diameter. Volume and number histograms are also available based on the Pade-Laplace analysis combined with a Mie algorithm. The NanoQ™ does not provide results expressed as continuous distribution curves for polydisperse samples.

Sample preparation

Dispersions for analysis are prepared by mixing particulate material into a dispersion medium. A sub-sample of a suitable concentration is added to suitable measurement cuvettes. Dispersions are typically produced by sonication in a dispersion medium; SOPs were developed for dispersing the NMs, see e.g. http://www.nanogenotox.eu. The dispersion medium must be filtrated before use to avoid any dust contamination. This can be done by using syringe filters or filter paper with high efficiency. Usually filters with a 0.2 to 0.45 μm pore-size are sufficient for filtration of dispersion media.

The concentration required for analysis depends e.g. on the relative refractive index between particles and dispersion medium, the particle size and polydispersity and the sample absorption. Malvern apparatus is designed to measure samples over a large range of concentration and size of particles. Specifications of sample properties (concentration range, size of nanoparticles, medium) is found in the documentation from Malvern Instrument on their website. The dispersion must be stable during the measurement.

Measurements

Summary

Measurements are performed at ambient temperature according to the procedure appropriate for each type of apparatus. Sample properties such as material and dispersant refractive indices and viscosity are entered in the software for analysis. Number and duration of run and optical configuration are automatically optimized by the software for Malvern apparatus. For Cordouan apparatus, 15 runs of 60s are performed.

About ZetaSizer NanoZS from Malvern Instrument

DLS measurements can be performed in disposable polystyrene cuvettes (optical path 1 cm, volume 1 mL) or alternatively glass cuvettes (at NRCWE) or in semi micro polystyrene disposable cuvettes (optical path 1 cm, volume 500 µL) or in clear disposable zeta cells DTS1061 just before zeta potential measurements (at CEA). The measurements are repeated 3 (CEA) or 6 (NRCWE) times with automatic determination of duration and number of runs, and averaged. The repeated analyses are conducted to enable omission of measurements with poor correlation data or abnormal solutions to the correlation function (must be carefully considered).

The following standard procedure is recommended as the general approach for DLS measurement of NM dispersions:

- Turn on the computer and DLS instrument
- Allow the instrument to warm up according to the manufacturer's recommendation (30 min).
- *Optional: Complete viscosity measurement using the SV-10 Vibro Viscometer mounted with the 10 ml flow-reactor placed in a thermostated water jacket. The measured dynamic viscosity is used as input data for the specific dispersion measured in the DTS software.*
- Upload the DTS software and the "Measurement" window for entering material specific data on dispersion medium, test material and specific analytical settings:
    - Refractive index and absorption values for dispersant and NM.
    - Temperature conditions (25°C) and equilibration time for measurement.
    - The General purpose model is selected for initial evaluation of data and is the most generic model for calculation of size.
- Select a sample cuvette, ensure that it is dustfree and has no defects or scratches in the measurement area of the cuvette. Some producers have been found to deliver cuvettes with scratches or folding structure in the measurement area at one side of the cuvette. Dust may be cleaned out by rinsing the cuvette in dispersion medium.
- Fill in a suitable volume of dispersion into a measurement cuvette using a pipette.
- Place the sample cuvette in the sample holder in the DLS instrument.
- Run analysis (click "play" on the measurement window).
- The size analysis may be immediately accepted if the DTS Expert advice denotes the result quality as "Good". If the result is not of good quality, the sample should be further analyzed for presence of dust, cuvette errors, large particles, sedimentation, wall-deposition etc.
- If the sample contains particles with large spread in size distribution, one may consider filtering the sample through different syringe filters to investigate presence of small nm-size particles. Small nm-size particles may not be fully resolved when larger particles are present due to the large drop (10^6 per factor of ten in size ratio) in scattered light intensity with size.
- If parameters such as refractive indexes, absorption coefficient or viscosity were wrong or unknown at the measurement time, the correction can be made afterwards using the command Edit (right click on the measurement) in the DTS software.

The measurement conditions generally used at CEA and NRCWE are listed in Tables A1 and A2, respectively. The viscosity considered for measurement is generally the one of pure water, 0.8872 cP, but the data can be corrected afterwards for the values measured.

At CEA, the viscosity of water is considered for all samples prepared without addition of BSA or in the pH-adjusted protocol. For suspensions prepared according to the validated NANOGENOTOX protocol, all data were corrected considering the real viscosities measured by NRCWE (usually around 0.99 cP – 1 cP).

Table A1. Conditions used at CEA, refractive index (R_i), absorption or imaginary part (R_{abs}) and dynamic viscosity.

	Water (STP)	**$SiO_{2(amorphous)}$**
R_i	1.33	1.50

R_{abs}		0.01
Viscosity [cP]	0.8872	-

Table A2. Conditions used at NRCWE, refractive index (R_i), absorption or imaginary part (R_{abs}) and dynamic viscosity.

	Water (STP)	**$SiO_{2(amorphous)}$**
R_i	1.33	1.544
R_{abs}		0.20
Viscosity [cP]	0.8872	water

DLS measurements for stability over time

DLS measurements for stability over time were performed on 500 µL suspension in semi micro polystyrene cuvette (CEA) or 1 mL in standard disposable cuvette (NRCWE). The first measurement at t_0 is performed as usual DLS measurements (described above) with automatic determination of parameters. The number of the run, duration, position and choice of attenuator are then recorded and used for the following measurements, which are scheduled over a period of approximately 16 h, usually every 30 min.

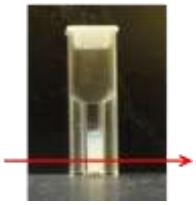

Figure A3. Semi micro cuvette used at CEA for DLS measurements over time. The arrow represents the position of the laser beam probing the suspension.

On Vasco™ from Cordouan Technologies

The following procedure was used and is recommended:

- Turn on the Vasco™ 30 minutes before starting a measurement.
- Run the NanoQ™ software, enter the material specific data on dispersion medium and test nanomaterial as well as specific analytical settings (see table below). Temperature is set to 21 °C.
- Prior to any measurement, it is strongly recommended to carefully clean the cell to avoid pollution from previous measurements. The cleaning operation has to be made gently according to the manufacturer's recommendations.
- Once the cell is perfectly clean, introduce the sample to analyse. For that, use a plastic pipette to extract a sample from the suspension to analyse and drop off a small volume (≈ 2 µl) in the

centre of the cell as shown on the picture below. In order the perform measurements under good conditions, the suspension to be analysed should cover entirely the bottom of the cell, as this correspond to the upper surface of the glass prism guiding the laser beam. For the suspensions analysed in NANOGENOTOX, the thickness of the liquid was set to about 1.5mm (position "up" of the dual thickness controller). After closing the mechanical system, measurements can begin.

- Run the analysis.
- Process the data.

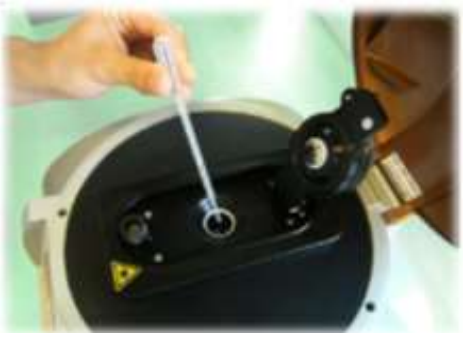

Figure A.4. Illustration of sample deposition on Vasco™ apparatus.

The conditions used at INRS for the analysis with the Vasco™ are reported in Table A3.

Table A3. Conditions used at INRS, refractive index (R_i), absorption or imaginary part (R_{abs}) and dynamic viscosity.

	Water	**$SiO_{2(amorphous)}$**
R_i	1.33	1.54
R_{abs}		0.2
Viscosity [cP]	0.97	0.97

For all measurements performed with the Vasco™ in the NANOGENOTOX project, the "statistical mode" was used, i.e. 15 successive measurements, each with a duration of 60 seconds.

Data treatment

Summary

A monomodal model, the cumulant analysis is used to treat the raw data correlograms (decaying as exponential). It determines a Z-average (diameter of particles scattering with higher intensity) and a polydispersity. Since these samples are quite polydisperse, more sophisticated models, such as the CONTIN method, are applied as multimodal analysis to reveal size distributions.

About ZetaSizer NanoZS from Malvern Instrument

The actual raw data obtained from a dynamic light scattering experiment is the autocorrelation function, which is an exponential decay with a characteristic time related to the size of the diffusing object. An example of correlation data is shown on Figure A5 for two NM104 samples (0.5 g/L TiO_2, 0.036 mol/L of monovalent salt), one stable suspension at pH 2.8 (red curves) and the supernatant of an aggregated sample at pH 10.1 (green curves). The data used are the averaged data for 3 consecutive measurements.

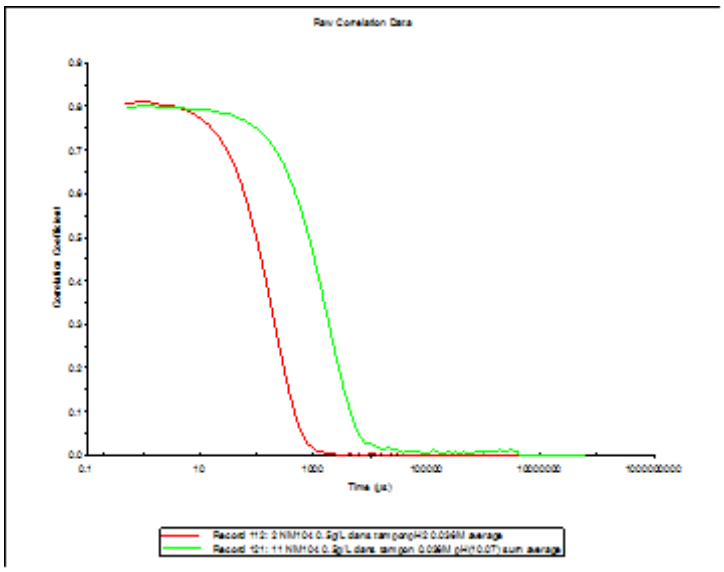

Figure A5. Example of raw correlation data for two NM104 samples (0.5 g/L TiO_2 in 0.036 mol/L ionic buffer), one stable suspension of relatively dispersed particles at pH2.8 (red curve), and one unstable sample of big aggregates at pH10.1 (green curve, measure on supernatant).

The raw correlation data are analysed to extract information on size and distribution. Various algorithms can be used and the simplest is the *Cumulants analysis* which fits the data by approximating the single exponential decay by a degree 2 Taylor development function. This provides a Z-average mean value, which corresponds to the particle size diffusing with the highest intensity, and a polydispersity index (PdI) for this monomodal distribution. In the DTS software, the corresponding graph is entitled "Cumulants fit". The method applies to monomodal distributions with polydispersity lower than 0.25, and is in agreement with ISO 13321 standard. For higher polydispersity, the two parameters Z-average and PdI alone do not accurately describe the sample size distribution and a multimodal analysis is necessary.

Some examples of Cumulant fits analysis applied to NM-104 (TiO_2) are shown in Figure A6. The high PdI obtained for the sample at pH 10 indicates that this model is not advanced enough to determine an accurate size distribution for this sample.

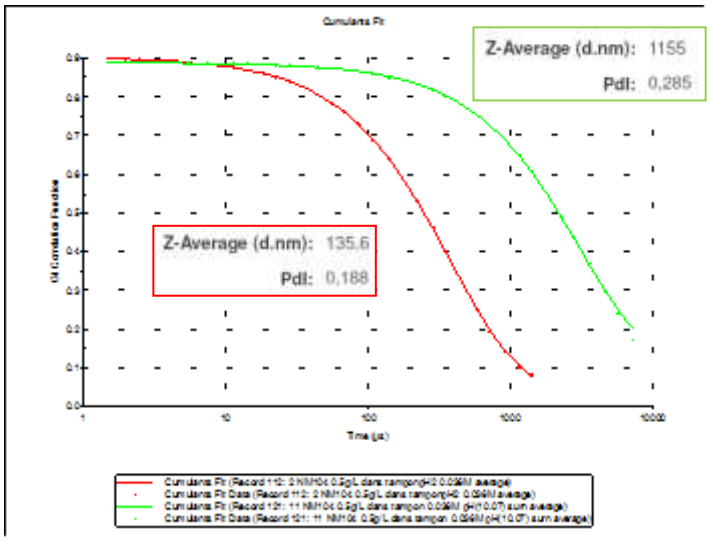

Figure A6. Example of data and fits by the Cumulant method, together with calculated values of Z average and polydispersity, for two NM-104 (TiO_2) samples (0.5 g/L TiO_2 in 0.036 mol/L ionic buffer, stable suspension at pH2.8 in red and unstable sample of big aggregates at pH10.1 in green).

For polydispersity indices between 0.08 and 0.5, the correlation data can be better analyzed by the *CONTIN method*. It fits the correlation data to the best combination of a set of 24 exponential functions, giving rise to a size distribution over 24 granulometric classes. In DTS software, this fit is denominated as "distribution fit", "data fit" or "size fit" (Figure A7).

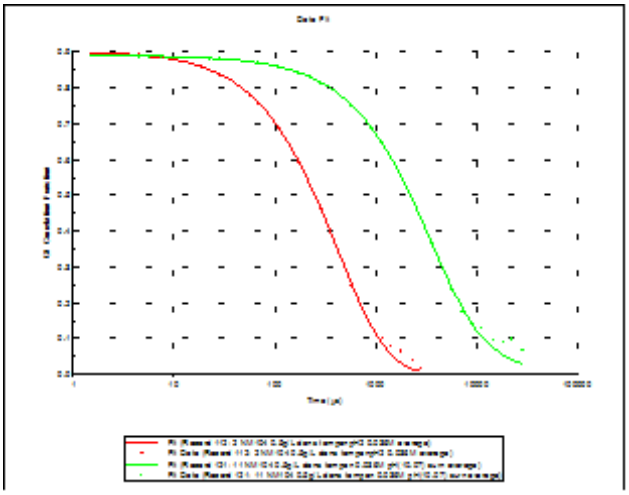

Figure A7. Example of data and fits by the CONTIN method, for two NM-104 (TiO_2) samples (0.5 g/L TiO_2 in 0.036 mol/L ionic buffer, stable suspension at pH2.8 in red and unstable sample of big aggregates at pH10.1 in green).

Taking into account the refractive indices of material and dispersant, Mie Theory can be applied to represent size distribution in volume. The number size distribution can then be calculated from simple geometrical considerations (Figure A8). Distribution data can be retrieved from DTS software in the form of tables of diameter, percentage and width for the three main peaks.

It should be noted that for 2 particles with a size ratio of 10, the bigger particle contributes 10^3 times more than the smaller one to the volume distribution, and 10^6 times more to the distribution by intensity. Since DLS measurements are based on intensity, this means that the light scattered by a few large particles may totally cover the signal from the smaller ones.

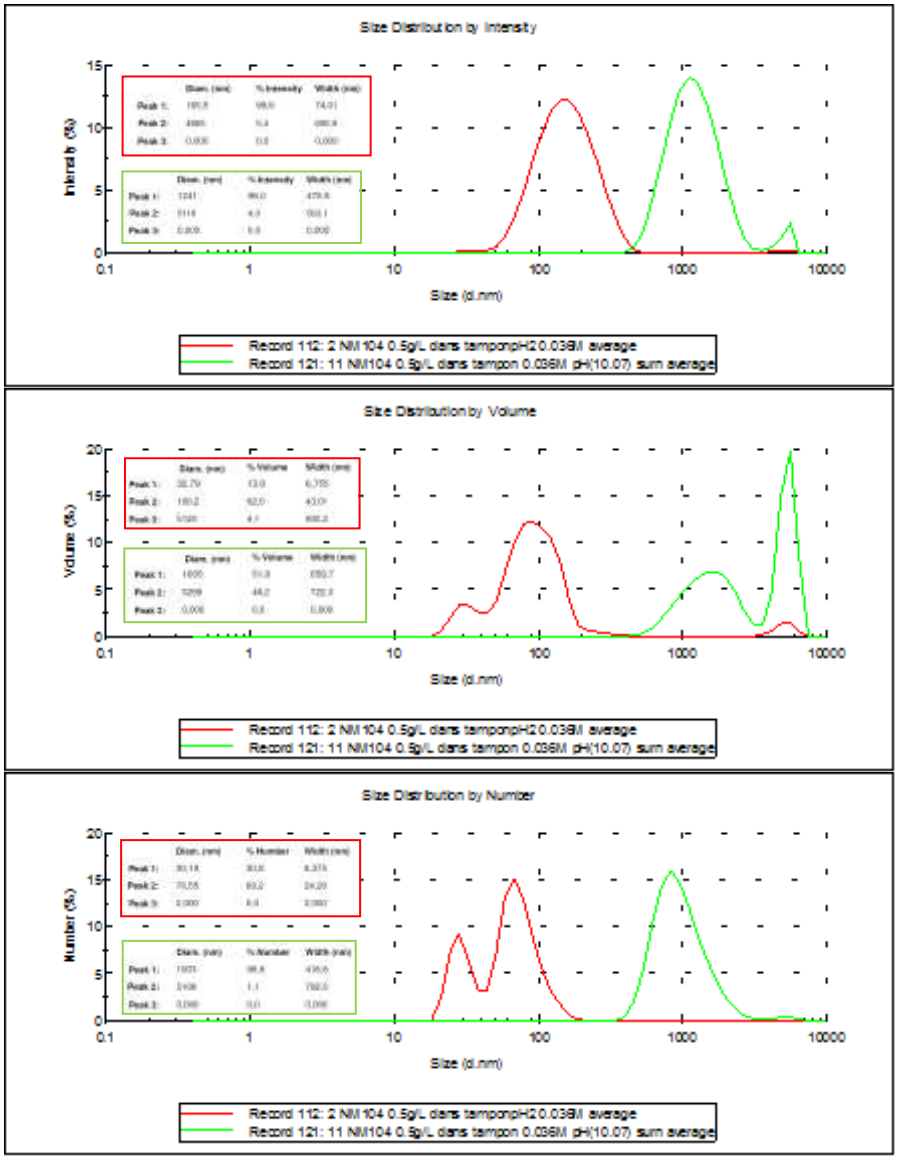

Figure A8. Example of size distributions by intensity, by volume and by number, together with tables of numerical values for the three main peaks of each distribution, for two NM-104 (TiO_2) samples (0.5 g/L TiO_2 in 0.036 mol/L ionic buffer, stable suspension at pH2.8 in red and unstable sample of big aggregates at pH10.1 in green).

After controlling correlation data and fits, an average measurement is calculated with the software. As an example, the main graphs observed for the 3 initial measurements of a sample of NM-104 at pH 2.8 (0.5 g/L TiO_2, 0.036 mol/L of monovalent salt) are displayed on Figure A9. Since the correlation data are good, all 3 measurements are taken into consideration for the averaged data.

The main parameter reported in the results section is *"Z-average"*, which represents the mean size contributing to the major part of the signal **in intensity**. For polydisperse samples, this value mostly gives a hint about the aggregation state of the particles but does not reflect the hydrodynamic size of most of the dispersed particles (in number), which of course is much lower. When Z-average is higher than approximately 500 nm, it can only be deduced that there are big aggregates in suspension but the numerical value is usually meaningless.

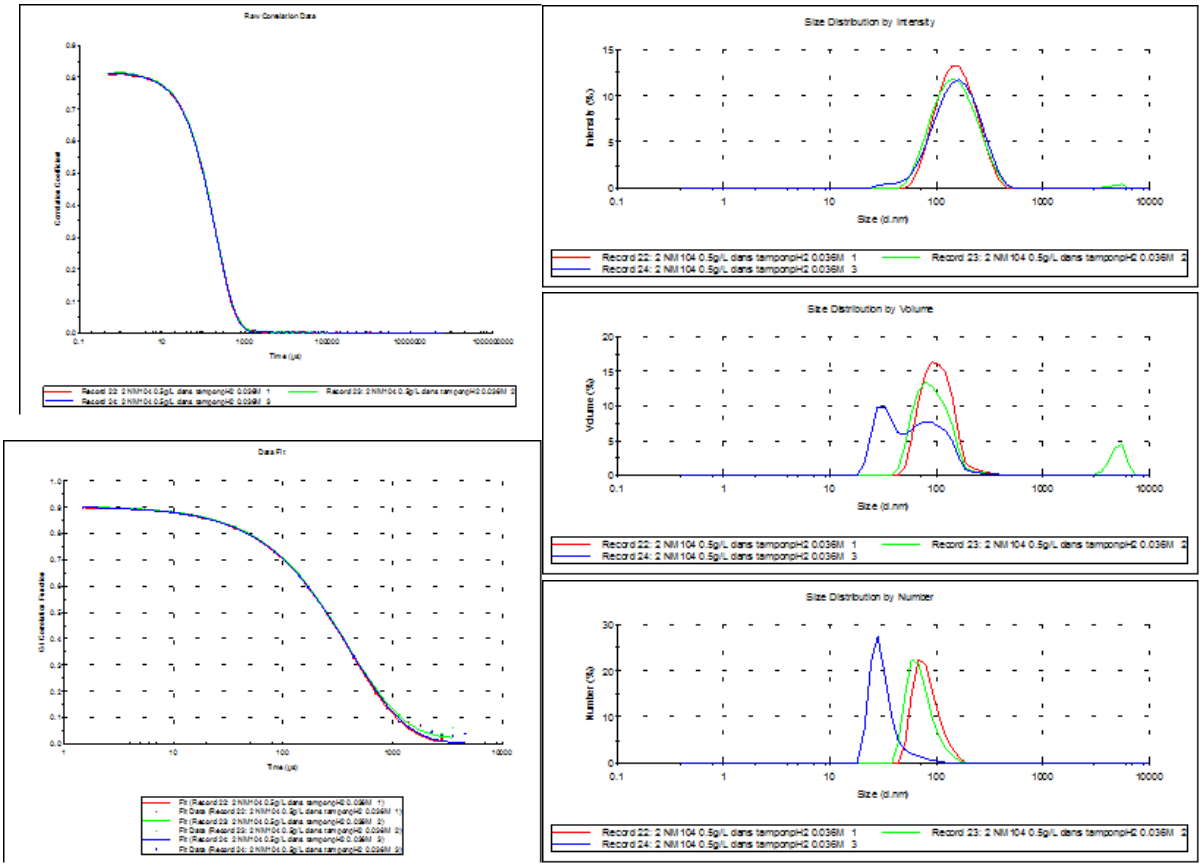

Figure A9. Main graphs reported by DTS software for 3 consecutive measurements of a NM-104 (TiO_2) sample (pH 2.8, 0.5 g/L TiO_2 in 0.036 mol/L aqueous ionic medium)

On Vasco™ from Cordouan Technologies

As for the Zetasizer NanoZS, the raw data obtained from Vasco™ is the autocorrelation function, which is an exponential decaying function with a characteristic time related to the size of the diffusing object.

Comments on use and applicability

DLS is very suitable for size and stability analysis of particles in liquid dispersions. However, great care should be taken in interpretation of data; especially when the sample contains both μm- and small nm-size particles.

For better accuracy of size-determination, it is important to obtain true values of the optical properties and viscosity of the dispersion liquid.

References

Support documents can be downloaded from http://www.malvern.com, application library section.

VIII. ANNEX VIII: THE SENSOR DISH READER SYSTEM

The hydrochemical reactivity was assessed regarding acid-base reactivity and influence on the oxygen balance using a recently developed 24-well SDR (Sensor Disc Reader) system (PreSens Precision Sensing GmbH, Germany) intended for use for in vitro assays (Figure B1). Determination of the acid-base reactivity is particularly important in cell media, where a buffer usually is applied to ensure pH stability in the bioassay. However, if a NM is particular reactive, this pH buffer may be insufficient at sufficiently high NM doses. The O_2 reactivity may another important parameter and relates to hydrochemical reactions that consume or liberate oxygen. Deviations in the O_2-balance can be caused by different reactions including redox-reactions, protonation and deprotonation in the dispersion. These phenomena may be caused by catalytic reactions, but also dissolution, transformation of molecular speciation and precipitation in the medium under investigation.

Figure B1. Sensor Dish Reader, examples of sensor products and illustration of the SDR measurement principle. In this study we used the 24-well Oxy- and HydroDish for O_2 and pH monitoring. Source: PreSens Precision Sensing GmbH, Germany.

The pH variation was measured using the HydroDish® fluorescent sensor plate for pH detection with up to ± 0.05 pH resolution for pH 5 to 9. Measurement is not possible outside of this range.

The O_2 variation was measured using the OxoDish® fluorescent sensor plate for O_2 detection with ± 2 % air saturation resolution. The OxoDish® sensor can measure O2 concentrations between 0 and 250% saturation, corresponding to 0 to 707.6 µmol/l.

In brief, the fluorescent sensor spots are placed at the bottom of each wells in the dishes. For our study, we used 24 well plates. The sensor spot contains a luminescent dye. It is excited by the SensorDish® Reader using a laser diode, placed below the multidish, which is only active when analyses are done, and the sensor luminescence lifetime is detected through the transparent bottom. The luminescence lifetime of the dye varies with the oxygen partial pressure (OxoDish®) and the pH of the sample (HydroDish®), respectively. This signal is converted to oxygen and pH values by the instrument software. The sensor plates are pre-calibrated and the calibration data are uploaded and used for the specific plates used.

Experimental Procedure

Samples were prepared by prewetting the NMs with 0.5% v/v ethanol and dispersion in 0.05% w/v BSA water by probe-sonication following the generic NANOGENOTOX dispersion protocol. Chemically pre-analyzed and approved Nanopure filtered water was used for the batch dispersion to ensure minimum background contamination in the test.

The incubation media included 0.5% BSA-water, low-Ca Gambles solution and Caco 2 medium. The BSA water was included in the study to assess the behavior of the NMS in the batch dispersion medium, which is the first stage in all the biological tests in NANOGENOTOX. The reactivity was tested at doses 0.32, 0.16, 0.08 and 0 mg/ml and a total volume of 2 ml was entered into each well of the SDR plates. Figure B2 illustrates the general procedure.

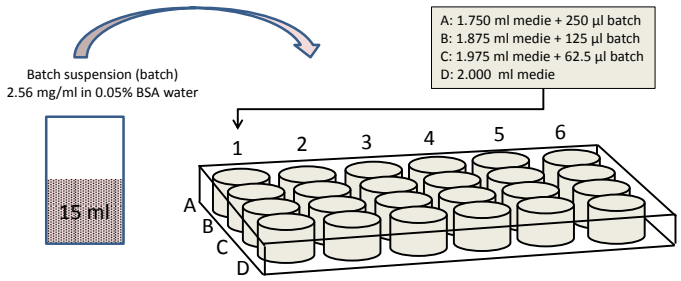

Figure B2. Principal sketch of the dosing into the SDR plates resulting in 2 ml test medium in each well. In this way six dose-response measurements can be made in one test round.

After 24-hours incubation, the maximum dose and control media from the pH and O_2 wells were retrieved by pipette, filtered through a 0.2 µm CAMECA syringe filter and centrifuged in Eppendorf tubes for 60 minutes at 20,000xG RCF using a Ole Dich table top centrifuge. NM samples were placed in the outer ring and pure reference media in the inner ring. Then the upper 1.25 ml of each filtrate from the pH and O_2 wells were sampled, pooled (2.5 ml) in Eppendorf tubes and stabilized with 1 ml 2% HNO_3 water (sample diluted 5/7). The liquids were then stored in darkness until sent for analyses. All vials were washed and rinsed in acid before use.

Data Treatment and Evaluation

The reactivity of each NM was evaluated qualitatively from the evolution of the pH and O_2 over time for each NM at the four dose levels, including the blank control. The SDR pH-values were plotted directly as function of time. The data were then evaluated visually comparing the SDR values of exposed wells with that of the un-exposed control media as well the readings from the initial medium readings in each of the wells to assess if there would be any systematic off-set in some of the sensors. This sensor-evaluation was always done using the blank control as the assumed correct internal reference value.

For the O_2 analyses, the difference between time-resolved readings from ”exposure doses” and the medium control ($dO_2 = (O_{2,dose} – O_{2,medium\ control})$) were plotted as function of time.

For both pH and O_2, if the SDR readings from the dosed media showed no difference or followed the same trend as the reference media, the NM was assumed to have negligible pH reactivity or influence on the oxygen balance through redox reactivity or dissolution.

Nanomaterial dissolution and biodurability

The NM dissolution and biodurability was assessed from elemental analyses of the solute adjusted for background concentrations in the three test media. It was assumed that maximum dissolution would be observed at the 0.32 mg/ml dose and that equilibrium was reached in 24 hours. Consequently, if the elemental composition of the test materials is given, the results enable calculation of the solubility limit as well as the durability (the un-dissolved residual) of the specific NM in the batch dispersion, the lung lining fluid and the Caco2 media. However, in this study, we have only semi-quantitative elemental composition data on the SAS.

Elemental analysis

The concentrations of dissolved Si elements in the media were analysed using Inductively Coupled Plasma-Optical Emission Spectroscopy. Ti, Al, Fe, Co, and Ni were determined by ICP Mass-spectrometry. Both element series were analysed as a commercial service by Eurofins, DK-6600 Vejen, Denmark. The elemental background concentrations in the three test media were determined on three doublet samples for each media. The elemental concentrations after dissolution were determined in two sub-samples for each NM.

IX. ANNEX IX: NANOGENOTOX STANDARD OPERATING PROCEDURE FOR SURFACE CHARGE AND ISOELECTRICAL POINT BY ZETAMETRY

General description

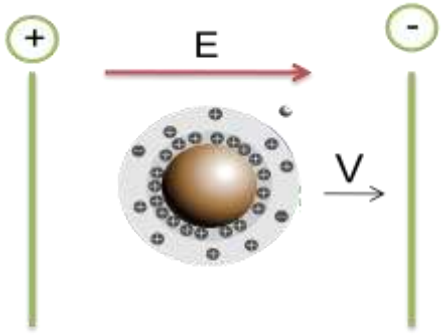

Figure C1. scheme of charged particle in electric field applied between

Dispersion state and stability of suspensions are governed by an equilibrium between attractive (mainly van der Waals) and repulsive (electrostatic or steric) interactions. A stable suspension is obtained if repulsive interactions overcome the attractive ones, which are responsible for aggregation and subsequent sedimentation. Zeta potential is a good indicator of the magnitude of repulsive interactions between charged particles. The charge at the very surface of the particles is not accessible and Zeta potential corresponds to the potential at the shear plane. This is the boundary between the bulk dispersant and the double layer of solvent and ions moving together with the particles, see Figure C1. The reciprocal Debye length, κ^{-1}, represents the thickness of this double layer. The zeta-potential varies with pH due to protonation-deprotonation of the material surface. From colloid science, a suspension of small particles is considered stable if the zeta-potential exceed |30| mV.

For low pH (acidic medium), the surface of metal oxide (MO) materials is protonated (MOH_2^+), i.e. positively charged. For high pH the deprotonation results in negatively charged particles (MO^-). The pH-value at which the charge is reversed determines the so-called isoelectric point (IEP) where the dispersion is unstable. IEP can be determined by titration, but can also be measured from manually prepared different dispersions displaying the same ionic strength for various pH. The zeta potential can be highly influenced by the properties of the medium, such as ionic strength (by compression of the double layer), or adsorbing molecules or ions (especially multivalent ions).

The zeta potential (ζ) is not directly measurable and is calculated from the measurement of electrophoretic mobility U_E using Henry's equation:

$$U_E = \frac{2\,\varepsilon\,\zeta\,f(\kappa a)}{3\eta}$$

ε: dielectric constant of medium
η: viscosity
κ: inverse of the Debye length, a: radius of a particle
$f(\kappa a)$ = 1.5 for aqueous suspensions in the Smoluchowski approximation

In practice, the sample is exposed to an electric field which induces the movement of charged particles towards the opposite electrode.

Chemicals and equipment

- HNO_3 (analytical grade)
- NaOH (analytical grade)
- $NaNO_3$ (analytical grade)
- Purified water (MilliQ or Nanopure water)
- Ultrasonic probe Sonics & Materials, VCX500-220V, 500 W, 20 kHz equipped with a standard 13 mm disruptor horn, or equivalent
- pH-meter with standard pH probe
- Zetasizer Nano ZS (e.g, Malvern Instruments), equipped with laser 633 nm
- Autotitrator (Malvern MPT-2) –*optional for automatic determination of IEP*
- Malvern computer software (DTS 5.03 or higher) to control the Zetasizer
- Clear, disposable zeta cells (DTS1061 - DTS1060C)

Sample preparation

Summary

Samples for zeta potential measurements are prepared as aqueous suspensions of 1 g/L for SiO_2 nanomaterials with constant ionic strength of 0.036 mol/L (monovalent salt) and controlled pH. They are prepared by dilution of concentrated sonicated stock suspensions of 10 g/L into pH and ionic strength controlled "buffers" prepared by addition of HNO_3, NaOH and $NaNO_3$ in various proportions.

Stock suspension preparation

20 mL of stock suspensions of 10 g/L NM in pure water are prepared as follows:

200 mg of NM are weighed and introduced in a 20 mL gauged vial (with protective gloves, mask and glasses, and damp paper towel around the weigh-scale).

- The 20 mL gauged vial is completed with ultrapure water (MilliQ®)
- The suspension is transferred into a flask suitable for sonication (a 40 mL large-neck glass flask of internal diameter 38 mm was used, height of 20 mL liquid 20 mm), making sure that all the settling material is recovered.
- The suspension is dispersed by ultrasonication for 20 min at 40% amplitude in an ice-water bath. Probe, sample and bath are placed in a sound abating enclosure, and in a fume hood.

Preparation of "buffer" solution

Denominated *"buffer"* solutions are aqueous ionic solutions of Na^+, H^+, NO_3^- and OH^-, designed to display the same ionic strength with a modulated pH.

- A first set of concentrated buffer solutions (0.1 mol/L of salt, various pH) are prepared by addition of HNO_3, NaOH and $NaNO_3$ in various proportions in ultrapure water.
- Then 20 mL of these concentrated buffers are poured into 50 mL gauged vials completed with ultrapure water, giving a new set of buffers with a salt concentration of 0.04 mol/L and a pH ranging from 1.5 to 12.5. The combination of the two buffers gives access to the necessary intermediate pH.
- By this procedure, acidic buffers contain 0.04 mol/L of NO_3^- and various ratios of Na^+/ H^+ as counter ions; likewise, basic buffers contain 0.04 mol/L of Na^+ and various ratios of NO_3^-/OH^- .

Preparation of suspensions for zeta potential measurements and determination of isoelectric point

In this SOP Zeta potential measurements are performed on 1 g/L suspensions for SiO_2 samples. 10 g/L suspensions of the SiO_2 samples are used right after sonication. Series of samples are prepared by addition of 400 µL of concentrated NM suspension and 3.6 mL of 0.04 mol/L buffer solutions in a 5 mL glass flask. This leads to samples of 1 g/L SiO_2 and a constant ionic concentration of 0.036 mol/L in monovalent salt.

For each NM, an additional sample is prepared in MilliQ or Nanopure water with the same NM concentrations, i.e. 400 µL of concentrated NM suspension and 3.6 mL of water.

Measurements and data treatment

Summary

For each suspension of known pH, fixed ionic strength and fixed NM concentration, the measurements for determining the zeta potential are performed on a general purpose mode with automatic determination of measurement parameters. Three measurements are performed and averaged for reporting. For unstable samples, measurements are performed on supernatants. Zeta potentials are then plotted against pH to determine the stability domains and isoelectric points (IEP).

Equilibrium pH of the suspensions are measured and considered as pH values for the reported results. The suspension to be characterized by zetametry are inserted in Malvern patented folded capillary cells with gold electrodes (volume 0.75 to 1 mL), DTS1061. Zeta measurements (electrophoretic mobility) are performed on the "*general purpose"* mode at 25°C with automatic optimization of laser

power, voltage settings, the number of runs (10 - 100) and run duration, and repeated 3 times with no equilibration time as the sample is already at ambient temperature.

The Smoluchowski model (F(κa)=1.5) was used, considering the high polarity of aqueous solvent, and hence a thin double layer around the particles. For the dispersant, the refractive index R_i, absorption R_{abs}, viscosity and di-electric properties considered are the ones of pure water and the table below lists the parameters used for dispersant and material properties.

Table C1. Properties of dispersant and material phases used for zeta potential measurements

	Water (STP)	**$SiO_{2(amorphous)}$**
R_i	1.33	1.5
R_{abs}		0.01
Viscosity [cP]	0.8872	-

Data treatment

Electrophoretic mobility is measured by a combination of laser Doppler velocimetry, a technique based on the phase shift of the laser beam induced by the movement of particles under an electric field, and phase analysis light scattering (patented M3-PALS technique). In this "mixed mode measurement" (M3), the measurement consists of the application of an alternative electric field in two modes, a fast field reversal mode, and a slow field reversal mode. The light scattered at an angle 17° is combined with the reference beam and the resulting signal is treated by the computer (Figure C2). During the fast field reversal mode, the electro-osmose effect is negligible, allowing to determine an accurate mean zeta potential, whereas the slow field reversal mode helps modelling the distribution of potentials.

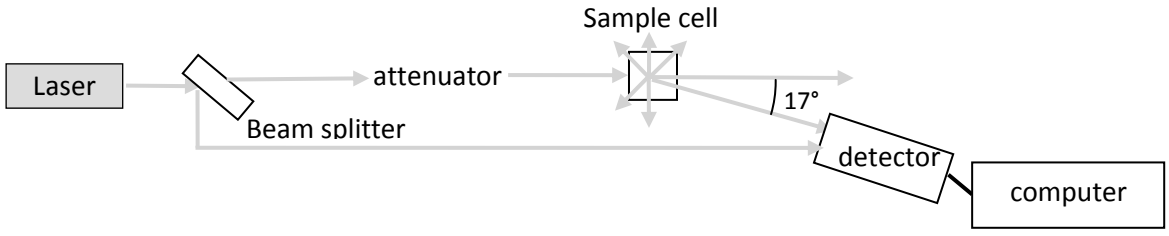

Figure C2. Simplified scheme of optical configuration for zeta potential measurement on Zetasizer NanoZS.

An example of the main data plots returned by DTS software from zeta potential measurements is shown on figure C3 (phase plot and corresponding electric field applied, mean zeta potential and zeta potential distribution).

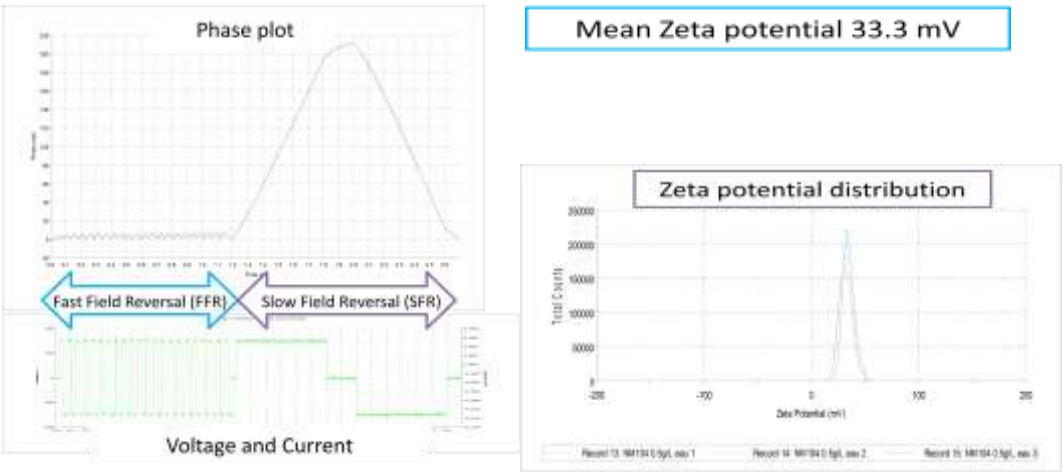

Figure C3. Data plots retrieved from zeta potential measurements on Nanosizer ZS, example of 3 consecutive measurements on a suspension of NM-104 (TiO_2) at 0.5 g/L in pure water.

More details on the results of zeta potential measurements with the M3-PALS technique are available in the documentation from Malvern Instruments and can be downloaded from http://www.malvern.com, application library section. The reported value is the average of zeta potential values from the 3 measurements (determined during the fast field reversal step), with possible exclusion of diverging data.

X. ANNEX X: NANOGENOTOX STANDARD OPERATING PROCEDURE FOR SMALL ANGLE X-RAY SCATTERING

This annex describes the general procedure applied at CEA/LIONS (Laboratoire Interdisciplinaire sur l'Organisation Nanométrique et Supramoléculaire) to perform Small Angle X-ray Scattering measurements and the data treatment to extract physical-chemical properties of materials. This procedure was applied to characterize the SAS NMs as powders and in aqueous suspension.

General description

Small-Angle X-ray Scattering is a technique based on the interaction between X-rays and electrons to probe the structure of materials. The processed data is the number of X-rays scattered by a sample as a function of angular position of a detector, see Figure D1.

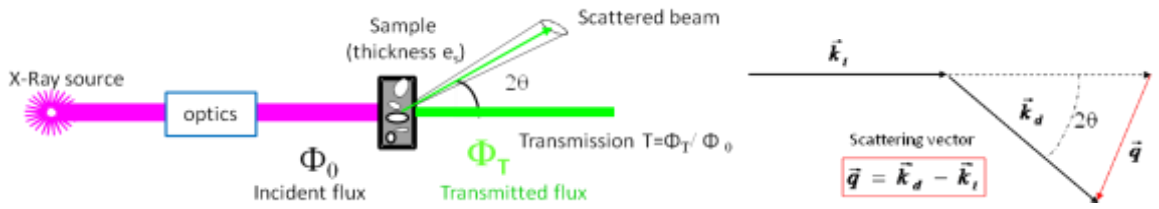

Figure D1. Schematic set up for SAXS and physical quantities

2D raw data images are converted into diffractograms displaying the **scattered intensity *I*** as a function of scattering vector *q* defined by:

$$q = \frac{4\pi \ sin\theta}{\lambda}$$

λ : X-ray wavelength

The experimental scattering intensity is defined as the differential scattering cross-section per unit volume of sample and can be expressed as follows:

$$I(q) = \frac{1}{V}\frac{d\sigma}{d\Omega} = \frac{\eta_1 C_{ij}}{\eta_2 (\Phi_0 ST) dt}\frac{1}{\Delta\Omega}\frac{1}{e}$$

σ : scattering cross-section

V : volume of sample

C_{ij}: number of counts detected on a pixel ij during dt

η_1: detector quantum efficiency when measuring the direct beam

η_2: detector quantum efficiency for the count Cij

(φ_0ST): flux (in detector unit counts/s) integrated over the whole beam transmitted by the sample

T: transmission of the sample

$\Delta\Omega$: solid angle covered by one pixel seen from the center of the sample ($\Delta\Omega = p^2/D^2$ with p the pixel size and D the sample to detector distance)

The intensity is then expressed in **absolute scale** (in cm^{-1}) to be independent of the experimental set up parameters (X-ray wavelength, experimental background, time for acquisition, sample thickness, etc.).

General theorems of experimental physics have been developed to extract different properties of nanostructured material from the diffractograms, such as shape of nanoparticles, surface area, interactions occurring, etc. *I(q)* curves can also be theoretically calculated from assumed nanostructures to fit the experimental curves.

In the simple case of binary samples, the scattering intensity is proportional to:

- the electronic contrast, more precisely the square of scattering length density difference between the two materials $(\Delta\rho)^2$,
- the concentration of the scattering object (in volume fraction), in case of suspensions for example.

Ultra Small Angle X-ray Scattering (USAXS) measurements give access to X-ray scattering data for a range of smaller *q* and then complement the SAXS diffractograms. It requires a specific and very precise set-up, different from the one used for SAXS.

Equipment

The experimental set up (X-ray source, optical elements, detectors, etc.) and the procedure for absolute scaling of data has been thoroughly described by Zemb (Zemb et al., 2003) and Né (Né et al., 2000).

Apparatus

The main set up components used for SAXS and USAXS experiments at CEA/LIONS are listed below:

- X-ray generator : Rigaku generator RUH3000 with copper rotating anode (λ= 1.54 Å), 3kW
- Homemade optic pathways and sample holders (with two channel-cut Ge (111) crystals in Bonse/Hart geometry for USAXS set up (Lambard et al.,1992)
- Flux measurement for SAXS set up : pico amperemeter Keithley 615
- Flux measurement for USAXS set up : DonPhysik ionization chamber
- Detector for SAXS set up : 2D image plate detector MAR300

- Detector for USAXS set up: 1D high count rate CyberStar X200 associated to a scintillator/ photomultiplier detector.

All experimental parameters are monitored by computer by a centralized control-command system based on TANGO, and interfaced by Python programming. 2D images are treated using the software *ImageJ* supplemented with some specific plugging developed at CEA/LIONS by Olivier Taché (Taché, 2006).

Calibration

A sample of 3 mm of Lupolen® (semi crystalline polymer) is used for the calibration of the intensity in absolute scale, the maximum intensity being adjusted to 6 cm^{-1}.

A sample of 1 mm of octadecanol is used for the calibration of the q range (calculation of sample-to-detector distance), the position of the first peak standing at 0.1525 $Å^{-1}$.

Calibrations in intensity and in q range are performed before each series of measurements.

Sample preparation

Almost any kind of material can be analysed by SAXS, whether as a powder, a colloidal suspension, a gel, or even self-supported hybrid materials, as long as the sample prepared meets some requirements of transmission and scattering properties.

Depending on the X-ray absorption coefficient of the material and its scattering properties, the sample thickness has to be adjusted to get a transmission as close as possible to the target transmission of 0.3 (optimal absorption/transmission ratio).

The sample thickness *e* is directly linked to the transmission *T* by the following equation:

$$e = -\frac{1}{\mu}\ln(T)$$

μ: X-ray absorption coefficient of the material,

T: transmission, *T* = transmitted flux/ incident flux of the direct beam

If not self-supported (liquids, powders or gel), the material to be analysed is inserted in a cell, which can be made of glass (capillary), or X-ray transparent material such as Kapton® (polyimide). A measurement of the empty cell is performed and subtracted as a background for the sample measurement. See Figure D2 for examples of cells used at CEA/LIONS.

Powders

The absorption coefficient depends on the material and on the energy. For the Cu K-alpha emission (8 keV) used here, the coefficient, $\mu_{SiO2,}$ for SiO_2 is 77 cm^{-1} and the optimal sample thickness (equivalent thickness of dense material) to get a transmission of 0.3 is 150 µm.

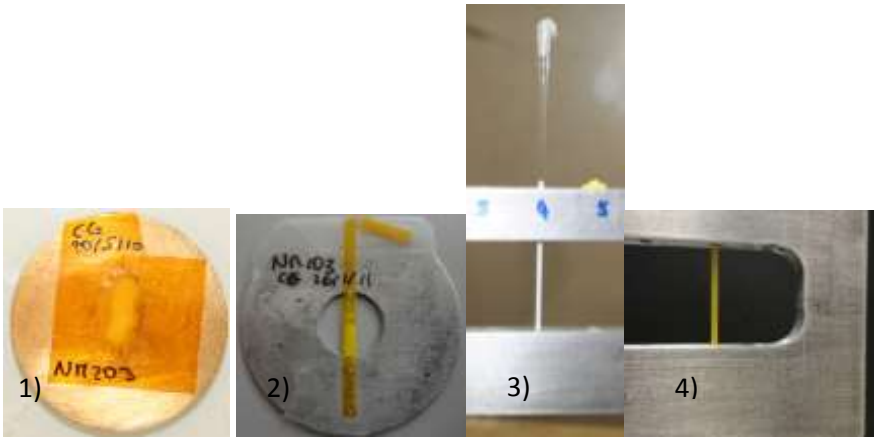

Figure D2. Examples of different type of cells used for SAXS measurements, 1) double sticky kapton® cell for powders, 2) 1.5 mm flattened polyimide capillary for powders, 3) 1.5 mm glass capillary for powder or liquid samples, 4) 1.5 mm polyimide capillary for powder or liquid samples.

The SiO_2 powder samples, except NM-203, were prepared in 1.5 mm glass capillaries leading to typical equivalent thickness of dense material from 100 to 200 µm. NM-203 powder is very sticky and was very difficult to insert into capillaries, so it was measured in a double sticky kapton® cell.

Aqueous suspensions

The usual thickness of aqueous samples for SAXS measurement is 1mm with an acquisition time of 1 hour. Dispersions for analysis are typically produced by sonication in a dispersion medium. The concentration required for analysis depends on the relative scattering length densities between particles and dispersion medium, and the density of materials. The sample must be stable within the time-frame of the measurement.

Typical concentration in oxide for NANOGENOTOX suspensions is 3 g/L. Since the scattering length density of silicon dioxide is relatively low, higher concentrations were used when possible.

Measurements

In order to calculate the sample transmission, the flux of incident and transmitted beam are measured and averaged over 200 s before running the SAXS measurement. The time of acquisition necessary for SAXS experiment depends on the sample properties. For SiO_2 powders, two measurements were performed: one

with a short time of 200 s or 150 s to get unsaturated data for small angles (low q), and one for a long time of 1800 s to get data in the high q region with low signal/noise ratio.

For aqueous suspensions prepared for NANOGENOTOX, SAXS measurements were performed in kapton capillaries of internal thickness 1.425 mm and run for 3600s, leading to transmissions of about 0.25. USAXS measurements were performed in 1 mm or 1.5 mm non-sticky double kapton cells, cell types are shown on Figure D2.

Data treatment

Raw data, translated into intensity as a function of the scattering vector q, are first normalized by parameters of the experiments such as acquisition time, sample thickness and calibration constants determined using reference samples, thus expressing data in absolute scale (cm^{-1}). Backgrounds are then subtracted. To get continuous diffractograms for the whole q range SAXS data obtained for short and long times are combined with USAXS data.

For powder samples, the Porod law is applied to extract specific surface areas of raw materials. Data from suspensions are fitted with a model describing fractal aggregates of primary particles. In this model, the whole q range is divided into sections reflecting different structural levels in the sample, and fitted by local Porod and Guinier scattering regimes. Intensity average parameters are then determined such as radius of gyration for the primaries and for the aggregates, and a fractal dimension for the aggregates. Invariants are calculated, which give a correlation between the sample concentration and the specific surface area obtained in suspension.

Raw data treatment

SAXS data

Radial averaging of 2D image (ImageJ)

2D images from the detector are converted into Intensity = f(scattering vector q) graphs by the software ImageJ together with SAXS plugging. The process follows mainly these steps:

- Determination of the centre coordinates (direct beam position)
- Application of a mask to remove pixels corresponding to the beam stop and around the photodiode
- Radial averaging of the intensity, knowing pixel size, sample-detector distance and wavelength (example of parameters in Figure D3), conversion of pixel position into scattering vector *q*, and creation of a .rgr file containing *I(q)* data.

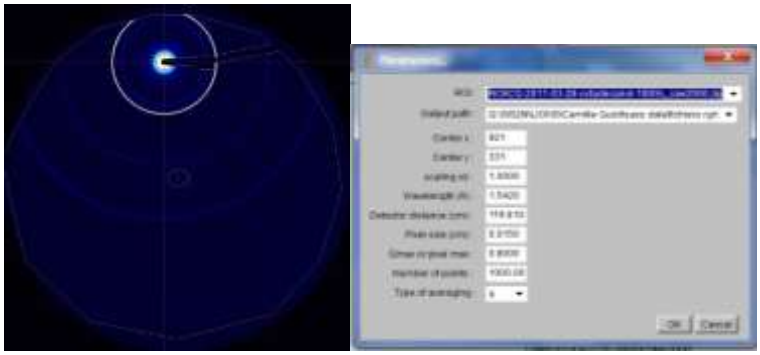

Figure D3. Example of raw 2D image (octadecanol) and parameters used for radial averaging with ImageJ

Absolute scaling of I(q) (pySAXS)

In order to scale the data to the absolute scale in cm^{-1}, *I(q)* data generated by *ImageJ* as .rgr files are treated by a homemade program called *pySAXS* and based on python programming.

The scaling involves a subtraction of the detector background and normalization by exposition time, sample transmission, sample thickness and K constant. The K constant is calibrated with Lupolen® sample and allows conversion of intensity in photons into absolute intensity in cm^{-1}. An example of parameters used for the scaling is shown on Figure D4.

The subtraction of the empty cell signal and normalization by the sample thickness can be done in a subsequent step.

USAXS data

Raw USAXS data are generated as intensity vs angle data in .txt files. Data treatment is achieved using *pySAXS* and involves the following steps:

- Subtraction of the "rocking curve" (signal with empty cell) normalized by the intensities at 0° (transmission).
- Desmearing, taking into account the effective size of the "punctual" detector (cf reference 0)
- Conversion of angle into q range
- Normalization by the sample thickness.

Figure D4. Example of SAXS scaling parameter file from PySAXS software

Data analysis

General theorems of X-ray scattering have been developed to analyze SAXS data. Here are presented some simple laws for **binary systems** (two phase samples) that may be of use in NANOGENOTOX framework.

Porod's Law

In the high q range, sample diffractograms display an intensity decreases in a q^{-4} trend, called the "Porod region". This region corresponds in the "real space" to the scale of the interfaces (for smooth interfaces).

Therefore, for a binary sample, the asymptotic limit of the so-called "Porod's plateau", when data are represented in Iq^4, is related to the total quantity of interface Σ (in m^2/m^3) between the two phases, as follows:

$$\Sigma[\mathrm{m}^{-1}] = \frac{\lim_{\text{plateau}} (I.q^4)}{2\pi(\Delta\rho)^2}$$

where $\Delta\rho$ is the difference in scattering length density between the two phases. For a binary sample of **known thickness**, the volume fraction of a material φ_A, its specific surface area S_A/V_A (surface developed/ volume of A in the binary sample) and Σ are linked by the following relation:

$$\Sigma[\mathrm{m}^{-1}] = \frac{S_A}{V_A}\varphi_A$$

For example, for a suspension of oxide in water, the determination of Porod plateau gives access to the concentration of the sample if the specific surface area of particles suspended is known (and vice versa).

Specific surface area determination from SAXS on powders

To treat raw SAXS data and get absolute intensities, the intensity by the thickness of the scattering material need to be normalised. However, for powder samples, the sample thickness is not well defined and cannot be precisely controlled as it depends on the powder compaction and the different scales of porosity, see Figure D5. To elude this problem, a model system is used, considering the effective thickness of material crossed by X-rays, called e_B, corresponding to an equivalent thickness if all the material would be arranged in a fully dense (no inner or outer porosity) and uniform layer.

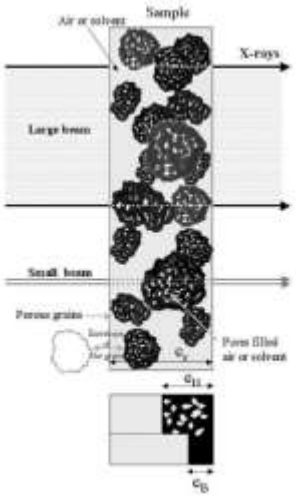

Figure D5. Schematic representation of a powder sample for SAXS measurement, and definitions of equivalent thick-nesses e_H and e_B.

The sample transmission is related to this equivalent thickness by the following equation:

$$e_B = -\frac{1}{\mu}\ln\left(T_{exp}\right)$$

where μ is the material absorption coefficient for X-Ray (μ_{SiO2} = 77 cm^{-1}) and T_{exp} is the **experimental transmission** (transmitted flux Φ_T/ incident flux Φ_0), i.e. transmission of the sample with regard to the transmission of the empty cell (kapton® alone, empty capillary, etc). The intensity scaled by this thickness e_B is called I_1. The Porod's law can then be applied for I_1 to access the specific surface area of the powder.

Specific surface areas of powders are determined on the Porod plateau from the equation. The values in m^{-1} are then converted into m^2/g taking into account the material density ρ_m:

$$\sum[\frac{m^2}{g}] = \frac{\sum[m^{-1}]}{\rho_m[\frac{g}{m^3}]}$$

If no uncertainty is considered for the material density, the relative uncertainty of the specific surface area calculated is directly linked to the determination of the Porod plateau:

$$\frac{\Delta\sum[\frac{m^2}{g}]}{\sum[\frac{m^2}{g}]} = \frac{\Delta\sum[m^{-1}]}{\sum[m^{-1}]} = \frac{\Delta\lim(I)_1 q^4}{\lim(I)_1 q^4}$$

However, if we consider a quantifiable uncertainty on the material density, it is passed on to the calculated sample thickness e_B and the theoretical scattering length density of the material. Finally, the relative uncertainty on the specific surface area is increased by the uncertainty on the material density:

$$\frac{\Delta \sum[m^{-1}]}{\sum[m^{-1}]} = \frac{\Delta \lim(I)_1 q^4}{\lim(I)_1 q^4} + \frac{\Delta \rho_m}{\rho_m}$$

The uncertainty on the material density even contributes twice when the specific surface area is expressed in m^2/g:

$$\frac{\Delta \sum[\frac{m^2}{g}]}{\sum[\frac{m^2}{g}]} = \frac{\Delta \lim(I)_1 q^4}{\lim(I)_1 q^4} + 2\frac{\Delta \rho_m}{\rho_m}$$

All specific surface area results, together with their uncertainty calculations are presented below. Errors on the Porod's plateaus have been determined manually for each diffractogram, and the uncertainty on the material density is considered to be about 5%.

Invariant theorem

When *I(q)* can be extrapolated to zero values of *q* (no interaction at a large scale, i.e. a flat signal for low q) and at infinite *q* (usually with the Porod law), the following invariant theorem can be applied:

$$Q = \int_0^\infty I_{Abs}\, q^2 dq = 2\pi^2 \varphi(1-\varphi)(\Delta\rho)^2$$

This implies that the invariant *Q* is a constant for a defined composition, which gives access to the volume fraction ϕ, or to the evolution of interactions for a fixed composition.

Guinier regime

For dilute samples of monodisperse objects (negligible position correlation between scattering objects, i.e. structure factor 1), the intensity in the low q region ($qR_G << 1$) can be approximated to:

$$I(q) \approx A\left(1 - \frac{(qR_G)^2}{3} + Bq^3\right)$$

which gives access to the radius of gyration of the particles R_G with the slope of $\ln(I)=f(q^2)$.

Data fits

Assuming values of parameters such as volume fraction, size, shape and polydispersity of scattering objects for a model sample, it is possible to calculate theoretical curves of *I(q)*. Therefore, the adjustment of such parameters to fit experimental curves allows for the modelisation of the sample properties.

Unified model of aggregates in suspension for SAXS data treatment

A unified fitting approach, developed by Beaucage et al. (Beaucage et al., 1996; Kammler et al., 2004; Kammler et al., 2005) was used to treat X-ray scattering data from SiO_2 suspensions composed of aggregates of primary particles. In this model, the whole q range is divided into sections reflecting different structural levels in the sample, and fitted by local Guinier, fractal and Porod scattering regimes, see Figure D6.

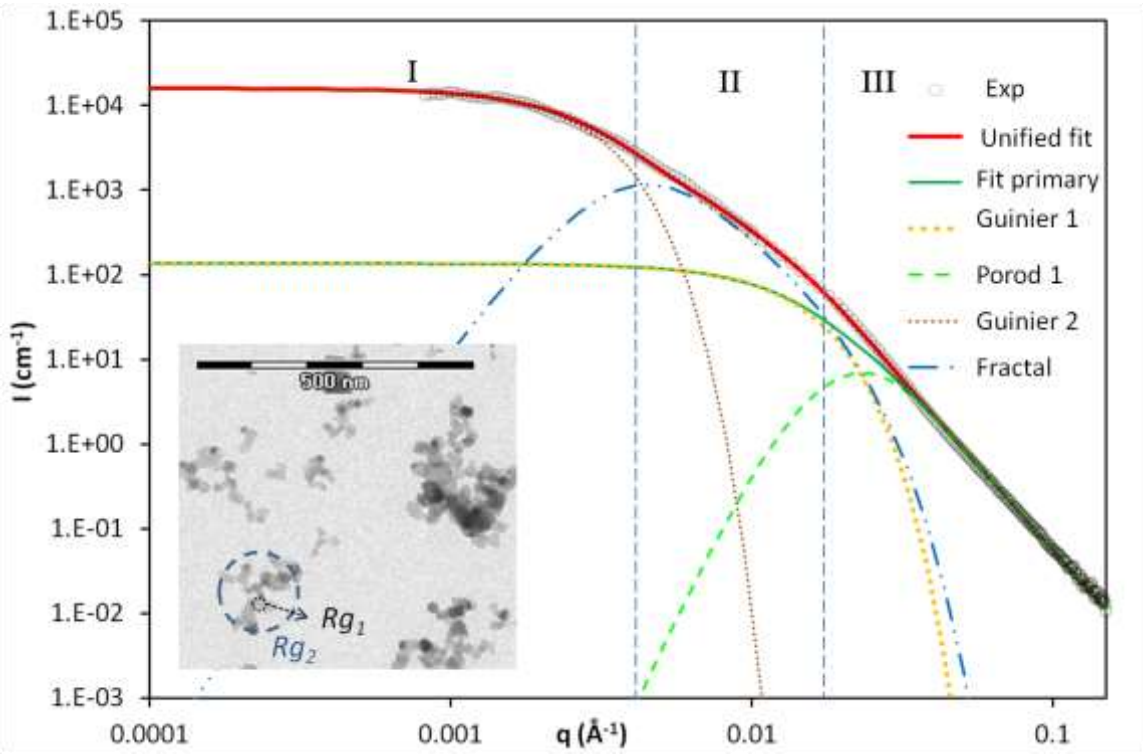

Figure D6. Example of SAXS diffractogram (NM-105, a TiO_2, suspension sonicated at pH 2 as circles) illustrating the unified fit (solid red line) and its components prevailing in each q-domain (dashed-dotted lines). Insert of TEM micrograph (by CODA-CERVA) illustrating the gyration radius of primary particles (Rg1) and aggregates (Rg2) used in the model. Exp = experimental data.

The scattering vector *q* is homogeneous to the reverse of a length, so large q values actually corresponds to small observation scale in the direct space.

For a smooth surface of primary particles, **at large q** (the scale of interfaces) the intensity decays as a power-law of q^{-4} defining the Porod regime:

$$I_{Porod\ 1}(q) = B_1\ q^{-4}$$

The coefficient B_1 is directly linked to the specific surface area of the primary particles:

$$B_1 = 2\pi N(\Delta\rho)^2 S$$

with N and S respectively the number density and the average surface area of primary particles and $\Delta\rho$ the difference of scattering length density between scattering object (SiO_2) and medium (water).

This Porod regime is preceded **at lower q** by a Guinier regime, signature of the size of primary particles, and is described by:

$$I_{Guinier\ 1}(q) = G_1 \exp\left(\frac{-q^2 {Rg_1}^2}{3}\right)$$

The sum of these two regimes (***Fit primary*** in Figure D6) would describe scattering intensity resulting from individual uncorrelated primary particles, *i.e.* if they were perfectly dispersed and non-aggregated. It prevails in the large q range (domain III, Figure D6). The upturn of the intensity at small q is due to the association of primary particles into aggregates of finite size.

These aggregates also present a finite size and inner structure. Thus, a second Guinier regime is associated with the structural size of aggregates and prevails in the domain I defined in the Figure D6:

$$I_{Guinier\ 2}(q) = G_2 \exp\left(\frac{-q^2 {Rg_2}^2}{3}\right)$$

The coefficients G_1 and G_2 are defined by:

$$G_i = N_i(\Delta\rho)^2 V_i^2$$

where N_i and V_i are respectively the number density and volume of object i (primary particle or aggregate).

These two Guinier regimes give access to the radii of gyration of the primary particles, Rg_1 and of the aggregates, Rg_2.

The ratio of G1 to B1 is a measure of the anisotropy of the primary particles since

$$\frac{G_1}{B_1} \alpha \frac{V^2}{2\pi S}$$

with *V* the volume of the particles and *S* their surface.

For intermediate q range between the scale of aggregates and the scale of primary particles (domain II in Figure D6), the intensity decays with a slope typical for the fractal regime of an aggregate and described by a power-law linked to the mass-fractal dimension D_f:

$$I_{Fractal}(q) = B_2\, q^{-D_f}$$

The coefficient B_2 is linked to D_f, G_2 and Rg_2 by:

$$B_2 = \frac{G_2}{Rg_2^{\,D_f}} D_f \Gamma\left(\frac{D_f}{2}\right)$$

Γ is the gamma function.

The fractal dimension D_f is a measure of the degree of ramification and density of aggregates (value between 1 and 3), see Hyeon-Lee et al., 1998.

An average number of primary particles per aggregate can be derived from the Guinier coefficients:

$$N_{part/agg} = \frac{G_2}{G_1}$$

The global unified fit is obtained by addition of the different terms, see Bushell et al., 2002.

To fit the experimental diffractograms, the total model curve

$$I(q) = I_{Porod\,1}(q) + I_{Guinier\,1}(q) + I_{Fractal}(q) + I_{Guinier\,2}(q)$$

is plotted and parameters (B_1, G_1, G_2, D_f, Rg_1 and Rg_2) are adjusted manually so that the model fits the best the experimental data. Three parameters are there to describe the primary particles, and three are also necessary to describe the aggregates structures of primary particles. Also in TEM three independent parameters were required to describe the aggregates.

Some geometrical restrictions have to be respected ($D_f < 3$; volume of N primaries < volume of aggregate, total surface area of primaries cannot be smaller than the corresponding surface area for ideal spheres).

All SAXS data are treated to be represented in the absolute scale (intensity in cm^{-1}). Therefore quantitative measurements are accessible and through the use of the invariant theorem and it is possible to calculate the exact concentration of samples, and then correlate the specific surface area developed in the suspension to the specific surface area of raw materials obtained from powder samples.

References

1. T. Zemb, O. Taché, F. Né, and O. Spalla; “A high-sensitivity pinhole camera for soft condensed matter”; J. Appl. Crystal., 36, 800-805, **2003**.
2. F. Né, I. Grillo, O. Taché, and T. Zemb. ; “From raw image to absolute intensity: Calibration of a guinier-mering camera with linear collimation”; J. de Physique IV, 10(P10), 403-413, **2000**.
3. O. Spalla, S. Lyonnard, and F. Testard; “Analysis of the small-angle intensity scattered by a porous and granular medium”; J. Appl. Crystal., 36, 338-347, **2003**.
4. J. Lambard, P. Lessieur and Th. Zemb; “A triple axis double crystal multiple reflection camera for ultra small angle X-ray scattering”; J. de Physique I France, 2, 1191-1213, **1992**. Lambard, J.; Lesieur, P.; Zemb, T., A triple axis double crystal multiple reflection camera for ultra small angle X-ray scattering. J. Phys. I France 1992, 2 (6), 1191-1213.
5. O. Taché ; « Une architecture pour un système évolutif de contrôle commande d'expériences de physique », Engineer thesis, **2006**, available at http://iramis.cea.fr/sis2m/lions/tango/tango-ds/memoire.pdf
6. Beaucage, G., Small-Angle Scattering from Polymeric Mass Fractals of Arbitrary Mass-Fractal Dimension. J. Appl. Crystal. **1996**, 29 (2), 134-146.
7. Kammler, H. K.; Beaucage, G.; Mueller, R.; Pratsinis, S. E., Structure of Flame-Made Silica Nanoparticles by Ultra-Small-Angle X-ray Scattering. Langmuir **2004**, 20 (5), 1915-1921.
8. Kammler, H. K.; Beaucage, G.; Kohls, D. J.; Agashe, N.; Ilavsky, J., Monitoring simultaneously the growth of nanoparticles and aggregates by in situ ultra-small-angle x-ray scattering. J. Appl. Physics **2005**, 97 (5), 054309-11.
9. Hyeon-Lee, J.; Beaucage, G.; Pratsinis, S. E.; Vemury, S., Fractal Analysis of Flame-Synthesized Nanostructured Silica and Titania Powders Using Small-Angle X-ray Scattering. Langmuir **1998**, 14 (20), 5751-5756.
10. Bushell, G. C.; Yan, Y. D.; Woodfield, D.; Raper, J.; Amal, R., On techniques for the measurement of the mass fractal dimension of aggregates. Advances in Colloid and Interface Science **2002**, 95 (1), 1-50.
11. Porod, G.; Glatter, O.; Kratky, O., General theory: Small-angle X-ray scattering. Academic Press ed.; Academic Press: New York, **1982**.